Process Development For

Metal Soaps

By
Mehmet GÖNEN

A Dissertation Submitted to the
Graduated School in Partial Fulfillment of the
Requirement for the Degree of

MASTER OF SCIENCE

Department: Chemical Engineering
Major: Chemical Engineering

İzmir Institute of Technology
İzmir, Turkey

We approve the thesis of **Mehmet GÖNEN**

Date of Signature

....   **24.01.2003**

Prof. Dr. Devrim BALKÖSE

Supervisor

Department of Chemical Engineering

....   **24.01.2003**

Prof. Dr. Semra ÜLKÜ

Co-Supervisor

Department of Chemical Engineering

....   **24.01.2003**

Assist. Prof. Dr. Fikret İNAL

Co-Supervisor

Department of Chemical Engineering

....   **24.01.2003**

Prof. Dr. Levent ARTOK

Department of Chemistry

....   **24.01.2003**

Assist. Prof. Dr. Turgut BATTAL

Department of Chemical Engineering

....   **24.01.2003**

Prof. Dr. Devrim BALKÖSE

Head of Department

ACKNOWLEDGMENT

İzmir, January 2003

Mehmet GÖNEN

ABSTRACT

Zinc stearate ($ZnSt_2$) is an important compound among the metallic soaps. It has many applications e.g., in resins, paints, cosmetics, textile, lubricants and Langmuir-Blodgett films. Double decomposition (precipitation) and fusion processes are widely used techniques in $ZnSt_2$ production. The product purity has been a major concern in most of the $ZnSt_2$ applications such as PVC stabilization, coating of textile goods, additive in cosmetic products. In this study, the production of $ZnSt_2$ using precipitation, fusion and modified fusion processes was investigated based on product purity. Raw materials and $ZnSt_2$ were characterized by using various techniques.

In the precipitation process, in order to maximize the solubility of sodium stearate and to minimize the water evaporation, the reaction was carried out at 70°C. 2.5% (w) NaSt was used in the reaction at this temperature. The equivalent, excess Zn and deficient Zn cases were studied to determine the raw materials ratio on product purity. Equivalent raw materials produced highest product purity. From washing experiment, it was seen that Na_2SO_4 adsorption did not take place on to wet $ZnSt_2$. The washing water to zinc stearate ratio was found to be 40 dm^3/kg for effective removal of by products and raw materials unreacted at room temperature. Any further increase in the amount of water did not bring any significant removal results. In the drying of wet $ZnSt_2$ at 100°C, it was determined that it has 85% (w) water. In IR spectra, characteristic $ZnSt_2$ peak was observed at 1540 cm^{-1}. $ZnSt_2$ obtained by this process did not contain any free Na^+ and SO_4^{-2} ions as indicated by ICP, EDX and elemental analysis results. Only two of the characteristic peaks of $ZnSt_2$ at 2θ values of 6.40 and 19.58 were obtained in XRD pattern of the dried product due to low crystallinity. From SEM micrographs, it was seen that zinc stearate has lamellar structure and particle size changes between 2-4 μm. Melting point of the zinc stearate was found to be about 122°C using optic microscopy with temperature controlled hot stage.

In fusion process, reaction was carried out at 140°C in equivalent amounts for different stirring rates 400, 600 and 750 rpm. The increase in mixing rate decreased the delay time occurring at the beginning of the reaction. The conversion was found to be 80% using the developed method from IR spectra. In the comparison of the experimental conversion data with shrinking core model no relation was established. In

IR spectra, two peaks observed at 1540 cm^{-1} and 1700 cm^{-1} which belong to ZnSt$_2$ COO$^-$ stretching and stearic acid C=O stretching vibrations, respectively. All of the characteristic 2θ values of zinc stearate were observed for product, which means that the crystallinity of the product is high. From SEM micrographs, it was seen that zinc stearate structure is in the form of layered lamella and particle size change between 4-6 μm. The melting point of zinc stearate samples from fusion process was found to be slightly lower than 122°C by optic microscopy with temperature-controlled hotstage.

In the modified fusion process, reaction was carried out at 80°C for 1 h. with equivalent amounts of stearic acid and zinc oxide in the presence of H$_2$O. Sodium stearate 1.5% (w) was added into reaction mixture as a surfactant and its effect was examined. At the end of reaction it was seen from IR spectra that it does not significantly increase the reactants dispersion. The presence of unreacted raw materials was determined in IR spectras and XRD patterns. This result was confirmed by SEM micrographs too.

In TGA analysis, thermal decomposition temperature of zinc stearate was found to be 250°C. The use of zinc stearate in n-paraffin wax shifted the thermal decomposition temperature of wax 10°C. Increasing the amount of zinc stearate in n-paraffin increased the decomposition temperature of wax.

According to the results of this study, for pure zinc stearate production precipitation process should be preferred in spite of high wash water consumption. The fusion and modified fusion processes needs to be studied further to increase the conversion and decrease the delay time.

ÖZ

Çinko stearat metal sabunları arasında önemli bir bileşiktir. Reçinelerde, boyalarda kozmetik ürünlerinde, tekstilde, yağlarda ve Langmuir-Blodgett filmlerinin hazırlanmasında olmak üzere bir çok uygulama alanına sahiptir. Çift bozunma (çöktürme) ve ergitme prosesleri çinko stearat üretiminde yaygınca kullanılan tekniklerdir. PVC'nin ısıl kararlı kılınması, tekstil ürünlerinin kaplanması, kozmetik ürünlerinde katkı olarak kullanılması gibi birçok uygulamasında ürün saflığı önemli bir konu olmuştur. Bu çalışmada çinko stearat üretimi, ürün saflığı göz önünde bulundurularak çöktürme, ergitme ve modifiye edilmiş ergitme prosesleriyle çalışılmıştır. Hammaddeler ve çinko stearat değişik teknikler kullanılarak karakterize edilmiştir.

Çöktürme prosesinde sodyum stearatın çözünürlüğünü arttırmak için reaksiyon 70°C'de çalışılmıştır. Bu sıcaklıktaki sodyum stearatın en yüksek çözünürlük değeri 2.5% (w) reaksiyonda kullanılmıştır. Ürün saflığı üzerine hammadde oranlarının etkisini belirlemek için eşdeğer, ağırlıkça %10 fazla çinko ve %10 eksik çinko durumları çalışılmıştır. En yüksek ürün saflığı eşdeğer miktarlardaki hammaddeler ile sağlanmıştır. Yıkama deneylerinden Na_2SO_4'ın ıslak çinko stearat üzerine adsorplanmadığı gözlenmiştir. Oda sıcaklığında reaksiyona girmemiş hammaddelerin ve yan ürünlerin etkili bir şekilde ayrılması için yıkama suyunun çinko stearate oranı 40 dm^3/kg olarak bulunmuştur. Su miktarındaki artış önemli bir uzaklaştırma sağlamamıştır. Islak çinko stearatın 100°C kurutulmasıyla yapısında ağırlıkça %85 su olduğu tespit edilmiştir. IR spektralarında 1540cm^{-1}'deki karakteristik çinko stearat piki gözlenmiştir. Bu metot ile üretilen $ZnSt_2$ ICP, EDX ve elemental analiz sonuçlarında belirtildiği gibi Na^+ ve $SO4^{-2}$ iyonlarını içermemiştir. Çinko stearatın karakteristik piklerinden sadece iki tanesi düşük kristal düzeninden dolayı 2θ değeri 6.40 ve 19.58'de elde edilmiştir. SEM mikro fotoğraflarından çinko stearatın lameller yapısına sahip olduğu ve partikül büyüklüğünün 2-4 μm arasında değiştiği gözlenmiştir. Çinko stearatın erime noktası optik mikroskopta sıcaklık kontrollü plaka kullanılarak 122°C civarında bulunmuştur.

Çöktürme prosesinde reaksiyon 140°C'de, eşdeğer miktarlarda, 400, 600 ve 750 rpm değişik reaksiyon hızlarında çalışılmıştır. Karıştırma hızının arttırılması reaksiyon

başlangıcındaki gecikmeyi azaltmıştır. IR spektralarından geliştirilen metot ile dönüşüm %80 olarak bulunmuştur. Deneysel dönüşüm verileri ile kinetik modellerin karşılaştırılmasında bir bağlantı kurulamamıştır. IR spektralarında 1540cm^{-1} ve 1700cm^{-1}'de gözlenen iki pik sırasıyla çinko stearatın COO$^-$ yapısı gerilme ve stearik asitin C=O grubu titreşimlerine aittir. Çinko stearatın karakteristik 2θ değerlerinin hepsi ürün için gözlenmiştir. Bu sonuç kristalliğin yüksek olduğunu gösterir. SEM mikro fotoğraflarından çinko stearat yapısının düzlemsel lamelle formunda olduğu görülmüştür ve partikül büyüklüğünün 4-6 μm arasında değiştiği bulunmuştur. Ergitme prosesinden elde edilen çinko stearat örneklerinin erime noktaları optik mikroskopta sıcaklık kontrollü plaka kullanılarak 122°C'den az düşük olarak bulunmuştur.

Modifiye çöktürme prosesinde reaksiyon 80°C'de, 1 saat süresince eşdeğer miktarlardaki stearik asit ve çinko oksit ile su ortamında çalışılmıştır. Sodyum stearat yüzey aktif madde olarak reaksiyon ortamına ağırlıkça %1.5 eklenmiş ve etkisi incelenmiştir. Reaksiyon sonunda IR spektrumlarından sodyum stearatın hammaddelerin dispersiyonunda önemli arttırma sağlamadığı görülmüştür. Ürün içinde reaksiyona girmemiş hammadde olduğu IR spektrumlarından ve XRD patternlerinden bulunmuştur. Bu sonuç SEM mikro fotoğraflarında da doğrulanmıştır.

TGA analizinde çinko stearatın bozunma sıcaklığı 250°C olarak bulunmuştur. Çinko stearatın n-parafinde katkı olarak kullanılmasının n-parafinin termal bozunma sıcaklığını 10°C yükseltmiştir. Çinko stearat miktarının arttırılması parafinin bozunma sıcaklığını yükseltmiştir.

Bu çalışmanın sonuçlarına göre, saf çinko stearat üretiminde, yüksek yıkama suyu tüketimi olmasına rağmen çöktürme prosesi tercih edilmelidir. Ergitme ve modifiye edilmiş ergitme prosesleri, dönüşümü arttırmak ve reaksiyondaki gecikme süresini azaltmak için daha ayrıntılı çalışılmalıdır.

TABLE OF CONTENTS

LIST OF FIGURES

LIST OF TABLES

CHAPTER I

INTRODUCTION

Metallic soaps are defined as the reaction products of alkaline, alkaline earth, or transition metals with saturated, unsaturated straight chain or branched aliphatic carboxylic acids with 8-22 carbon atoms. They are commercially important compounds and find applications in areas such as driers in paints or inks, components of greases, stabilizers for plastics, fungicides, catalysts, waterproofing agents, fuel additives and etc. (Elvers et al., 1990). The soaps of di- and trivalent metal ions are those most commonly used. In addition to above applications mentioned, a number of other uses of polyvalent metal soaps have been suggested. Current interest in low dimensional compounds has led to a number of investigations on the potential application of metal soaps in this area, particularly as Langmuir-Blodgett (LB) multilayers.

The physicochemical properties of metallic soaps are determined by the nature of the metal ion and the organic acid. They are generally water insoluble, but may be soluble in various organic solvents in which they commonly exhibit Krafft-type behaviour, with solubilities increasing dramatically above a particular temperature (Akanni et al., 1992). The metallic soaps of saturated straight chain carboxylic acids are solids and either have a sharp melting point or melting range or carbonize heating without melting. Unsaturated fatty acids and branched synthetic acids form metallic soaps with plastic properties. They are, therefore, usually produced and used in solutions.

Metallic soaps are manufactured by using one of the following three processes: Double decomposition (precipitation) process, direct reaction of carboxylic acids with metal compounds (fusion) process and direct reaction of fatty acid with metals (DMR). Since some of the metals give no reaction with organic acids, first two processes are generally preferred in the production of pure compounds (Akanni et al., 1992).

Zinc stearate ($ZnSt_2$) is one of typical ionic surfactant of metallic soaps. Precipitation and fusion processes are widely used in $ZnSt_2$ production. Product purity has been a major concern in most of the $ZnSt_2$ applications such as PVC stabilization, coating of textile goods, an additive in cosmetic products and etc. The use of

commercial Ca/Zn stearates in PVC stabilization accelerates the PVC degradation (Gökçel et al., 1999). Due to the lack of studies for pure $ZnSt_2$ production and a few detailed structural study of $ZnSt_2$, production of pure $ZnSt_2$ by using fusion and precipitation processes and comparison of the processes based on product purity have become necessary.

In this study, our objective was to produce $ZnSt_2$ with high purity using precipitation process, fusion process and modified fusion process. The raw materials and produced $ZnSt_2$ samples were characterized by different techniques. A comparison between three processes has been made by taking account the separation of unreacted raw materials and formed by products. Reaction parameters such as reaction temperature, mixing rate, and raw materials ratios were investigated to attain high product purity.

CHAPTER II

METALLIC SOAPS

Metallic soaps are defined as the reaction products of saturated or unsaturated fatty acids (carboxylic acids) with alkaline, alkaline earth or transition metals. As an organic acid source, both natural and synthetic carboxylic acids are used for various products. Metallic soaps are industrially important compounds and find applications in wide spectrum including as waterproofing agents, thickening and suspending agents and as lubricants; in powder metallurgy, as mold release agents, flattening agents, fillers, antifoaming agents, and driers in paints, inks and in tablet manufacture (Blachford, 1982).

2.1. Types of Metallic Soaps

Metals (M) and carboxylic acids (R-COOH) can form the following metallic soaps depending on their valance and properties.

Neutral Soaps:

$R\text{-}COOM_I$

$(R\text{-}COO)_2M_{II}$

$(R\text{-}COO)_3M_{III}$

Acid Soaps:

$(R\text{-}COO)_2M_{II}. R\text{-}COOH$

$(R\text{-}COO)_3M_{III}. R\text{-}COOH$

Acid soaps contain bound free organic acid that can be removed by extraction.

Basic Soaps:

$(R\text{-}COO)_2M_{II}.(MO)_X$ x=1-2
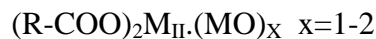
Complex metal oxides can also be present in the form of metal hydroxides or as mixture of metal oxides and hydroxides.

Mixed Soaps:

$(R\text{-}COO)(R'\text{-}COO)M_{II}$
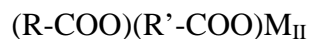
Mixed soaps consist of mixed crystals or mechanically produced mixtures.

Complex Soaps:

Lead can form complex-basic salts:

$(PbO)_X.PbSO_4.[(R\text{-}COO)_2Pb]_X$
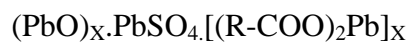
Other inorganic anions can also be present instead of sulfate. A list of industrially important of metallic soaps is given in Table 2.1. (Elvers, et al., 1990).

Table 2.1. Metallic soaps

Element	Setarate	12.Hydroxystearate	Laurate	Oleate	Naphthanate	2Ethylhexanoate
Ag	+	+	+	+	+	
Al	+	-	+	+	+	+
Ba	+	+	+	-	+	+
Be	+	-	+	-	-	-
Bi	+	-	-	+	-	+
Ca	+	-	+	-	+	+
Cd	+	+	+	+	+	+
Ce	+	-	-	-	+	-
Co	+	-	-	+	+	+
Cr	+	-	-	-	+	+
Cu	+	-	-	+	+	+
Fe	+	-	-	+	+	+
Hg	+	-	+	+	+	-
Li	+	+	-	-	-	-
Mg	+	-	+	+	+	+
Mn	+	-	-	+	+	+
Ni	+	-	-	+	+	+
Pb	+	-	-	+	+	+
Sb		-	-	+	-	-
Sn	+	-	-	+	+	+
Sr	+	-	-	-	+	-
Th	+					
Ti	+					
U	+			+		
V	+				+	
Zn	+	+	+	+	+	+
Zr	+				+	+

(+: formed metallic soaps, -: no information about these metallic soaps)

2.2.   Raw Materials for Metallic Soaps

A monobasic carboxylic acids with 6-30 carbon atoms and metals from 1A, 2A and transition metals are generally employed in metallic soap synthesis. The selection of fatty acid and metal depends on the desired product properties. The mostly used metallic soaps and their constituents are given Table 2.1.

The fatty acids of common triglycerides are long, straight chain carboxylic acids. Most fatty acids contain even numbers of carbon atoms, because they are derived from two carbon acetic acid units. Some of the common fatty acids are saturated, while others have one or more elements of unsaturation; generally carbon-carbon double bonds. The structures of some common fatty acids derived from fats and oils are shown in Table 2.2.

Table 2.2. Structures and melting points of some common fatty acids

Name	Carbons	Structure	Melting point ($^\bullet C$)
Lauric acid	12	COOH	44
Myristic acid	14	COOH	59
Palmitic acid	16	COOH	64
Stearic acid	18	COOH	70
Oleic acid	18	COOH	4
Linoleic acid	18	COOH	-5

As can be seen from Table 2.2. the saturated fatty acids have melting points that increase gradually with their molecular weights. The presence of a cis double bond in the fatty acid lowers its melting point. For example, the C18 saturated fatty acid (stearic acid) has a melting point of 70°C while the C18 with a cis double bond (oleic acid) has a melting point of 4°C. This lowering of the melting point results from the unsaturated acid's "kink" at the position of the double bond (Figure 2.1.). The kinked molecules can not pack as tightly together in the solid as the uniform zigzag chains of the saturated acids (Wade, 1987).

Figure 2.1. The presence of the cis double bond in oleic acid lowers the melting point by 66°C.

Alkaline, alkaline earth and transition metals or their compounds e.g., oxides, hydroxides, carbonates and sulfates, chlorides are used in metallic soaps' production (Scott et al., 1974). Sodium and potassium are out of the above classification since the synthesized soaps by these metals are traditional soaps, which exhibit different properties than metallic soaps. For instance, while sodium and potassium soaps are soluble in water, metallic soaps are sparingly soluble or insoluble. The mostly used metallic soaps are given Table 2.1. The selection of metal ion source and fatty acid depends on process type.

2.3.   Composition and Properties of Metallic Soaps

Metallic soaps are composed of a metal and acid portion supplied as solutions in solvent or oil. The general formula for a metal soap is $(RCOO)_xM$. In the case of neutral soaps, x equals the valance of the metal M. Acid soaps contain free acid (positive acid number) whereas neutral (normal) soaps contain no free acid (zero acid number); that is, the ratio of acid equivalents to metal equivalents is greater than one in the acid soap and equal to one in neutral soap. Basic soap is characterised by a higher metal to acid equivalent ratio than the normal metallic soap. Particular properties are obtained by adjusting the basicity.

The nature of the organic acid, the type of metal and its concentration, the presence of solvent and additives, and production technique determine properties of metallic soap. Higher melting points are characteristics of soaps synthesised of high molecular weight, straight chain, saturated fatty acids. Branched-chain unsaturated fatty acids form soaps with lower melting points (Howe-Grant, 1990). Table 2.3. lists the properties of some solid metal soaps.

The most important property of metallic soaps is that they are sparingly soluble or insoluble in water. Based on this property, they are widely used in waterproofing materials formulation (Liao et al., 1997).

6

Table 2.3. Properties of solid metallic soaps

Compound	Total ash	Free fatty acid	Sp. gr.	Mp., °C	Colour
Al	5.5-16.0	3.0-3.5	1.01	110-150	white
Ba	19-28	0.5-1.0	1.23	Decomposes	white
Ca	8.8-10.6	0.5	1.12	145-160	white
Mg	8.0	0.5	1.03	145	white
Ni	9.4	5.2	1.13	180	green
Zn	13.5-17.7	0.5-0.9	1.09-1.11	120	white

When metallic soaps are employed as a powdered material as in most of the applications, they are, therefore, produced in powder form with particle size smaller than 44 μm (Howe-Grant, 1990). They are mostly white colored powder materials. Metal content of the soap is another important property, which is determined by titration and atomic absorption spectrophotometry.

Lastly, free fatty acid (FFA) value has commercially important property which shows the unreacted carboxylic acid amount in the product. For the determination of FFA, synthesized soap is mixed with ethanol, which extracts the unreacted fatty acid from metallic soap. After a certain time of stirring, the mixture has two phase systems, one phase consisted of the solid metallic soap and the other phase consisted of liquid ethanol having dissolved unreacted fatty acid. The liquid ethanol phase is separated from the solid metal soap phase by filtration. After filtration, the free fatty acid content is determined by titrating the ethanol phase to a pH of about 7 with 0.05 N sodium hydroxide (Lally and Cunder, 1969).

2.4. Analysis of Metallic Soaps

Metallic soaps can be characterized by using a number of techniques and equipments. The phase of metallic soap depends on the acid source used that is the length of the alkyl chain and the presence of double bond in the chain. For solid metallic soaps, metal content, total ash, free fatty acid, melting point, structural components, moisture content and particle size must be determined for industrial applications.

Metal content of the soap can be determined by one of the usual analytical methods after acid decomposition of the metallic soap in an aqueous extract or it can be determined directly by using atomic absorption spectroscopy. For the determination of the *total ash* value, the soap is preheated carefully in an incinerator and then heated slowly to 800 or 1000°C in a muffle furnace as soon as the organic part has decomposed. After being cooled in a desiccators the ash is determined by back weighing. Thermal gravimetric analysis is also used in *total ash* value determination. *Free fatty acid* in the product is extracted by using acetone or ethanol. The extract is then titrated by using alcoholic potassium hydroxide in the presence of indicator. *Melting point* of the soap is characteristically important and determined by using differential scanning calorimetry (DSC) or one of the commercial melting point apparatus. Even though metallic soaps are generally hydrophobic substances they may contain moisture due to the their porous structures. *Moisture content* of the product therefore needs to be calculated. The sample is weighed before and after heating at 110°C for 2 h in dry oven. *Particle size* of final product becomes mostly important according to the application area of the product. So it must be determined by using well-known sieving method or microscopy (Elvers, 1990).

Thermal decomposition of the calcium salts of several carboxylic acids were studied by using thermogravimetric analysis (TGA) and differential scanning calorimetry (DSC) (Valor et. al., 2002). Calcium salts of propionic, butyric, valeric, caproic, hetanoic, caprylic, decanoic, lauric, and tridecanoic acids (3,4,5,6,7,8, 10,12, and 13 carbon atoms in the chain respectively) were synthesized by mixing calcium hydroxide powder with an excess liquid acid in aqueous media at 85°C. The resultant insoluble mixture was washed in distilled water, filtered and dried in air at room temperature. From the TGA curves of the nine calcium carboxylate samples as shown in Figure 2.2. the transition occurred at about 110-120°C was attributed to the loss of the water of crystallization. In this figure, increasing aliphatic chain length of the salts decreased the decomposition temperature exponentially. SEM images of calcium caprylate are given in Figure 2.3. Microstructure of the calcium caprylate was observed as elongated plates of size that varied from one sample to another. A platelet shape of crystallites was evident and platelet faces were parallel to the (100) plane.
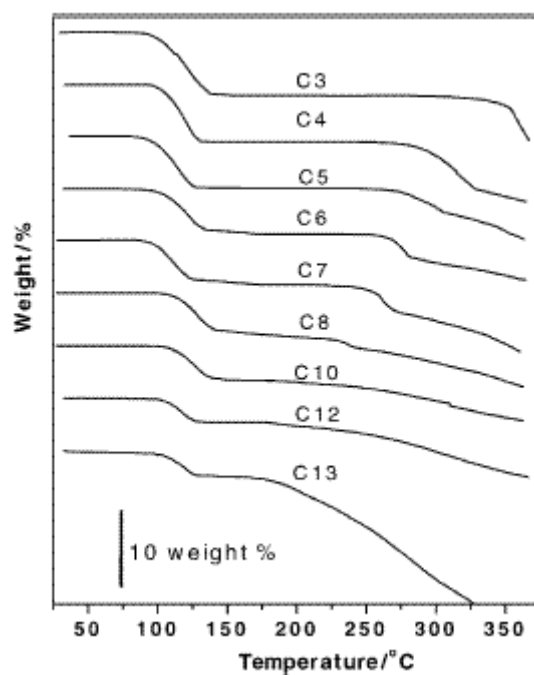
Figure 2.2. Thermograms for the decomposition of nine calcium carboxylates
(Valor et. al., 2002).
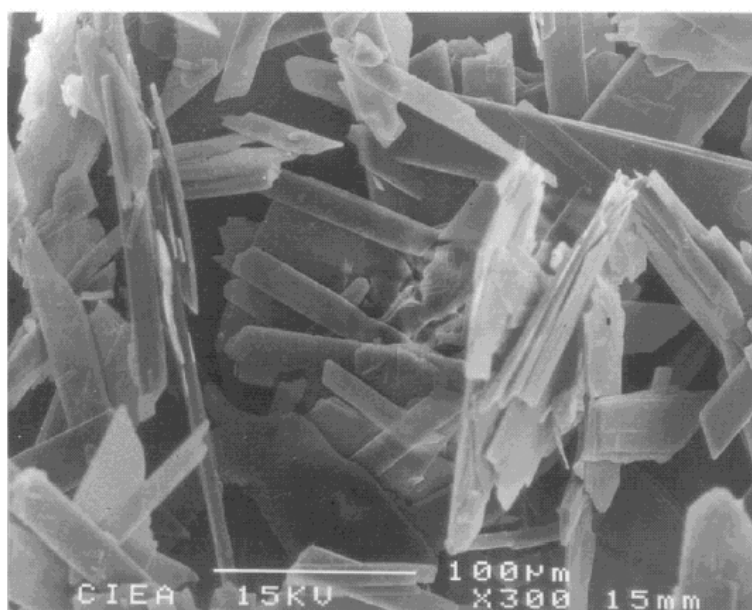
Figure 2.3. SEM microgram of calcium caprylate (Valor et. al., 2002).

Lee et al., (2001) examined the structure and phase behavior of nonmolecularly layered silver stearate by means of temperature dependent diffuse reflectance infrared transform (DRIFT) spectroscopy. Silver nitrate was synthesized by reaction of stearic acid and silver nitrate in aqueous phase. They calculated the interlayer spacing and d

values from X-Ray pattern of silver stearate, which is shown in Figure 2.4. The overall structure of the silver stearate proposed as in Figure 2.5.

2θ	$d(\text{Å})$	order (0k0)	interlayer spacing (Å)
5.26	16.80	3	50.4
7.1	12.45	4	49.8
8.94	9.89	5	49.45
10.76	8.22	6	49.32
12.62	7.01	7	49.07
14.48	6.12	8	48.96
16.16	5.48	9	49.32

$[Ag(O_2C(CH_2)_{16}CH_3)]_2$
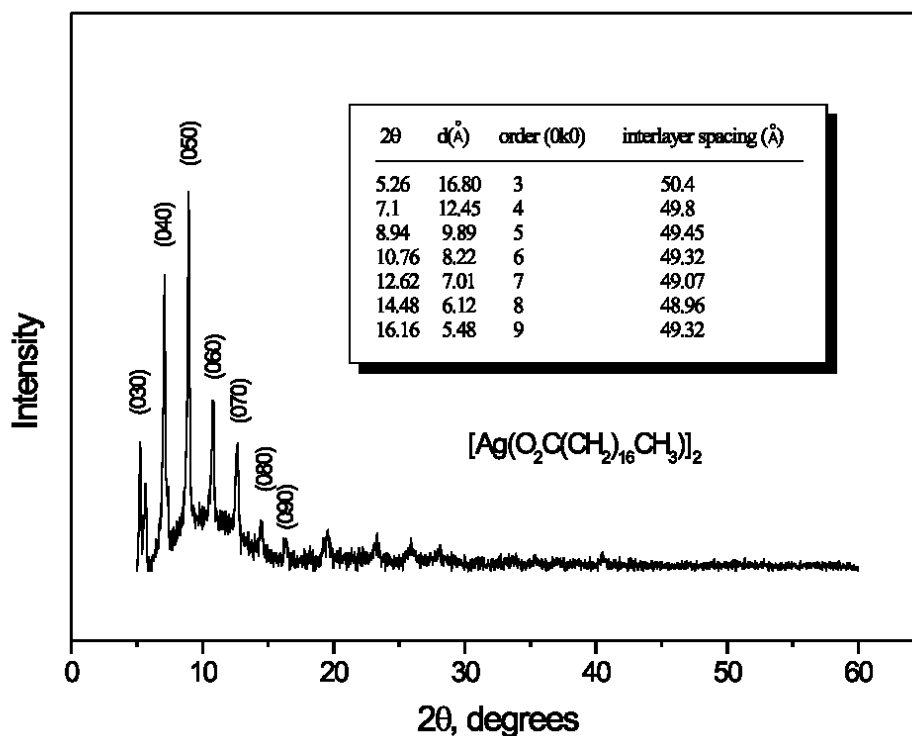
Figure 2.4. XRD Pattern of Silver Stearate (Lee et al., 2001).
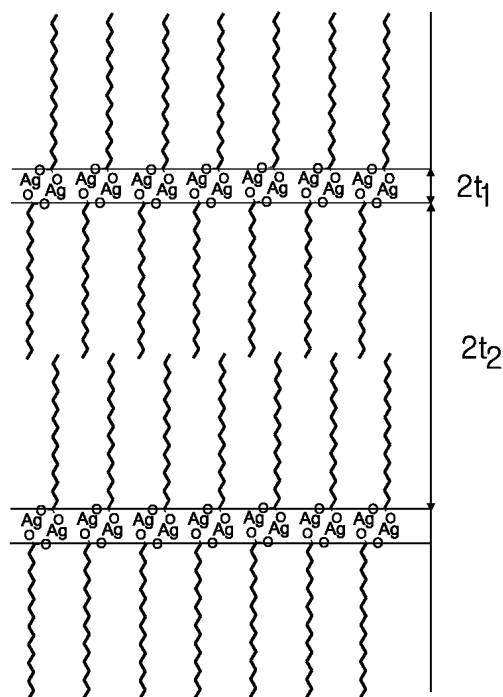
Figure 2.5. Structure of Silver Stearate (Lee et al., 2001).

10

CHAPTER III

PRODUCTION METHODS OF METALLIC SOAPS

Metallic soaps of the higher fatty acids, the most common of which are the metallic stearates are prepared mainly by three types of processes: Direct reaction with metal compounds (Fusion), double decomposition (precipitation), and direct metal reaction (DMR) process. The selection of a process and a solvent depends on the metal ion source, the desired final form of the product, acceptable purity, raw material availability and finally the fixed and overall manufacturing cost.

The most common soaps are those prepared from magnesium, calcium, and zinc and have found wide application in commerce as waterproofing agents, thickening and suspension agents, lubricating and anticaking agents. Calcium and zinc stearate are used together as stabilizing agents for plastics, particularly polyvinyl chloride (Scott et al., 1974).

3.1. Direct Reaction with Metal Compounds (Fusion) Process

In fusion process, a metal oxide, carbonate or hydroxide reacts with a carboxylic acid at temperatures between 100°C and 240°C. The formed by-product water is split out and resulting metal soap is solubilized in a hydrocarbon solvent since the metallic soaps themselves are generally hard, glassy, and difficult to grind (Howe-Grant, 1990). The postulated reactions for fusion process are as follows, where M is a bivalent metal and R is the alkyl chain.

$$MO + 2RCOOH \longrightarrow M(OOCR)_2 + H_2O \qquad\qquad \text{-3.1-}$$

$$M(OH)_2 + 2RCOOH \longrightarrow M(OOCR)_2 + 2H_2O \qquad\qquad \text{-3.2-}$$

$$MCO_3 + 2RCOOH \longrightarrow M(OOCR)_2 + H_2O + CO_2 \qquad\qquad \text{-3.3-}$$
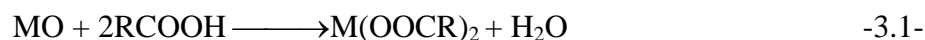
Fusion process can be further classified into three methods; these are melt process, reaction in aqueous phase and reaction in solvents.

3.1.1. Melt Process

In the melt process, metal oxides, metal hydroxides, or metal salts of volatile acids are fed into a stirred melt of organic acid at elevated temperature up to 230°C. The rate of addition should be adapted to the reaction rate to prevent foaming caused by evaporation of water or volatile acids. The reaction requires from 3 to 5 hours for completion (Scott et al., 1974). That long reaction time increases the production cost since during reaction, mixture must be maintained at the temperature higher than the melting point of formed metallic soap. With unreactive metal compounds, delay can occur in the initial phase. In order to initiate the reaction small quantities of water or, for metal oxides, volatile acids such as acetic acid are often added into mixture.

The melt process is suitable for metallic soaps with melting points below 140°C, which produce relatively nonviscous melts. Another important property of the metallic soaps is a colour of the final product. In this method, product turns into yellowish colour because of the high reaction temperature and the long reaction time. These are generally metallic soaps with sharp melting ranges such as lead, zinc, or cadmium stearate. Alkaline-earth stearates are not suited to this process because they have high melting points and exhibit rubber elastic properties in the melt. Since alkaline-earth metallic soaps are often used in combination with low melting metallic soaps are often used in combination with low melting metallic soaps (e.g., as polyvinyl chloride (PVC) stabilizers in the combinations barium-cadmium, barium-zinc, or calcium-zinc, or calcium-lead, a low-melting acidic metallic soap is first produced in the melt.) The high–melting is then formed in the melt of the low-melting one.

Hayasaka et al., (1983) studied a process for manufacturing of various metallic soaps such as lead, calcium, cadmium, magnesium, zinc and barium stearate. Metal oxide, hydroxide or hydrate was mixed with stearic acid under homogeneous agitation. The resultant mixture was agitated within a temperature range of 30°C lower than the melting point of the stearic acid to a temperature just under the melting point of metallic soap to convert part of mechanical energy generated into thermal energy and to obtain reaction between the powders. The mixture was further agitated within temperature range from melting point of stearic acid to a temperature just under the melting point of the metallic soap so as to remove the water under suction, produced by the reaction, while maintaining the mixture in the form of powder.

Conversions in these reactions were calculated analytically by performing simple titration procedure of stearic acid with KOH. X-ray diffraction was used to determine whether the product is formed or not. The proceeding of reactions was also controlled by X-ray analysis. The X-ray diffraction diagrams of lead stearate with elapsing time taken by Hayasaka et al. (1983), are shown in Figure 3.1. through Figure 3.3. The figures are drawn intensity (I) versus 2θ values.
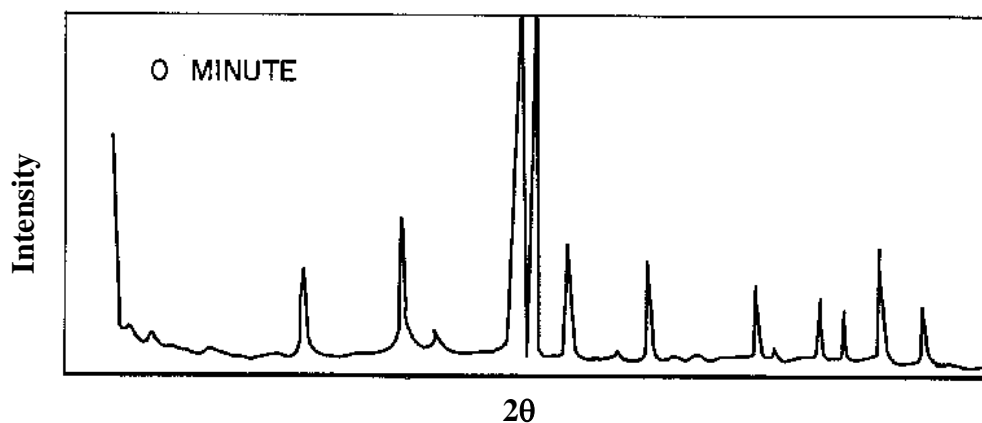
Figure 3.1. X-ray diffraction diagram of lead stearate at the initiation of reaction.
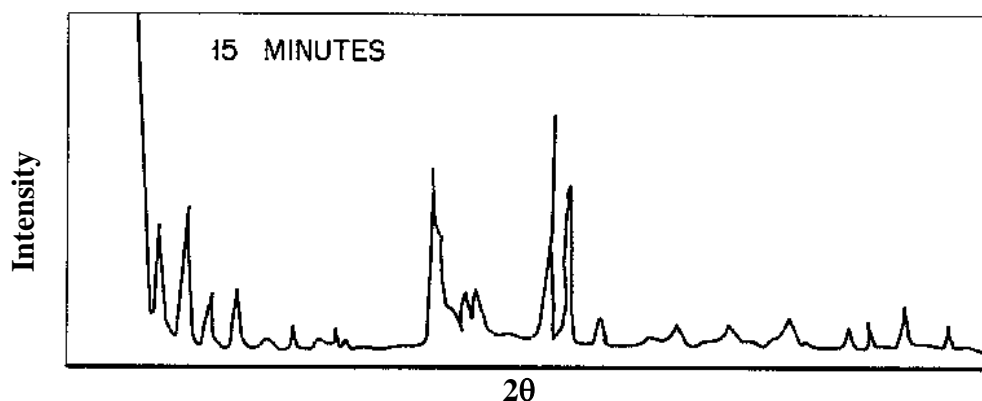
Figure 3.2. X-ray diffraction diagram of lead stearate at the 15 minute of reaction.
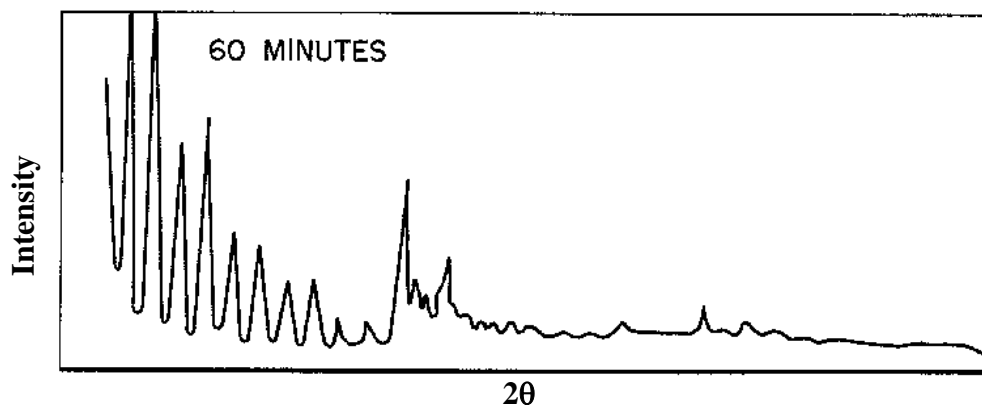
Figure 3.3. X-ray diffraction diagram of lead stearate at the 60 minute of reaction.

The reaction times used changes from 70 min. to 3 hours. They proved that the addition of pure acetic acid as a catalyst decreased the reaction time 60 min. in the calcium stearate production. The amount of the acetic acid was of 1% by weight based on the weight of the stearic acid. The conversion was 99.32 %. In this process, agitation of raw materials becomes difficult as the product is formed since the viscosity of the mixture increases. Increase in viscosity requires powerful mechanical mixing and results in high-energy consumption. Another important concern is the control of temperature, which must be lower than the melting point of the formed metallic soap. Ultimately, long reaction times up to 3 hours causes high energy consumption to maintain the mixture at the desired value of temperature.

3.1.2. Reaction in the Aqueous Phase

In aqueous phase reaction, metal oxides or hydroxides react in the presence of catalysts such as amine, sparingly soluble alcohols, or other wetting agents. The processes are applicable only to solid metallic soaps (e.g., barium, magnesium, zinc, lead, and calcium stearates).

Kato (2000), studied a process for preparing an aqueous dispersion of a higher fatty acid zinc salt which comprises the addition of a molten higher fatty acid to an aqueous dispersion of zinc oxide. Reaction takes place between the higher fatty acid and zinc oxide in the presence of a surfactant or water-soluble polyvinyl alcohol. The aqueous dispersion is maintained at a temperature that is higher than the melting point of the higher fatty acid used. The effect of surfactant type was examined on reaction conversion. The most effective catalyst was polyvinyl alcohol (PVA). The results are shown in Table 3.1.

Table 3.1. Effect of surfactant on conversion (Kato, 2000)

Surfactant name	Type	Amount (g)	Conversion (%)
Pentaethylenehexamine	Cationic	2.4	95.7
Aminoethylethanolamine	Cationic	2.8	96.1
Dodecyltrimethyl ammoniumchloride	Cationic	3.0	99.1
Ethylene oxide+lauryl alcohol	Nonionic	4.0	99
Sodium dodecyl sulfate	Anionic	2.0	97.3
Polyvinylalcohol	-	2.35	99.3

In this study, the reaction mixture was stirred for three hours while it was maintained at a temperature of 60°C. That long reaction time and presence of surfactant in the final product increases production cost and decreases product quality respectively. Another important concern is the separation of zinc oxide from the product since it was used in excess for the completion of reaction based on stearic acid.

A granular metallic soap production was investigated by Odashima and Kondo (1982). Cobalt stearate and zinc stearate were manufactured by reacting a water insoluble metal carbonate and fatty acid in a water dispersed state. The reaction was carried out at a temperature that is higher than the melting point of stearic acid, and below the melting point of the synthesized metallic soap. Stearic acid and zinc or cobalt carbonates were used in stoichiometric amounts. The quantity of water for dispersion phase was 20 times as much as the weight of the metal carbonate. The synthesized cobalt stearate and zinc stearate with a grain diameter of about 1 mm had melting points 90°C and 120°C respectively. The yields relative to the used cobalt and zinc carbonate were 97% and 98.9% respectively. Zinc carbonate was synthesized by the reaction of zinc chloride and sodium carbonate in chemical equivalents in aqueous phase. The melted stearic acid was added into liquid phase that contained dispersed zinc carbonate and other ionic matters. To increase the purity of zinc stearate at the end of process, mixture was washed with 1000 ml of water for three times. The quantity of water used was enormous and resulted in a new separation process of washing water. The resultant particle diameter of 1 mm is usually not suitable for many of the industrial applications and requires further grinding operation.

3.1.3. Reaction in Solvents

Reaction in solvents is preferred if the direct melt process is impossible or gives low quality products, or if the metallic soaps are to be used in a solution. This process mainly produces dryers and liquid PVC stabilizers that are based on branched-chain aliphatic carboxylic acids and naphthenic acids. The solvent (e.g., solvent naphtha or white spirits) also acts as an entrainer for removing reaction water by azeotropic distillation.

For solid metallic soaps the solvents can be replaced by organic compounds such as alkanes or fatty alcohols, which are solid at room temperature and can not be

saponified by metal oxides. The reaction medium can not be removed and remains in the final product, which may, for example, be used as a lubricant for plastics.

Martinus et al. (1982) examined the production of highly basic alkaline earth metal salts of organic acid in the presence of aromatic hydrocarbon and alcohol. An alkaline earth metal, calcium hydroxide, reacted with carbon dioxide in the presence of methanol and xylene. The reaction mixture thus obtained was mixed with salt of alkyl salicylic acid. The product obtained by mixing the salt of organic acid and the complex was then subjected to a further reaction with carbon dioxide. The carbonation temperature was between 15°C and 35°C. The reaction mixture containing the highly basic alkaline earth metal was centrifuged to remove the bulk of the solids. The resulting solution was then subjected to a liquid phase separation. Upper phase alcohol was removed and lower phase was mixed with lubricating oil to remove the used solvent. Finally, by the help of well-known distillation or stripping, volatile solvent was removed and the product was obtained.

They found that the use of alcohol, which contained 3% (v/v) of water, decreased the calcium hydroxide utilisation. The carbonisation temperature had to be lower than 30°C in order to prevent the vaporisation of solvent. The reaction between carbonated metal hydroxide and organic acid salt was carried out at a temperature below 50°C.

The metallic soaps formed by this method are synthesised in solvent or lubricating oil since they are glassy and hard materials. The use of solvent decreases the reaction temperature, thus energy consumption. However, the removal of solvent requires extra separation process and increases the production cost. Finally, if the metallic soap (e.g., calcium stearate and lithium stearate) is used in the composition of greases, this process might be advantageous.

3.2.   Double Decomposition (Precipitation) Process

The most important commercial process for the manufacture of metallic soaps is the precipitation process, which in most cases yields a product that is light fluffy powder having high degree of uniformity.

The raw materials used in the precipitation process are an alkali (usually caustic soda), an inorganic salt or hydroxide, and an organic acid or fat. The metal compound must be water-soluble, and includes sulfates, chlorides, acetates and carbonates, (e.g., aluminum sulfate, zinc sulfate, calcium chloride, and lithium hydroxide). The inorganic

salt must be examined for purity to guarantee against undesirable cations in the final soap. The organic materials are usually commercial fatty acids or sometimes natural glycerides. Acid number, iodine number, and titer must be obtained on all acids used, not only to safeguard against contamination but also as a necessary step in determining the relative amounts of raw materials needed for the production of a metallic soap with desired specifications (Howe-Grant, 1990).

Precipitation process consists of two main reaction steps. In the first step, the saponification of a glyceride or neutralisation of a fatty acid with caustic soda forms sodium or other alkali soaps. In the second step, the alkali soap is treated with aqueous solution of metal salt to precipitate the metallic soap, the soluble alkali salt remaining in the mother liquor. The soap solutions can also be added to the metal salt solution, or both solutions can be run simultaneously into a separate precipitation vessel. For sparingly soluble alkali soaps, alkaline solutions or alcohol-water mixture are used as reaction medium. Plastic metallic soaps are precipitated in the presence of a water-immiscible solvent, which absorbs the metallic soaps formed. The two steps might be represented as follows, where M is a bivalent metal and R is an alkyl radical usually a mixture, as in commercial stearic acid.

$$C_3H_5(O_2CR)_3 + 3NaOH \longrightarrow 3RCO_2Na + C_2H_5(OH)_3 \qquad \text{-3.4-}$$

$$RCOOH + NaOH \rightleftharpoons RCOONa + H_2O \qquad \text{-3.5-}$$

$$2\ RCOONa + MSO_4 \longrightarrow M(RCOO)_2 + Na_2SO_4 \qquad \text{-3.6-}$$
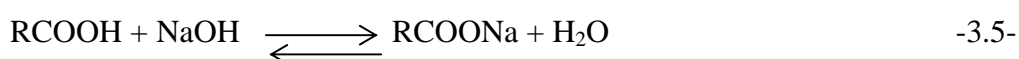
Reaction 3.4. is carried out by boiling the fat and alkali together with open steam. This reaction requires an induction period due to the immiscibility of the aqueous alkali and fat (oil) phases. Following the induction period, the reaction accelerates as the solubility of the fat in the alkali containing aqueous phase is increased by the formation of the soap. The manufacture of soap is often carried out by employing the niger of preformed soap from a previous batch. Addition of alkali and fat produces an exothermic reaction (by 65 cal/kg of fat saponified), which must be carefully controlled to avoid the boiling out of the mixture (Hui, 1996). This process is not used in the production of commercial soaps. Fats and oil are converted into fatty acids by steam assisted hydrolysis.

The reaction shown by equation 3.5. is an equilibrium reaction and carried out at the temperature of 100°C. In order to increase the reaction conversion, sodium salt is added in aqueous solution. The removal of the produced water with respect to reaction rate will also increase the fatty acid conversion and prevent the back reaction. The final step is the metallic soap synthesis which takes place by the addition of desired metal salt such, zinc sulfate, chloride, nitrate and carbonate.

This reaction is carried out at a temperature, in which solubility of sodium stearate is adequate. The temperature-composition phase diagram of water soluble surfactants for instance, sodium stearate, is characterised by a solubility boundary known as the Krafft boundary (Mul et al., 2000). Along the Krafft boundary, the surfactant solubility increases slowly as the temperature is increased, until a certain temperature range is reached. Above this temperature range the Krafft boundary forms a plateau, indicating a rapid solubility increase. The homogenous phase above the Krafft plateau is a micellar solution at low surfactant concentrations. At high concentrations, the Krafft boundary ends and hexagonal or lamellar liquid crystals may exist.

The phase behaviour of the pure sodium soaps such as, sodium stearate (NaSt), arachidate (NaAr), and behenate (NaBe) at high water content was determined by measurement of the soap solubility in aqueous solutions as a function of temperature (Mul et al., 2000). The Krafft boundary has its characteristic knee and plateau form as shown in Figure 3.4. for NaSt, NaAr, and NaBe.
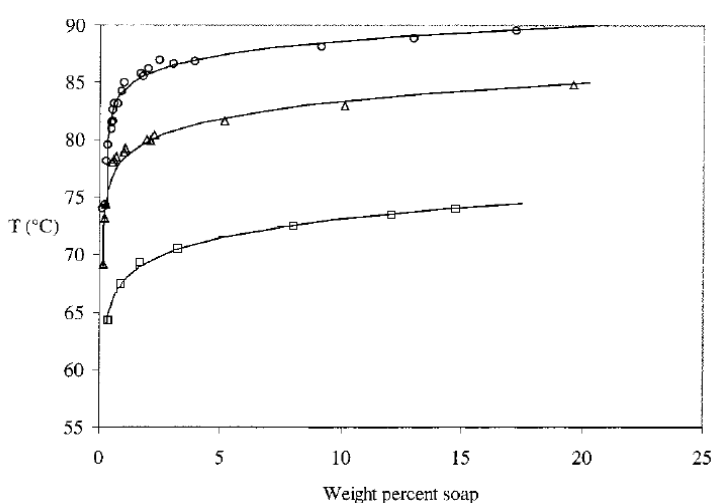
Figure 3.4. Krafft boundaries of long chain soaps in aqueous solution, Data NaSt (□), NaAr (Δ), NaBe (O) (Mul et al., 2000).

As a single characteristic of the Krafft boundary, a Krafft point can be defined as the temperature at which the solubility of the surfactant becomes equal to the cmc. The Krafft point increases linearly with the alkyl chain length of the soap. Below the Krafft point, the solubility increase with temperature is slow. After the knee in the solubility is reached, the solubility increases more rapidly, until a liquid crystalline region in the phase diagram is encountered.

The solubility properties of the alkali soap need to be known in the production of metallic soaps by precipitation process. The Krafft point for sodium soap is about 68°C. It is clear in Figure 3.4. that after a certain temperature, solubility of soap increases rapidly. However, at high concentrations, soap molecules form micelles in the solution. Micelles are aggregates of surfactant molecules. They form in surfactant solutions at or above a rather narrow range of concentration called critical micelle concentration (cmc) (Cutler and Davis, 1972). (Data for the critical micelle concentrations of long chain soaps can be determined by fluorescence microscopy using pyrene as the probe molecules (Mul et al., 2000)).

The temperature dependence of cmc of long chain soaps is shown in Figure 3.5. The cmc decreases rapidly and linearly when temperature increases. Due to this phenomenon, critical micelle concentration of soaps should be examined carefully in the production of metallic soaps.
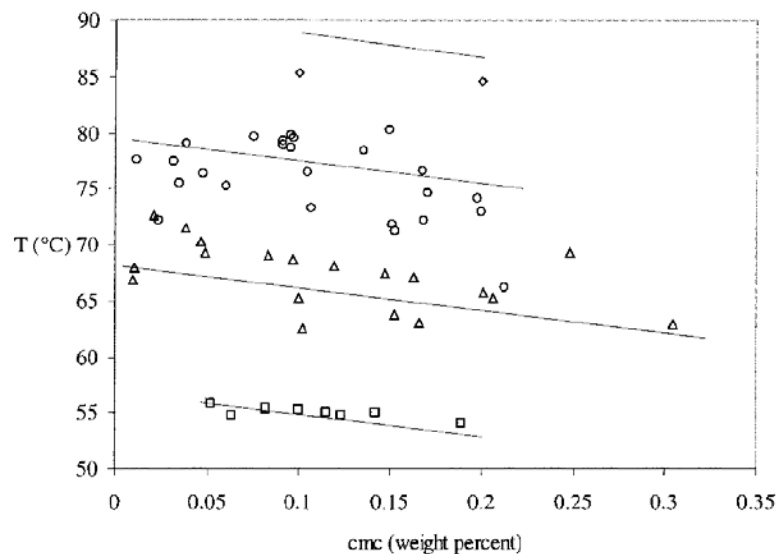
Figure 3.5. Critical micelle concentrations of long chain sodium soaps vs temperature, Data NaPa (□), NaSt (Δ), NaAr (O), NaBe (◊) (Mul et al., 2000).

A continuous process for preparing a metallic soap by double decomposition process was examined by Yoshizawa et al. (1992). In this study, an aqueous solution of an alkali soap and inorganic metal salt solutions were separately fed directly on the surface of the rotating impeller. The reactants were mixed instantaneously and resulting metallic soap slurry was discharged out from the mixer without delay.

The production of calcium stearate and zinc stearate were studied by using sodium soap solution as alkali soap source and calcium chloride and zinc sulfate solutions as metal source. The reaction was carried out at different temperatures ranging from 75°C to 95°C. The inorganic metal salt/alkali soap equivalent ratio used in the reaction was between 0.95 and 1.05. The aqueous slurry was then filtered and washed with water in an amount 5 times the volume of the dry product. The wet cake was dried in a hot air drier set at 105°C.

They showed that the increase in reaction temperature and mixing time increased the average particle size of the product. The results are given in Figure 3.6. The increase in mixing time might produce enough time for the agglomeration of formed molecules therefore, the particle size increased. In this process, the amount of water used in washing process is extremely high, and is not given any results regarding the purity of the product. So the washing process efficiency must be examined for optimum product quality and process conditions.
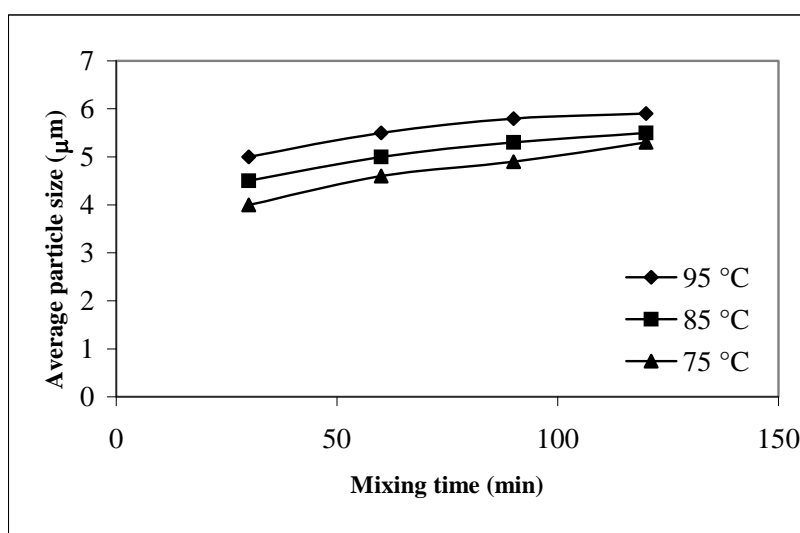
Figure 3.6. The effect of reaction temperature and mixing time on particle size (Yoshizawa et al., 1992).

The preparation of a silver salt of fatty acid which is used in photographic materials was studied by using precipitation process (Simons, 1974). Ammonium and sodium soaps were used as a soap source for the synthesis of silver behenate. Ammonium and sodium soaps were firstly produced by the reaction of behenic acid with ammonia and sodium hydroxide respectively at 85°C. Silver nitrate reacted with one of the above soaps at 25°C to produce silver behenate. The resulting flocculent, white precipitate was filtered and washed three times with water (250 ml portions) and dried.

Examination under an optical microscope showed the particle size to be less than 1 μm, with exception of a few larger particles or aggregates. The silver ion in the filtrate was estimated gravimetrically by precipitation with chloride ion, and showed 11 percent of the silver added was not converted, corresponding to 88 percent conversion of behenic acid to silver behenate. The obtained silver behenate was used in photographic materials, the coatings were smooth and of good quality. Lastly, it was proposed that the precipitation process might be used in the production of light sensitive photographic materials.

The process for preparation of calcium stearate ($CaSt_2$) and zinc stearate ($ZnSt_2$) by saponification of hardened oil was studied by Zhou et al. (2000). The process comprises saponification of hardened oil at 70-80°C for 6 h and synthesis of calcium and zinc soaps. Calcium stearate was synthesized by mixing the sodium stearate (NaSt) with $CaCl_2$ under $NaSt:CaCl_2$ molar ratio 2:1, 2-1.3, adjusting pH to 8.0. The reaction was carried out at 90°C for 1 h. Filtering, washing, and drying operations took place to obtain $CaSt_2$. $ZnSt_2$ was produced by mixing the NaSt with $ZnSO_4$ under $NaSt:ZnSO_4$ molar ratio 2:1.0-1.2. The reaction was carried out at 90°C and pH 7.0 for 1 h. Again filtering, washing, and drying operation were used to obtain $ZnSt_2$. The effect of saponification time, catalyst, and temperature on the saponification rate was discussed.

3.3.   Direct Metal Reaction (DMR)

The DMR process is carried out over a catalyst with fatty acids in a melted state or dissolved in hydrocarbons. The acid reacts directly with the metal, supplied in a finely divided state, producing the metal soap and hydrogen gas. Catalysts include water,

aliphatic alcohols, and low molecular-weight organic acids. The postulated reaction is given in Equation 3.7.

$$2RCOOH + M \longrightarrow M(OOCR)_2 + H_2 \qquad \text{-3.7-}$$
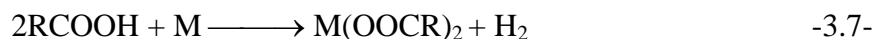
The DMR process has no aqueous effluent, gives high purity products, and is less expensive. However, if hydrogen is produced, it has to be removed carefully and should not reach explosive limits. Not all metals are sufficiently reactive to be suitable for the DMR process. Due to this phenomenon, in most cases it can not be used for the production of metallic soaps.

Basic metallic soaps are prepared by overbasing. That is, a normal metallic soap is treated in the presence of excess metal, metal oxide, hydroxide, or various salts, with reactive species, such as CO_2 or SO_2, capable of forming covalent bonds with the metal. The resulting moiety generally contains metal-oxygen bonds free of carboxyl groups. Overbasing can be carried out simultaneously with the general manufacturing techniques although the fusion and DMR processes are preferred; it can also be used as a post treatment (Howe-Grant, 1990).

Ross and Takacs (2002) investigated surface reactions of ethyl stearate and stearic acid with zinc, manganese and their oxides. The reactions were studied from ambient temperature to 600°C mainly using differential scanning calorimetry and thermogravimetry. The reaction products were analyzed by Fourier transform IR spectroscopy, scanning electron microscopy, and gas chromatography. For zinc and zinc oxide, first reaction zone began at about 160°C and extended to 280-290°C. Water and zinc stearate were formed. From 280 to 375°C zinc stearate was present in the reaction products of acid with both zinc metal and zinc oxide. At 600°C no acid soap was detected. They could not establish a clear relationship for the kinetics of any of reactions over the complete range of temperature because of difficulties in separating the contributions of a number of simultaneous and overlapping heterogeneous and homogeneous processes.

CHAPTER IV

ZINC STEARATE

Zinc stearate ($ZnSt_2$) is one of the typical ionic surfactant of metallic soaps. It is widely used in industry from pharmaceutical products to plastics. Up to today, there is no specific study concerning both production of zinc stearate and characterization of formed product. Two well-known processes, fusion and precipitation processes are used in $ZnSt_2$ production. The parameters of these processes have not been examined for the production of pure product.

The patents from U.S.A., U.K., and J.P. are the only cited studies on metallic soaps. However, the most of these studies do not include quantitative information about the characterization of the product. The main purpose of this study is to determine the parameters of the processes (fusion and precipitation) based on product purity.

4.1. Properties of Zinc Stearate

The general properties of $ZnSt_2$ are tabulated in Table 4.1. The most important and easily determined parameter, which gives qualitative information about the constituents of the product, is the melting point of the product. In early studies, melting point of the $ZnSt_2$ was given in the range of 118-130°C. The reasons for this, might be the purity of the product and different constituents of the acid source for instance, different carbon atoms in the alkyl chain.

Table 4.1. Properties of $ZnSt_2$ (Elvers, 1990)

Appearance	White Powder
Free fatty acid, wt.%	1
Total ash wt.%	13-14
Moisture wt.%	1
Bulk density (kg/dm^3)	0.16
Density (kg/dm^3)	1.1
Melting range (°C)	118-122

Ishioka et al. (2000) investigated the structure and transition behavior of $ZnSt_2$ by infrared and XAFS spectroscopies. From XAFS analysis, structure of $ZnSt_2$ was estimated as follows, the coordination number of the carboxylate group around the zinc atom was evaluated as 4 and the Zn-O distance as 1.95 A°. Based on the infrared spectrum and a normal mode analysis, the conformation of the alkyl chain was confirmed as all trans and sub-cell packing was considered as parallel type, and also coordination form of the carboxylate group was determined as briding bidentate type. It is pointed out that $ZnSt_2$ has a solid-liquid phase transition at 130°C with the increasing temperature. At the transition, the alkyl chains go into liquid like state.

Zinc stearate was synthesized by precipitation process in dry ethanol and water 50:50 % (v). Sodium stearate and zinc chloride solutions were used in the synthesis. The product was filtered and dried at 60°c under vacuum overnight. The purity of $ZnSt_2$ was confirmed by atomic absorption analysis; Zn=10.5 % (w) observed and 10.34 calculated, Na<0.1 % (w).

Fourier transform infrared spectroscopy is generally used to determine the chemical structure or components of the formed products. The infrared absorption spectra of zinc stearate complex prepared from sodium stearate and zinc thiocyanate were investigated by Sakai and Kojima, (2001). Patterns of the bands due to COO^- group of this compound (complex salt) were different from those of the ordinary zinc distearate. The tree COO^- peaks were observed at 1622, 1609, and 1595 cm^{-1}. The characteristic peak of zinc stearate is observed at 1540 cm^{-1} due to the antisymmetrical stretching vibration of the carboxylate group (Baltacıoğlu and Balköse, 1999).

Vibrational spectra and structure of zinc stearate was examined by Ishioka et al. (1998) considering the monoclinic anhydrous zinc acetate crystal in which the acetate groups had bridging bidentate coordination forms. Based on the spectral assignments of zinc acetate. A relation between the coordination structure of the carboxylate groups around the zinc atom and the vibrational frequencies of the carboxylate rocking mode was found. They found that the coordination form of zinc stearate is a bridging bidentate by using the obtained relation.

4.2.   Production of Zinc Stearate

Zinc stearate can be produced by double decomposition, direct reaction in the melt, direct reaction in the aqueous or organic phase and reaction of zinc metal powder with organic acid. In the precipitation process, water-soluble salts such as zinc chloride or sulfate reacts with sodium stearate. Sodium stearate can be produced from the reaction of stearic acid with sodium hydroxide. Raw materials in the fusion process are stearic acid and zinc oxide, hydroxide, carbonate, or acetate (Elvers, 1990).

4.2.1. Fusion Process

A fusion process for the continuous production of a granular metallic soaps was designed by Hudson et al. (1992). Process consists of mixing tank, pump, tubular reactor and spray dryer. The flowsheet of the process is shown in Figure 4.1. Molten fatty acid (stearic acid) and zinc oxide are mixed and fed into tubular reactor by pump.
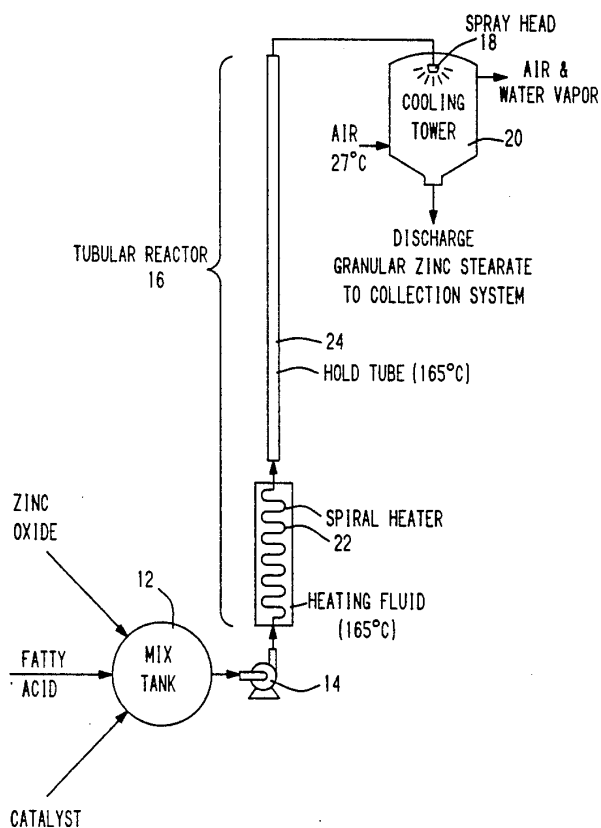
Figure 4.1. Flowsheet of the continuous ZnSt$_2$ production process (Hudson et al., 1992).

Azelaic acid was used as a catalyst in this reaction. It was pointed out in this study the amount of catalyst did not usually exceed about 0.1% by weight, based on the

weight of the metal oxide/fatty acid mixture. The mixture was heated to about 150°C by spiral heater before it entered the reactor. The reaction was conducted under pressure to maintain water generated by the reaction in the liquid state. Flashing of the reaction water in the cooling tower aids in cooling and formation of the fine granules. They examined the effect residence times within heating coil and tubular reactor. The residence times 2.2, 2.4, and 2.6 minutes produced $ZnSt_2$ with free fatty acid value of 0.3%, 0.8% and 0.4% respectively.

Chen et al. (2000) studied the method for direct synthesis of zinc stearate from stearic acid and zinc oxide in presence of catalyst. The optimum process conditions were obtained by orthogonal test and verification test as follows: the reaction time was 90 min, temperature was 135°C, peroxide was used as catalyst with amount of 3 % to the weight of stearic acid. This process had advantages of short flow, simple process, low cost, and no waste water. The quality of zinc stearate product was accorded with the demands of literature reported.

4.2.2. Modified Fusion Process

The synthesis of calcium and zinc stearate from stearic acid and calcium, zinc hydroxides were examined by Wu and Xiao, (1998). These metal oxides were synthesised from the reaction of sodium hydroxide with $CaCl_2$, and $ZnSO_4$ in aqueous medium. The reaction was carried out at 70°C and the reaction time was only 5 min. The liquid solid ratios of feed stocks were 4:1 (calcium stearate), and 3:1 (zinc stearate). They pointed that the yields of products synthesised by this method were greatly increased and consumption of energy and water were obviously decreased compared with traditional double decomposition method.

Production of zinc stearate was studied by Odashima et al. (1984). In their method, an aqueous solution of zinc chloride reacted with sodium carbonate to produce aqueous zinc carbonate dispersion. A granular stearic acid with melting point 56°C was added to this dispersion at 65°C. The reaction was carried out between 65-76°C, under stirring continuously for 40 minute. Zinc stearate generated in the upper layer of the reaction liquid was filtered out. It was washed with water three times, the quantity of water used for each time was 1000 ml. Thereafter, it was dried at 105°C. Finally, obtained granular zinc stearate had melting point of 120°C and average grain diameter

of 1 mm. Zinc content of the product was 10.38 % and the yield relative to the zinc used was 98.9%.

4.2.3. Precipitation Process

The synthesis of Cu(II) hexadecanoate for rubber additive was studied by Jona et al. (2002). They used the precipitation technique to prepare Cu(II) hexadecanoate from the reaction between aqueous solution of sodium salts (pH 7) of hexadecanoic acid (0.02 mol) with an aqueous solution of copper (II) sulfate (0.01 mol) dissolved in water. The fine compound that precipitated was filtered out (ca. 95% yield), washed with cold water and dried at room temperature. The crude product was purified by recrystallization from hot methanol with a yield of 80%. They found analytically that Cu(II) hexadecanoate consists of Cu, 11.00%; C, 66.64%; H, 11.04% by weight. As it is seen from this study, the use of methanol or other solvents for the removal of impurities decreases the product amount and increases the number of utilities in the process such as distillation, evaporation.

4.3. Uses of Zinc Stearate

Zinc stearate has a number of industrial applications particularly in the manufacture of plastics, paints, rubber, and cosmetics. It is used for following purposes:

- in the plastic industry as lubricants, release agents, and components of PVC stabilizers

- in the rubber industry, as release agents for unvulcanized products (wettable zinc sterate soaps and zinc stearate dispersions in water are also used)

- in paints as matting agents and abrasives

- in building protection as waterproofing agents

- for textile and paper industry also as waterproofing agents

- in the cosmetics and pharmaceutical industries as additive to body and face powders

- in paints as components of dryers and as anticaking agents for powdered products

Besides the zinc sterate use in plastic industry as a mold release agent and degradation inhibitor, it's use as a viscosity regulation agent was examined by Antony

and De, (1998). An ionomeric blend of maleated ethylene-propylene diene monomers (mEPDM) and maleated high-density polyethylene (mHDPE) exhibits higher melt viscosity than the corresponding non-ionomeric polyblend. The addition of zinc stearate decreased the melt viscosity of the ionomeric polyblend and caused an increase in tensile strength of the ionomeric polyblend (Antony and De, 1998). Table 4.2. shows the formulation of mixes.

Figure 4.2. shows a plot of log(apparent viscosity) against concentration of zinc stearate. It is evident that at all shear rates; the apparent viscosity decreases with increase in zinc stearate loading. At a particular zinc stearate level the viscosity decreases with increase in shear rates.

Table 4.2. Formulation of mixes (Antony and De, 1998).

Ingredient	Mix Number				
	PM0	PM1	PM2	PM3	PM4
MEDPM	60	60	60	60	60
MHDPE	40	40	40	40	40
ZnO	10	10	10	10	0
Stearic Acid	1	1	1	1	0
Zinc Stearate	0	10	20	30	0
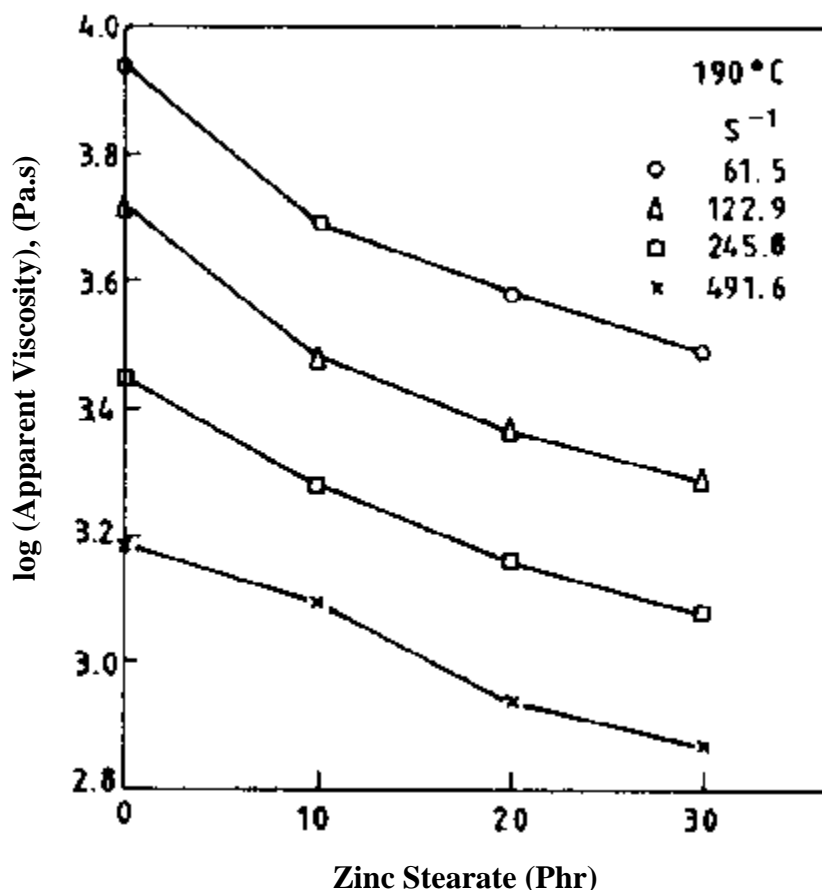
Figure 4.2. Plots of log(apparent viscosity) vs zinc stearate loading at different shear rates (Antony and De, 1998).

The molecular configuration in Langmuir monolayers with metal ions has attracted considerable interest because of many potential applications especially to Langmuir-Blodgett films. Sakai and Umemura (2002) examined the molecular structure in Langmuir monolayers of zinc stearate on a water surface using IR external reflection spectroscopy. They found that the wavenumbers and the absorbances of the antisymmetric and symmetric methylene stretching bands did not change during the monolayer compression, which means that orientational and conformational changes of the hydrocarbon chain did not occur. However, they pointed that wavenumber changes of the antisymmetric and symmetric carboxylate stretching bands were observed during the surface compression. These observations are shown in Figure 4.3.
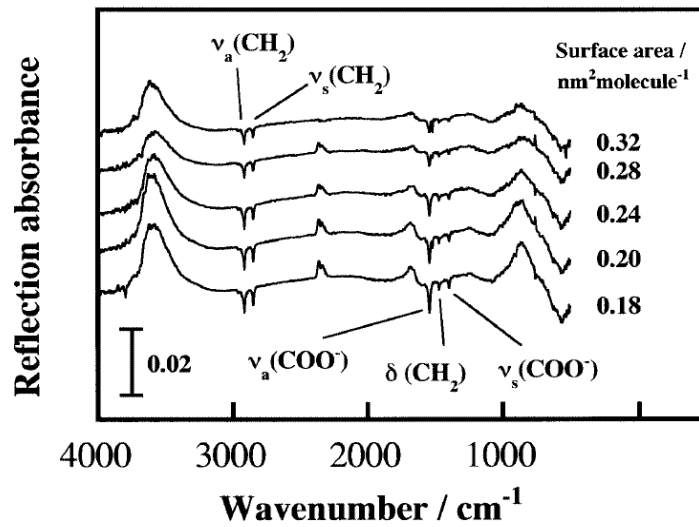
Figure 4.3. Fourier transform IR external reflection spectra of a Langmuir monolayer of zinc stearate measured by an s-polarized beam for various surface areas (Sakai and Umemura, 2002).

The structural changes occur only around the carboxylate group on surface compression of two dimensional crystal of the zinc stearate Langmuir monolayer.

One of the basic criteria influencing the properties of car tyres is the adhesion of the rubberizing compound to the steel cord. In order to achieve a high degree of rubber-to-metal adhesion, it is necessary to use an important group of substances known as adhesion promoters. The most widely used adhesion promoters are the carboxylates of metals such as Cu(II)hexadecanoate and zinc stearate Jona et al. (2001).

CHAPTER V

MATERIALS AND METHODS

Zinc stearate ($ZnSt_2$) samples were synthesized by using different methods, semi-batch precipitation process, batch fusion and modified fusion processes. In these methods different reaction times, reaction temperatures, different amount of raw materials and various mixing rates were studied. The separation of $ZnSt_2$ from reaction media (H_2O, Na_2SO_4) in the precipitation process was performed by the help of conventional filtration. Wet $ZnSt_2$ cake from filtration was washed by different amounts of deionized water with conductivity of 1.2 $\mu S/cm$, (produced by Labconco equipment) and dried in an oven at 100°C under vacuum. To prevent the oxidation oven was heated slowly. The fusion process was performed in a 200cc beaker and waited to the completion of reaction. Detailed description of studies is given below.

5.1.   Production of $ZnSt_2$ by Precipitation Process

The chemicals used for synthesis of $ZnSt_2$ by precipitation process are given in Table 5.1.

Table 5.1. Chemicals used for synthesis of $ZnSt_2$ samples

Chemicals	Origin of chemicals
$ZnSO_4.7H_2O$	99 %, Merck
$C_{17}H_{35}COONa$	Commercial product, Dalan Kimya A.Ş.

A 5.000 g (0.016 mol) sample of sodium stearate was dissolved in 200 ml of deionized water in the reactor at 70°C. NaSt is completely dissolved under this condition. Since the sodium stearate is partly soluble at low temperatures, temperature of dissolution was selected as 70°C. A 2.345 g (0.008 mol) of zinc sulfate heptahydrate was dissolved in 100 ml of deionized water at the 30°C. After sodium stearate was completely dissolved in water, zinc sulfate solution was fed to reactor by peristaltic pump (Masterflex C/L) at the constant flow rate of 13.64 ml.min^{-1}. The reaction temperature was maintained at 70°C by a PID temperature controller (Love Controls

Series2500). The upper limit for reaction temperature is boiling point of water (100°C) under atmospheric pressure. In this semi-batch process, mechanical stirrer at a rate of 500 rpm agitated mixture for 30 min. The postulated reaction is given in the Equation 5.1.

$$2C_{17}H_{35}COONa_{(aq)} + ZnSO_4.7H_2O_{(aq)} \longrightarrow (C_{17}H_{35}COO)_2Zn_{(s)} + Na_2SO_{4(aq)} \quad -5.1-$$
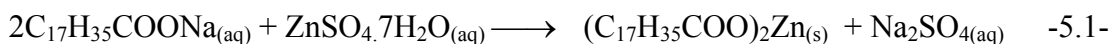
The reagents used in above step were in equivalent amounts. The reaction was repeated for 10% excess sodium stearate and 10% excess zinc sulfate. The schematic representation of reaction set up is given in Figure 5.1. Since the byproduct (Na_2SO_4) is soluble in water the reaction media was filtered by using buchner funnel and flask under 600-mmHg vacuum. To remove the Na_2SO_4 completely, wet $ZnSt_2$ was washed by deionized water of 200 ml for twice. Wet $ZnSt_2$ cake was dried in oven under 600-mmHg vacuum.

1. Stirrer(IkaLabortechnik)
2. Temperature Controller (Love Controls Series2500)
3. Thermocouple
4. Reactor (Stainless Steel, 304)
5. Heating Coil (Waage Electric 350W SF35)
6. Peristaltic Pump (Masterflex C/L)
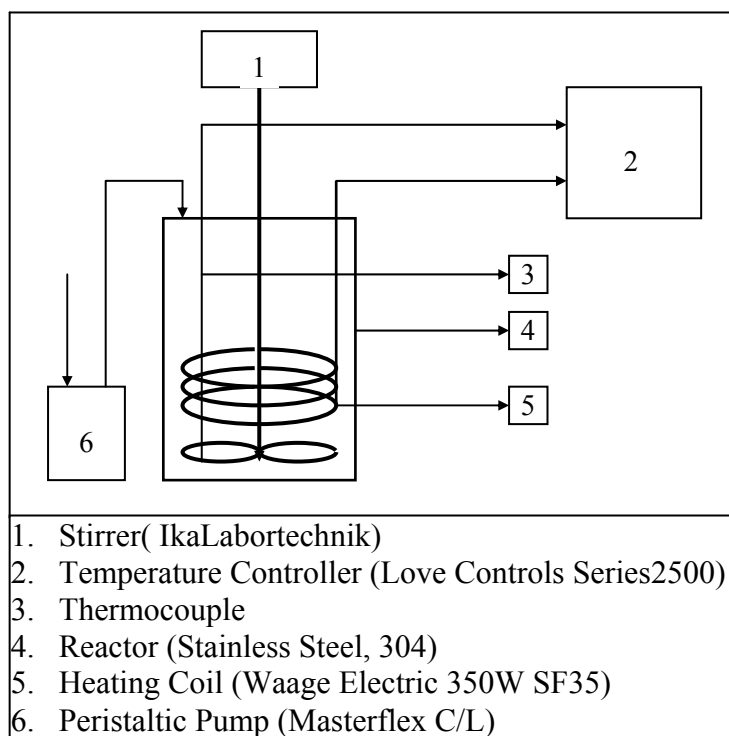
Figure 5.1. Experimental setup.

An experiment with a sudden mixing of reactants adding 100 ml of 2.34% (w) $ZnSO_4$ at 25°C to 200 ml of 2.5% (w) NaSt solution at 70°C. Samples were taken for different time intervals for studying the rate of reaction.

Impeller used in the 100 mm diameter reactor is four-bladed type and its blades are pitched. Blade diameter of the impeller is 50 mm and its width is 8 mm. The photograph of impeller is shown in Figure 5.2. Size of the impeller depends on the kind of impeller, operating conditions described by the Reynolds, Froude and Power numbers as well as individual characteristics (Walas, 1990). In this study, the effect of impeller on reaction and formed zinc stearate was not examined.

Figure 5.2. Photograph of the impeller.

5.1.1. Washing of $ZnSt_2$ Cake

Reaction was carried out using 200ml of 5% (w) NaSt and 100ml of 4.69% (w) $ZnSO_4$ solutions at 70°C and 500 rpm for 30 minute. 60.28 g of $ZnSt_2$ was obtained after filtration of reaction mixture.

Wet $ZnSt_2$ formed by equivalent reactants after filtration was washed by different amounts deionized water. In the washing process 5.00 g of $ZnSt_2$ with 85 % water content was mixed with 10 ml, 20 ml, 30 ml, 40 ml, 50 ml of deionized water and agitated by magnetic stirrer at room temperature for ten minutes. After $ZnSt_2$ was completely dispersed, it was filtered by blue band filter paper (Filtrak 391) under 600 mmHg vacuum. Conductivity of the filtrates was measured by conductivimetry. The relation between conductivity and concentration was established by measuring the conductivity of prepared Na_2SO_4 (99% Merck) solutions. Experiment details are given in Table 5.2. In this step, optimum amount of water was investigated by studying adsorption of Na_2SO_4 on $ZnSt_2$.

Table 5.2. Washing experiment details

Exp. #	Wet ZnSt$_2$ (g)	H$_2$O (ml)	Temp. (°C)
I	5.00	50	19.5
II	5.00	40	19.3
III	5.00	30	19.4
IV	5.00	20	19.3
V	5.00	10	19.7

5.2. Production of ZnSt$_2$ by Fusion Process

The chemicals used for synthesis of ZnSt$_2$ by fusion process are given in Table 5.3. Additionally, the acid value of stearic acid, consisting of C16-C18, is 208.2 mg KOH/g of stearic acid.

Table 5.3. Chemicals used for synthesis of ZnSt$_2$ samples

Chemicals	Origin of chemicals
ZnO	99 %, Merck
C$_{17}$H$_{35}$COOH	Commercial product, Dalan Kimya A.Ş.

113.78 g (0.40 mol) sample of stearic acid was molten in a reactor at a temperature of 70°C, which is above its melting point, and a 16.27 g (0.20 mol) of zinc oxide (ZnO) was added to molten stearic acid. The reaction was carried out at temperature of 140°C and under atmospheric pressure. In this batch process, mixture was agitated by mechanical stirrer at different rates of 400, 600, and 750 rpm. The postulated reaction is given in the equation 5.2.

$$ZnO_{(s)} + 2C_{17}H_{35}COOH_{(l)} \longrightarrow (C_{17}H_{35}COO)_2Zn_{(l)} + H_2O_{(g)} \qquad \text{-5.2-}$$

In order to determine the effect of stirring rate on reaction time, reaction was repeated for above mixing rates. Samples were taken for different time period to study the reaction kinetics.

5.3. Production of ZnSt$_2$ by Modified Fusion Process

The production of ZnSt$_2$ was investigated using the fusion process in the presence of water. 28.440 g (0.010 mol) of stearic acid was molten in 200 ml of deionized water. 4.070 g (0.005 mol) of zinc oxide was added into molten stearic acid at 70°C. The reaction was carried out at 80°C for 1 h. In order to investigate the effect of surfactant, a comparative experiment was performed by using NaSt 1.5% (w).

5.4. Characterization of ZnSt$_2$

The physico-chemical properties of each sample were identified by X-Ray diffraction, fourier transform infrared spectroscopy (FTIR), scanning electron microscopy (SEM), transmission optic microscopy, energy dispersive X-ray (EDX) analysis, optic microscopy with hot stage, thermal gravimetric analysis (TGA), inductively coupled plasma (ICP), and elemental analysis.

The crystalline structure and purity of the samples were determined by means of X-Ray powder diffractometer and Philips Xpert-Pro with CuKα radiation at 45 kV and 40 mA. The registrations were performed in the 5-60° 2θ range. Scanning Electron Microscopy, Philips XL30 SFEG (SEM) with energy dispersive X-ray (EDX) analyses were used for identification of particle size and product purity. The samples were coated with gold and palladium metals by using the sputtering technique.

The particle size of raw material, ZnO, was determined by using Micromeritics Sedigraph 5100. For the determination of ZnO particle size, 0.50 g of ZnO was dispersed in 100 ml of deionized water in the presence of Calgon.

Inductively Coupled Plasma Atomic Emission spectroscopy (ICP 96, Varian) and CHNS-932 LECO Elemental Analyzer (from TUBİTAK, Ankara Test and Analysis Laboratory) were used to determine the product constituents and the removal of by-product, Na$_2$SO$_4$.

In the determination of Zn content of the product, nitric acid is used for ICP analysis (Baltacıoglu, 1994). For this purpose, 200 mg of ZnSt$_2$ solid samples from precipitation process was mixed with 1 N 10 ml of HNO$_3$. The reaction was carried out at 100°C for 30 min. in tubes of rotary microwave oven (CEM Mars-5). At the end of

this reaction synthesized $Zn(NO_3)_2$ was used in ICP analysis to determine the Zn content of the product. The remained compounds in this reaction were subjected to IR analysis to check whether all of the zinc stearate was converted to stearic acid.

The melting behavior of each $ZnSt_2$ samples was determined by transmission optic microscopy (Olympus CH40) with heated hot stage controlled by a temperature controller (Instec STC 200C). Melting of $ZnSt_2$ particles was photographed by digital camera (Nikon Coolpix 995).

Fourier Transform Infrared Spectrophotometer (Schimadzu 8601) was used to determine chemical structure of the products, the impurities in products and reactant conversion by well-known ratio methods. In the preparation of $ZnSt_2$ samples KBr disc method wad used. 4.0 mg of $ZnSt_2$ weighed and 196 mg of KBr was added to it and mixed together. A pellet was obtained by pressing the powder under 8 tons of pressure.

Thermogravimetric analyses TGA utilized (Schimadzu TGA-51), $ZnSt_2$ samples (10-15 mg) were loaded into a Pt pan and heated from 30°C to 1000°C at 10°C min^{-1} under N_2 flow (40 ml.min^{-1}).

Fuel additive application of $ZnSt_2$ in n-paraffin wax with different weight percents was investigated by using TGA under the same parameters. The n-paraffin used in TGA is a commercial product obtained from Baykim Kimya. Its melting point is 58-60°C.

Density determination of $ZnSt_2$ pressed in form of a pellet was determined using the YDK01-OD density kit of Sartorius microbalance operating according to Archimedes principle.

The water content of zinc stearate after filtration was determined by moisture analyzer (Sartorius MA 100). In this determination, $ZnSt_2$ cake was kept in the moisture analyzer at 100°C until its weight does not change.

CHAPTER VI

RESULTS AND DISCUSSION

6.1.   Selection of Process Variables for Precipitation Process

Precipitation process is widely used for manufacturing of pure metallic soaps. However, it has some drawbacks regarding with high utility consumption such as washing and drying of the product and etc. Production of zinc stearate was performed by precipitation process in order to determine the process parameters for instance, solubility of raw materials, reaction temperature, conversion, removal of unreacted raw materials and formed by-products, and drying of the product.

6.1.1.   Concentration of Solutions

The raw materials in precipitation process are sodium stearate (NaSt) and zinc sulfate heptahydrate. The solubility of these materials in water is vitally important since reaction proceeds in aqueous phase as shown in Equation 5.1.

$$2C_{17}H_{35}COONa_{(aq)} + ZnSO_4.7H_2O_{(aq)} \longrightarrow (C_{17}H_{35}COO)_2Zn_{(s)} + Na_2SO_{4(aq)} \quad -5.1-$$
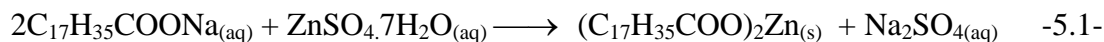
The solubility of the raw material, $ZnSO_4.7H_2O$ is in the range of 41.9-54.4 % (w) at the temperature range of 0-20 °C (Perry, 1963). 2.34% (w) zinc sulfate concentration was used in the reaction. However, the solubility of sodium stearate (NaSt) is extremely low and a major concern for this reaction. The phase behavior of the NaSt was studied by Mul et al., (2000). According to the Figure 3.4., NaSt has a Krafft point at 65 °C which means that it's solubility equals to 1% (w). This fact constitutes also a lower limit for the selection of concentration and reaction temperature. At 70 °C, the solubility of NaSt reaches about 3% (w) as seen in the Figure 3.4. Thus, concentration of NaSt was determined as 2.5% (w) for the reaction. The amount of water used in the reaction is 300 ml for 4.0 g of $ZnSt_2$. This value is extremely high and resulted due to the low solubility of the sodium stearate.

6.1.2. Reaction Temperature

The solubility of NaSt determines the reaction temperature since solubility is greatly affected by temperature. Reaction temperature was selected as 70 °C, which is in the solubility range of NaSt considering the Krafft point of the NaSt. The upper limit for the reaction temperature was chosen considering the vapor pressure of water, which increases with increasing temperature. As seen in Figure 3.4., at temperatures such as 80, 90, and 100 °C there is no significant increase in solubility of NaSt. The loss of water due to high vapor pressure causes the precipitation of NaSt. At 70 °C with 3% (w) concentration soap molecules form micelles in the solution Mul et al., (2000). The critical micelle concentration of 0.01% (w) for NaSt is obtained at 70 °C as seen in Figure 3.5. Thus, reaction was studied at 70 °C for initial concentrations NaSt and $ZnSO_47H_2O$ of 2.5% (w) and 2.34% (w) respectively.

6.2. Characterization of Raw Materials in Precipitation Process

The elemental and EDX analyses of sodium stearate and zinc sulfate heptahydrate were performed for characterization at three different points. The average results are as shown in Table 6.1. with theoretical values. As seen in Table 6.1. EDX and elemental analysis results of NaSt do not overlap with theoretical values. NaSt, obtained from Dalan Kimya, is a commercial product containing lower alkyl chain length as understood from higher Na and lower C content than the theoretical values. The O content is also higher than equivalent value. The presence of O not in the form of COO^- ion is indicated in another form.

Table 6.1. EDX and elemental analyses of raw materials % (w)

Sample	Element	Theoretical	EDX A.	Elemental A.
NaSt	Na	7.5	9.09	-
	C	70.54	66.14	59.61
	H	11.51	-	7.97
	O	10.44	14.45	-
$ZnSO_4$	Zn	22.74	39.27	-
	S	11.15	15.39	11.49
	H	4.9	-	4.68
	O	61.2	40.68	-

In EDX analysis, % (w) of H element in the sample could not be examined due to low atomic number of this element for EDX analysis. However percent values were recalculated by considering H in the compound. Zinc sulfate elemental analysis results confirm to the theoretical values. Since the EDX analysis is performed under vacuum, nearly 7 moles of hydrated water was removed from the sample. A low ratio of H/C was obtained than a saturated alkyl chain.
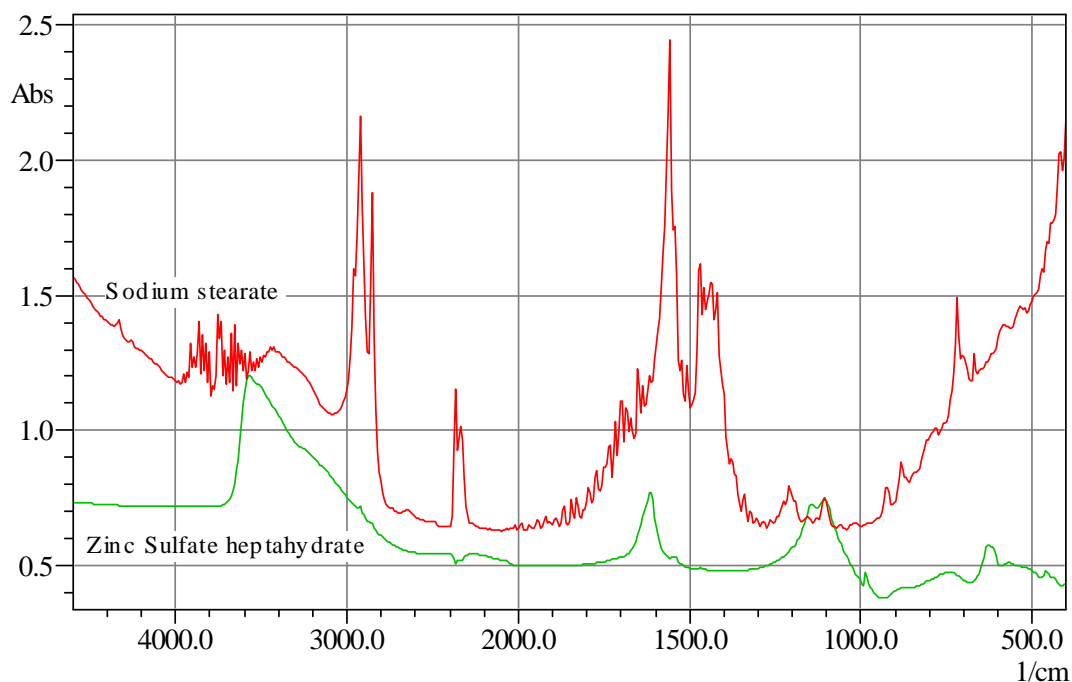
Figure 6.1. IR spectrum of sodium stearate and zinc sulfate heptahydrate.

In the IR spectrum of sodium stearate as shown in Figure 6.1., the characteristic absorption band of sodium salt of carboxylic acid was observed at $1560cm^{-1}$. This value is consistent with the value of $1560cm^{-1}$ from literature (Tandon et al., 2000). This characteristic band is assigned to the asymmetric stretching vibration ($\nu_{as}CO_2^-$) of the CO_2^- moiety. The characteristic absorption band of SO_4^{-2} ion was observed at $630cm^{-1}$ and 1120 cm^{-1}, which are consistent with literature values (Colthup et al., 1990). These bands are assigned to SO_4^{-2} bending and stretching vibrations.
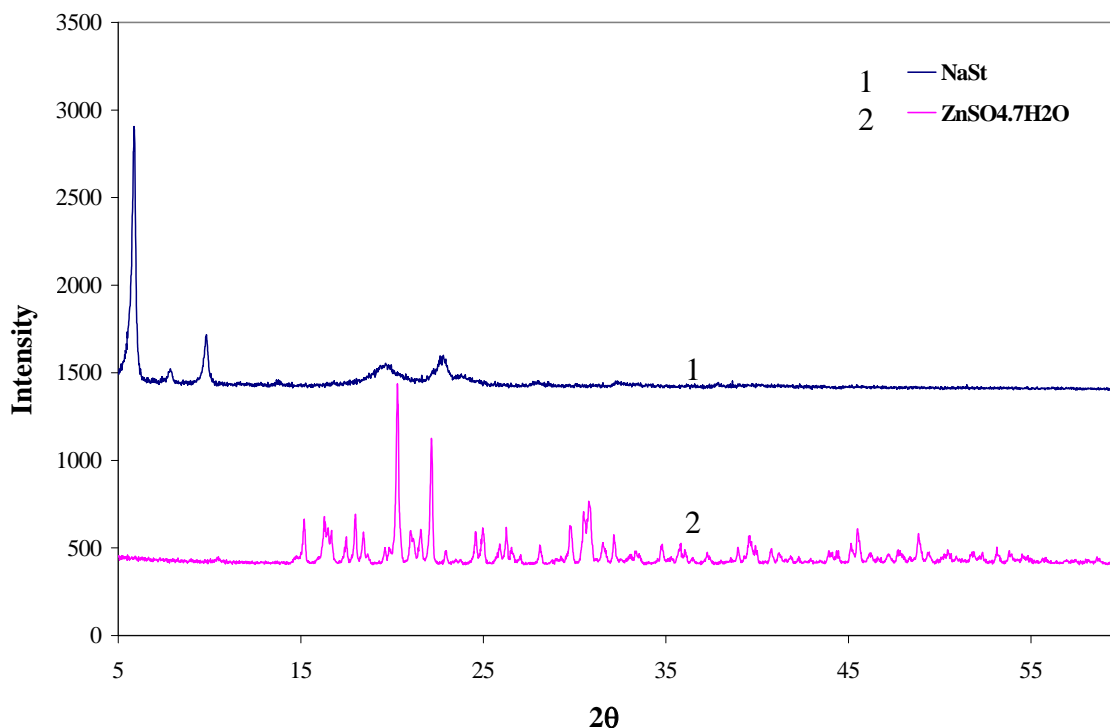
Figure 6.2. XRD pattern of sodium stearate and zinc sulfate heptahydrate.

XRD pattern of sodium stearate and zinc sulfate heptahydrate as shown in Figure 6.2. were obtained for determination of their purities and obtaining the unreacted raw materials in the product. The characteristic diffraction peaks of sodium stearate were observed at 2θ values 5.89, 7.99, 9.87, 19.87, and 23.03. The characteristic 2θ values for zinc sulfate hepathydrate were observed at 15.19, 18.01, 20.29, 22.17, and 30.87. These characteristic 2θ values are consistent with diffraction data library of the Philips Xpert-Pro., (PCPDFWIN v. 2.1).

6.3. Investigations on ZnSt$_2$ Produced by Precipitation Process

6.3.1. Reaction Stoichiometry

Different stoichiometric amounts of raw materials were studied in precipitation process for determining the effect of raw materials ratio on the ZnSt$_2$ synthesis. Experiments details are given in Table 6.2. For this purpose, manufactured ZnSt$_2$ samples were analyzed by EDX detector in scanning electron microscope (SEM), inductively coupled plasma (ICP) and elemental analyzer.

Table 6.2. Experimental details

Sample Code	NaSt	ZnSO$_4$7H$_2$O	Mixing R. (rpm)	Reaction T (°C)
ZnSt$_2$-1	Equivalent	Equivalent	500	70
ZnSt$_2$-2	Equivalent	10% Excess	500	70
ZnSt$_2$-3	Equivalent	10% Deficient	500	70

In EDX analysis, from three different points measurement has been done and average value of the these results were used. Zn^{++} ions were recovered from ZnSt$_2$ using nitric acid for ICP analysis. The weight percents of Na^+ and Zn^{++} ions were determined as shown in Table 6.3. The product obtained for three different conditions were very similar in composition. Elemental analysis results are lower than the theoretical values. This result is assigned to low C content in the sodium stearate. This situation produced higher Zn content in the product. Expected effect of excess and deficient zinc sulfate was observed based on the concentration of Na^+ ion in the product 0.02 and 0.521% (w) respectively.

According to the reaction Equation 5.1. the formed water soluble by product Na$_2$SO$_4$ is obtained. Synthesized ZnSt$_2$ samples were subjected to IR analysis to determine their structure and impurities coming from raw materials and by-products. IR spectra of ZnSt$_2$ samples are presented in the Figures 6.3. through Figure 6.5., for the equivalent, excess Zn, deficient Zn cases respectively.
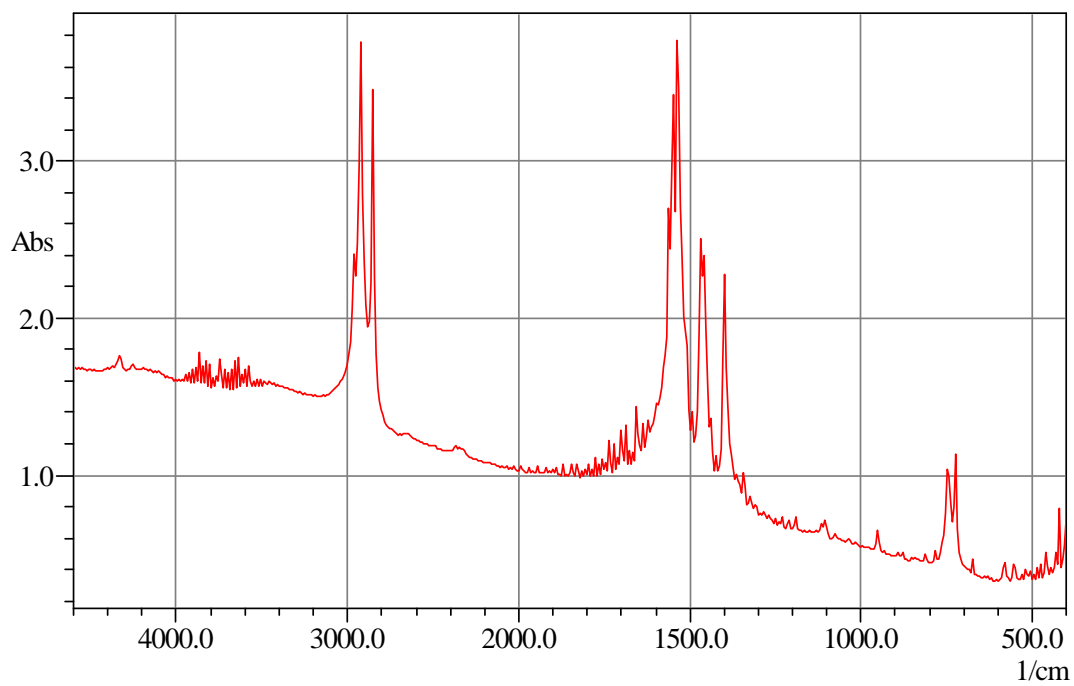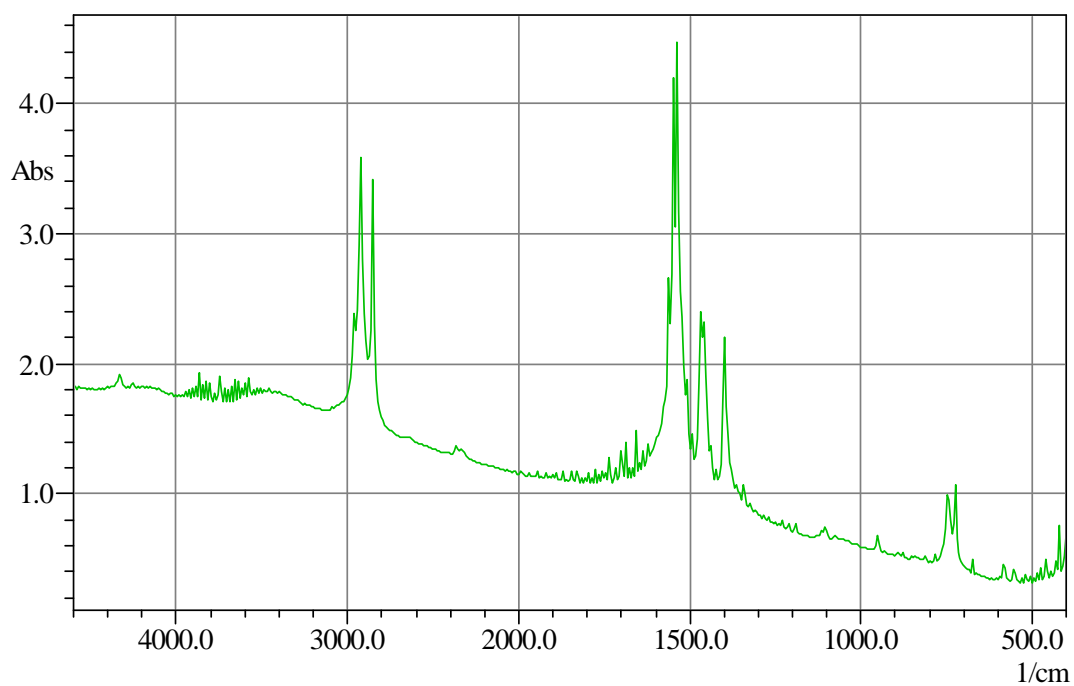
Figure 6.3. IR spectrum of equivalent case.

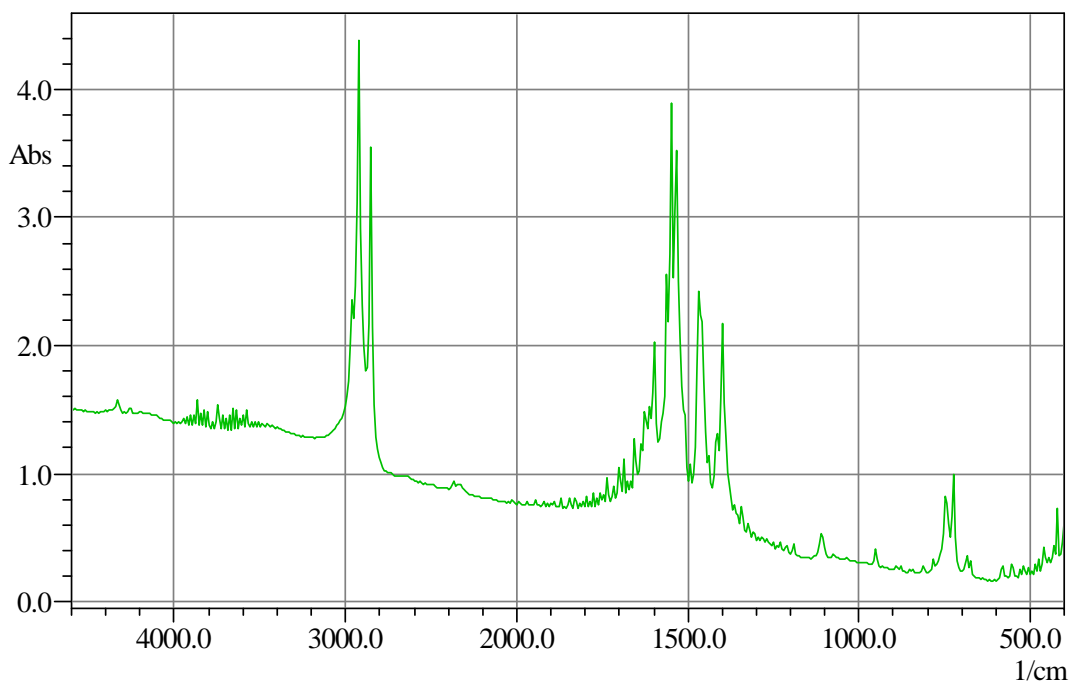Figure 6.4. IR spectrum of excess Zn case.

Figure 6.5. IR spectrum of deficient Zn case.

The characteristic peaks of zinc stearate at 1542 and 1398 cm^{-1} which are consistent with the literature (Sakai and Umemura, 2001) were observed for the three samples. These bands are due to antisymmetric and symmetric carboxylate stretching bands ($\nu_a COO^-$ and $\nu_s COO^-$) respectively. Antisymmetric and symmetric methylene stretching, and methylene scissoring bands ($\nu_a CH_2$, $\nu_s CH_2$, and $\delta_s CH_2$) were observed at about 2914, 2850 and 1472 cm^{-1} respectively. These bands are due to the alkyl chain in the zinc stearate structure. In Figure 6.5., the band observed at 1560 cm^{-1} belongs to asymmetric stretching vibration ($\nu_{as} CO_2^-$) of the sodium soap. This result shows the presence of unreacted sodium soap in the product even though it was washed with water two times, (each time 200 ml of water was used). From the IR analysis it was found that raw materials must be fed in equivalent amounts in the production of zinc stearate by precipitation process. It is anticipated that excess use of sodium stearate will result in some problems in washing process due to low solubility of the NaSt at washing temperatures.

The remained solid compounds from the reaction of ZnSt$_2$ and HNO$_3$ were subjected to IR analysis to determine whether all of the ZnSt$_2$ reacted or not. IR analyses of samples, equivalent, excess Zn and deficient Zn, are similar having a characteristic peak of stearic acid at 1700cm^{-1} due to the C=O stretching vibration.
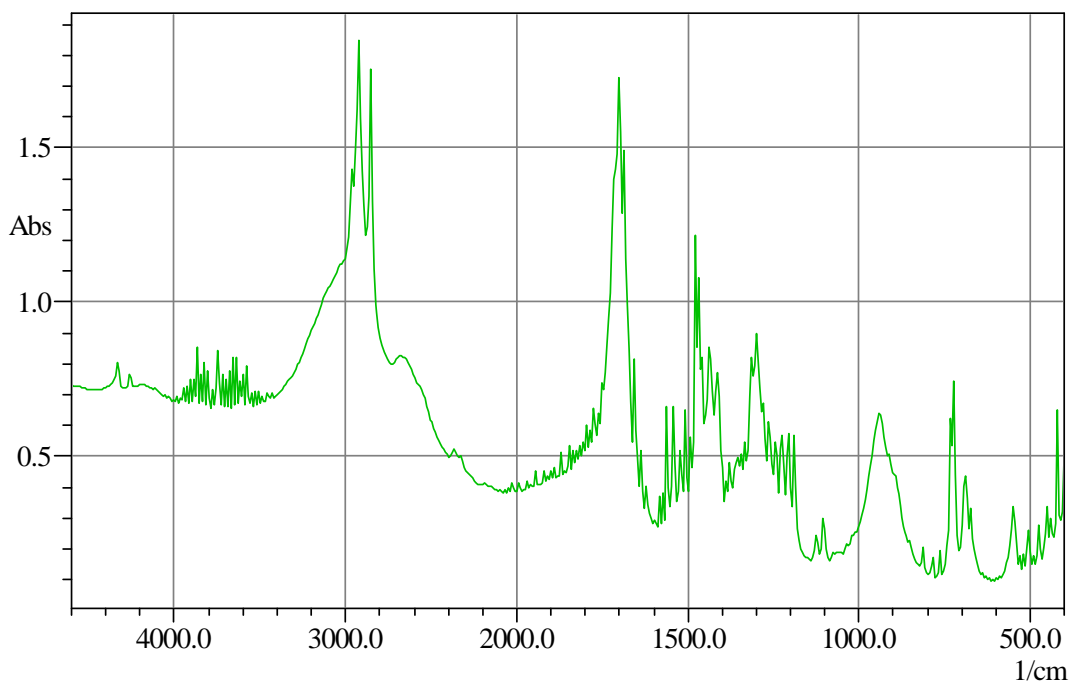
Figure 6.6. IR analysis of stearic acid obtained from ZnSt$_2$ and HNO$_3$ reaction.

As seen in Figure 6.6., the characteristic peak of ZnSt$_2$ around 1540 cm^{-1} is not observed and the characteristic peak of stearic acid at about 1700 cm^{-1} is observed. This result points out that 100% conversion of ZnSt$_2$ was achieved. Lastly, the results of Zn % (w) of the products from ICP analysis are reliable.

Aqueous phase of reaction and water from washing process were analyzed by ICP for determining the reaction proceeding and washing efficiency. As seen in Table 6.4. the amount of Na$^+$ ion is the lowest value in reaction aqueous phase for deficient Zn case. In the washing steps, the removal of formed sodium sulfate was achieved successfully except in the deficient zinc sulfate case. Because, the solution contains sodium stearate which might absorb the sodium sulfate. And it can be proposed that second washing is not necessary if high purity is not required.

The lowest amount of unreacted Zn was observed in the equivalent raw materials for the reaction. In the deficient Zn case, expected low zinc content was seen. However, its removal could not be achieved easily by washing. This result was assigned to the presence of sodium stearate in the solution.

SEM micrographs of the $ZnSt_2$ samples produced by precipitation process are given in Figure 6.7. through Figure 6.9. Figure 6.7. shows the equivalently produced $ZnSt_2$ crystalline morphology, it had a random platelike crystals. Figure 6.8 exhibits the crystal structure of $ZnSt_2$ produced in excess Zn case, which has similar crystal morphology with equivalent case product. As seen in Figure 6.9 crystal structure of $ZnSt_2$ produced in deficient case is similar to other product crystalline morphology. The particle size of samples changes between 2-4 μm.

Figure 6.7. SEM micrograph of $ZnSt_2$ sample produced in equivalent case.

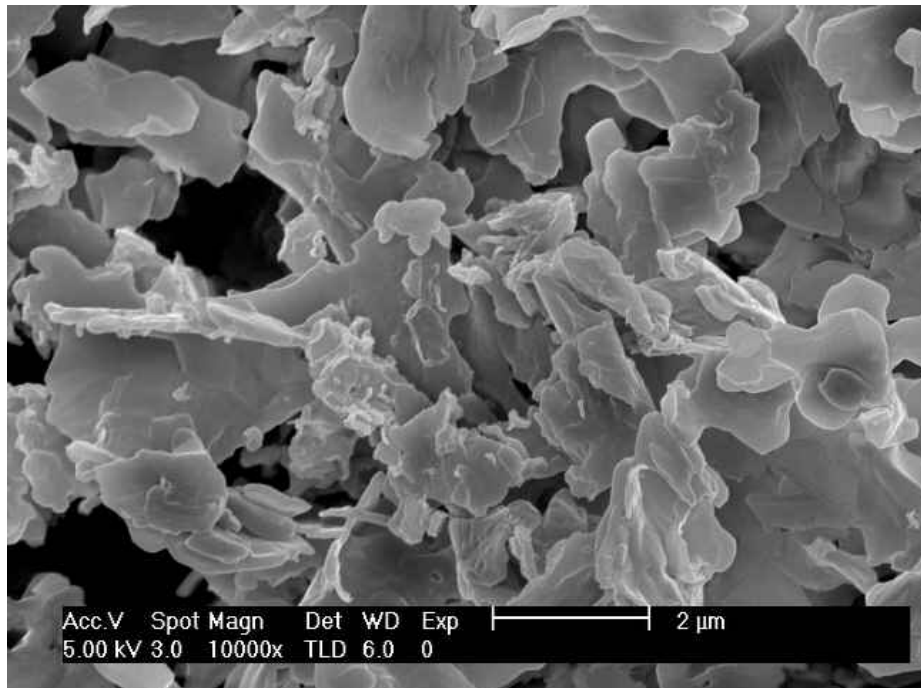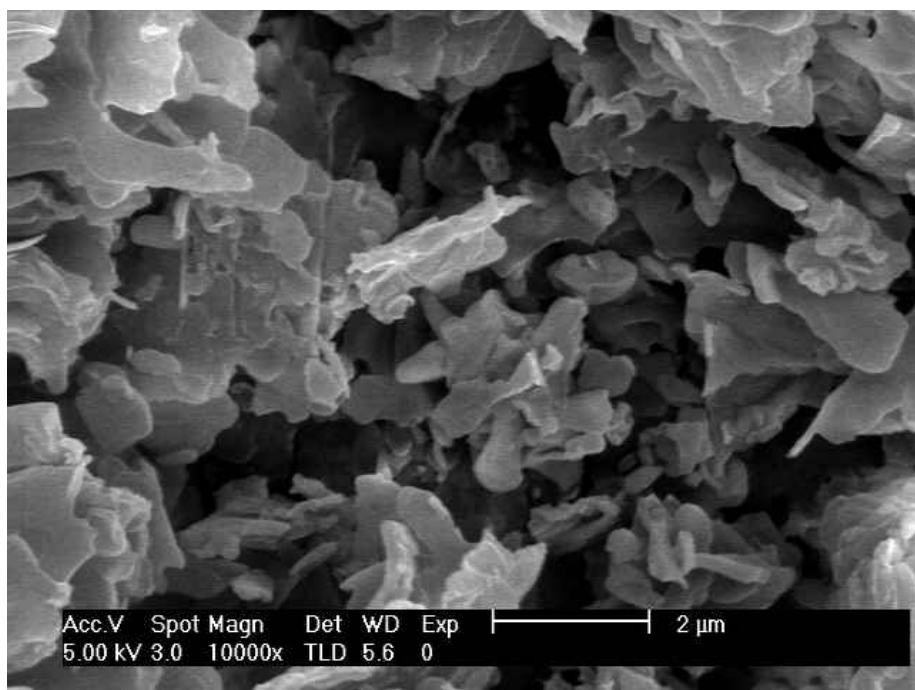Figure 6.8. SEM micrograph of ZnSt$_2$ sample produced in excess Zn case.
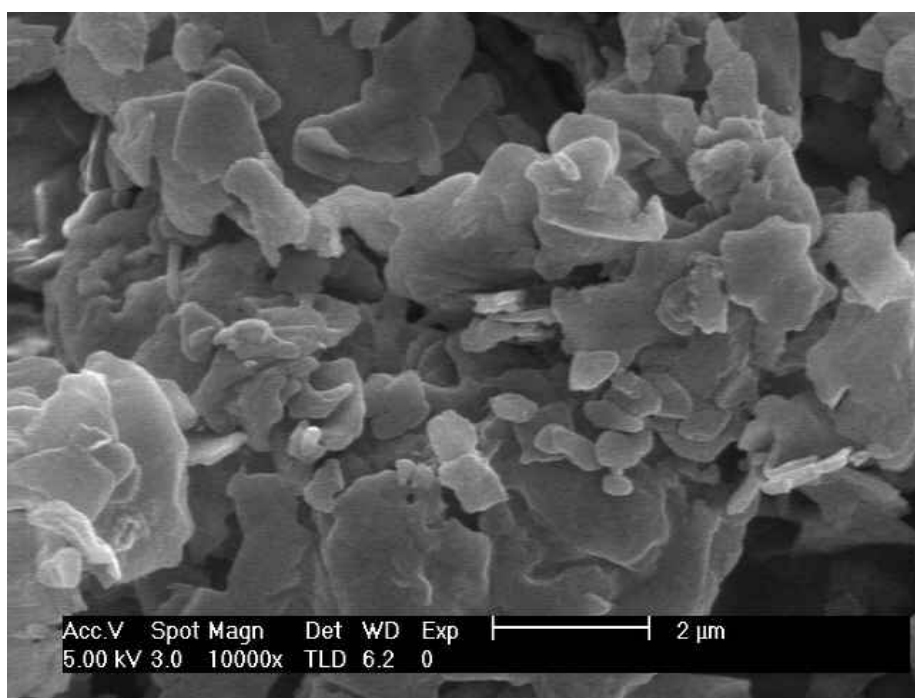
Figure 6.9. SEM micrograph of ZnSt$_2$ sample produced in deficient Zn case.

The melting point of the zinc stearates from experiments 1, 2 and 3 were determined by transmission optic microscopy with hot stage controlled by temperature controller. The reported temperatures are the hot stage temperature of the microscope.

The phase of the samples were recorded before and after the melting as shown in Figure 6.10.

(a) at 122°C	(b) at 123°C
(c) at 122°C	(d) at 123°C
(e) at 120°C	(f) at 123°C
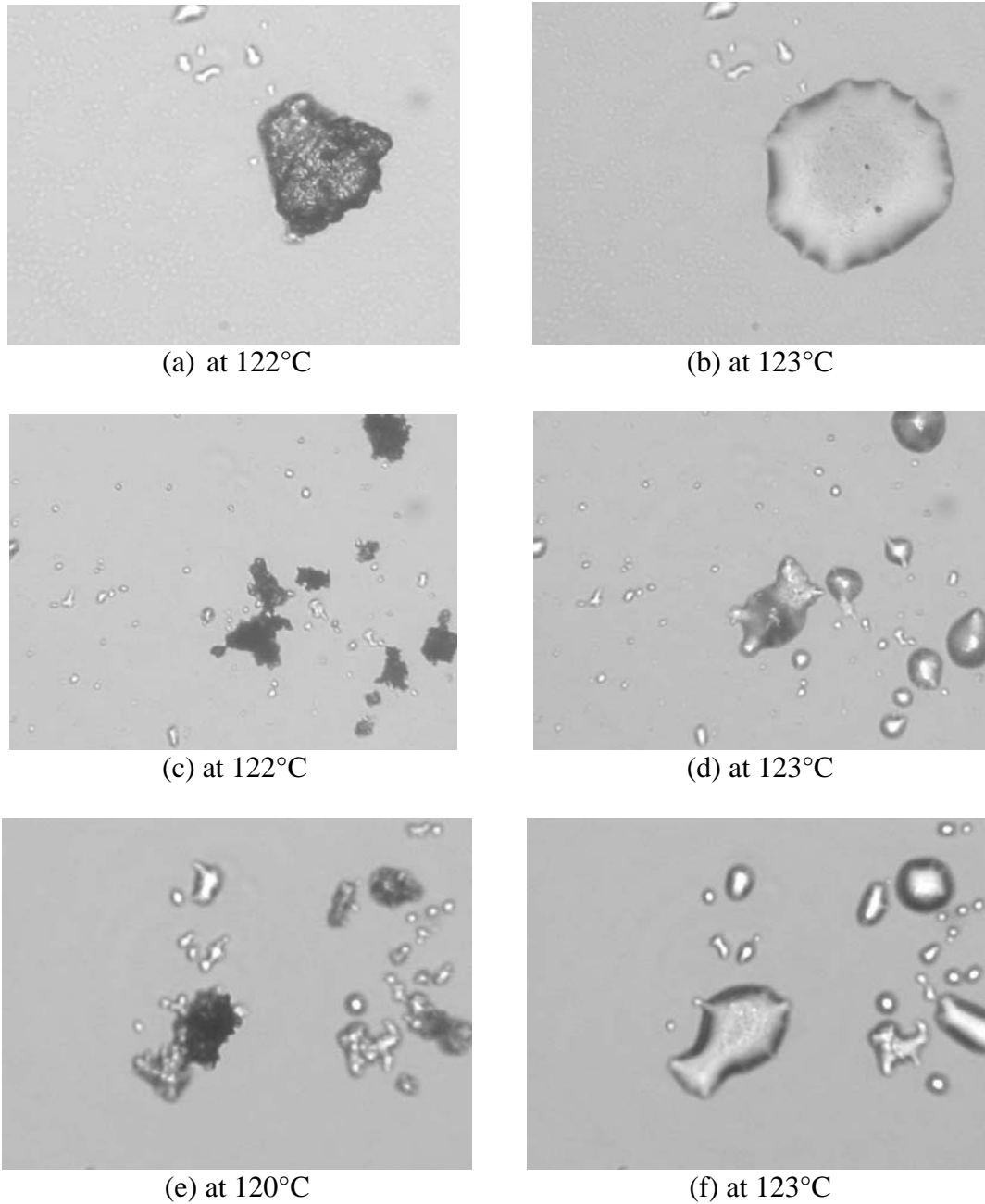
Figure 6.10. Transmission optic microscope photographs of ZnSt$_2$ samples before and after melting (with 320X magnification).

(a),(b) for equivalent case ; (c),(d) for excess Zn case; (e),(f) for deficient case.

The melting point of the equivalent case was determined as 122°C as shown in Figure 6.10.(a) and Figure 6.10.(b). The melting point of excess Zn case found as 122°C shown in Figure 6.10.(c) and Figure 6.10.(d). The melting point of deficient Zn case determined to be lower than 122°C given in Figure 6.10.(e) and Figure 6.10.(f). In

deficient Zn case product melt lower than 122 °C due to the presence of NaSt in the product. Generally, 122°C melting point is consistent with literature (Elvers, 1990).

The produced $ZnSt_2$ samples of equivalent, excess Zn, and deficient Zn cases were subjected to X-ray analysis in order to determine their structures and impurities. The XRD patterns of equivalent, excess Zn and deficient Zn are shown in Figure 6.11.
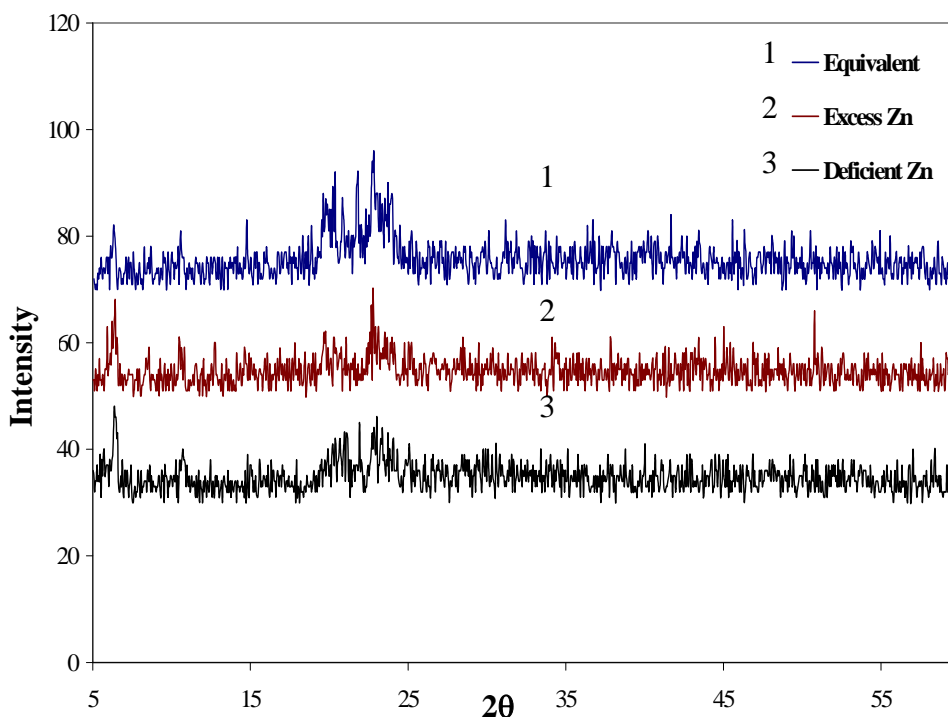
Figure 6.11. XRD pattern of $ZnSt_2$ samples produced by precipitation process.

Although, all of the XRD patterns are noisy, two of the characteristic 2θ values of zinc stearate at 6.40 and 19.58 were observed. The noise of the patterns are caused by amorphous structure of zinc stearate. The reason of this amorphous structure might be the reaction phase in which the product can not be orderly packed. On the other hand, the presence of micelles in the reaction phase might have some diminishing effects on crystallinity of the product.

6.4.   Washing of $ZnSt_2$ Cake From Precipitation Process

In precipitation process, the insoluble product and soluble by-product are formed in aqueous phase since the reaction as shown in Equation 5.1. is carried out in aqueous

phase. The separation of synthesized $ZnSt_2$ from reaction mixture is achieved by common filtration process since $ZnSt_2$ is insoluble in water. On the other hand, the porous structure of $ZnSt_2$ has tendency to adsorb the by-product sodium sulfate.

$$2C_{17}H_{35}COONa_{(aq)} + ZnSO_4.7H_2O_{(aq)} \longrightarrow (C_{17}H_{35}COO)_2Zn_{(s)} + Na_2SO_{4(aq)} \qquad -5.1-$$
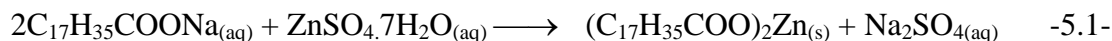
In order to examine the adsorption capability of $ZnSt_2$, a number of washing experiments have been performed. The $ZnSt_2$ cake which, is manufactured using precipitation process, was used in these experiments. 5.0 g of this wet product was used for each of the washing experiments. The details of the experiment were given in Table 6.5. The most interesting situation encountered in the filtration process is the floating of $ZnSt_2$ although it's density is greater than the water. This result induced to determine the synthesized $ZnSt_2$ density. Its density was calculated by using density kit and preparing a pellet from $ZnSt_2$ powders as a 1.09 kg/dm^3 which is consistent with literature. The reason of $ZnSt_2$ particles floatation is that they cover high volume with respect to their weight, which means that they have porous structure.

Table 6.5. Washing experiment details

Experiment Set	Wet ZnSt$_2$ (g)	H$_2$O (ml)	Conductivity (μS/cm)	Temperature (°C)
I	5.00	50	1128	19.5
II	5.00	40	1322	19.3
III	5.00	30	1634	19.4
IV	5.00	20	2150	19.3
V	5.00	10	3170	19.7

In the washing experiments, the removal sodium sulfate was observed by measuring the conductivity of the filtrate. For this purpose, a calibration curve of sodium sulfate solution as given in Figure 6.12. was prepared by using different sodium sulfate concentrations. The sodium sulfate, which is used in calibration, has 99%(w) purity (Merck). The conductivity of water (1-2 μS/cm) was ignored for calibration curve linearization.
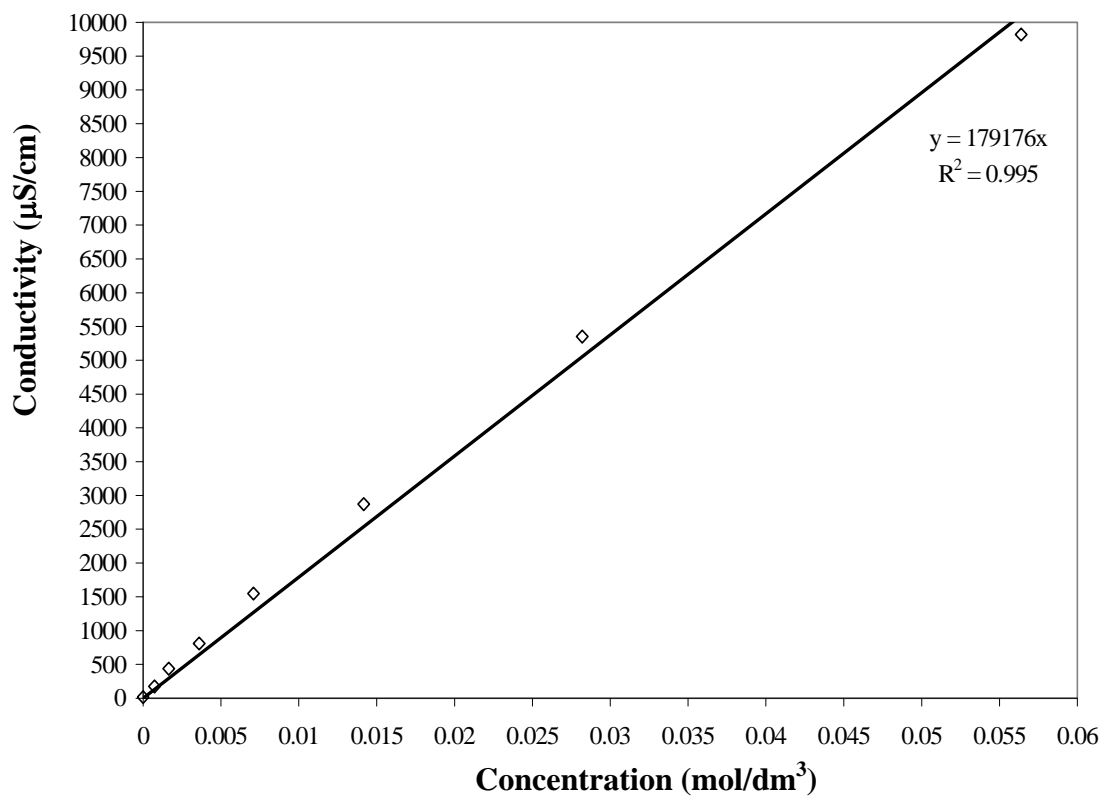
Figure 6.12. Calibration curve of Na_2SO_4.

Concentrations of the reaction mixture and filtrate from washing process were calculated using the linearization equation of the calibration curve. The results are given in Figure 6.13.
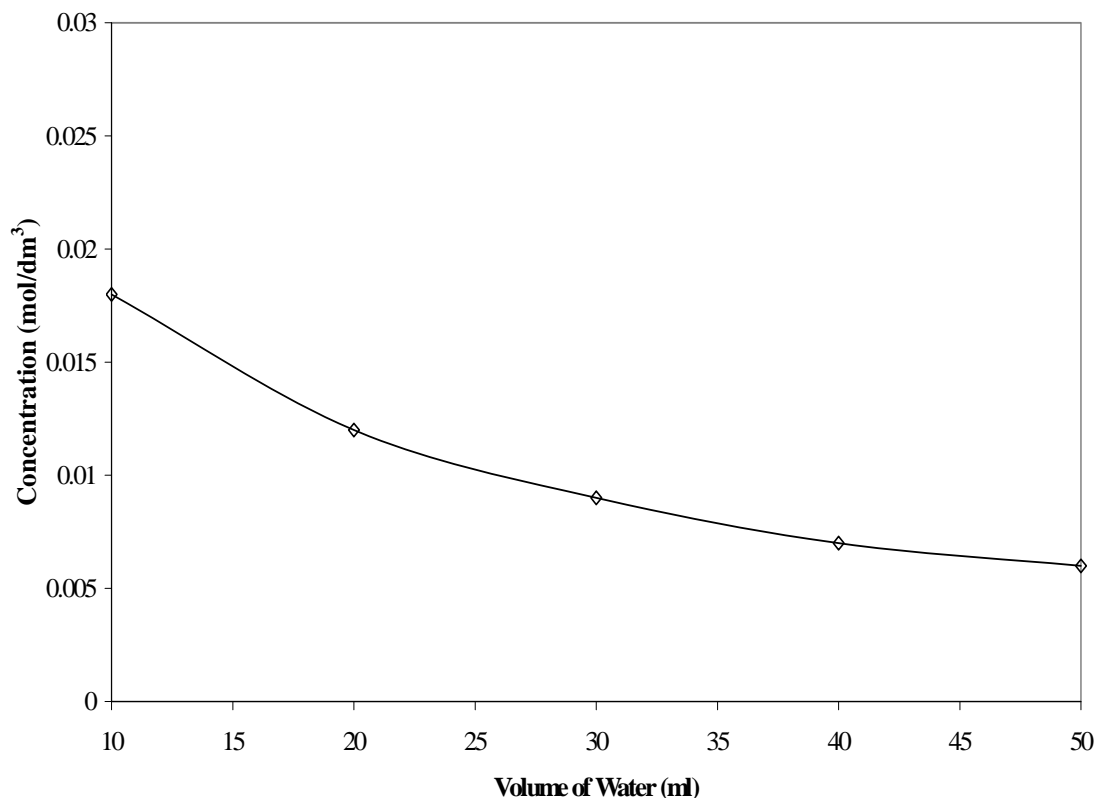
Figure 6.13. Concentrations of the reaction mixture and the filtrate from washing process.

The concentration of the filtrate obtained from the precipitation reaction was measured as 0.06 mol/dm³. The soluble salts were removed by washing from wet $ZnSt_2$. As seen in Figure 6.13., increasing the amount of washing water further more has no significant effect on removal of soluble salts. On the other hand, an increase in the amount of wastewater will produce environmental problems and need further separation processes. From these data, optimum amount of water was found as 30 ml for 5.00 g of wet $ZnSt_2$ cake. In order to determine the dry basis, wet $ZnSt_2$ is dried in moisture analyzer for 2 hours. It was observed that wet $ZnSt_2$ cake contains about 85% (w) water. The amount of washing water is 40dm³/kg of $ZnSt_2$ in dry basis.

In order to investigate the adsorption of sodium sulfate on wet zinc stearate, the concentration of Na_2SO_4 in solid phase and filtrate were measured. The measurements were translated into a graph as solid phase concentration by weight percent versus liquid phase concentration given in Figure 6.14. It was found that sodium sulfate was not significantly adsorbed on to wet zinc stearate.

The adsorption isotherm for Na_2SO_4 adsorption on wet $ZnSt_2$ cake is linear and can be expressed as;

$$q = 0.2 \times c$$

where q is the concentration of Na_2SO_4 in wet cake in g/g and c is the concentration in mol/dm^3 in aqueous phase at equilibrium. Very low solid phase concentrations could be achieved by washing with $40 dm^3$ H_2O per kg $ZnSt_2$ in dry basis.
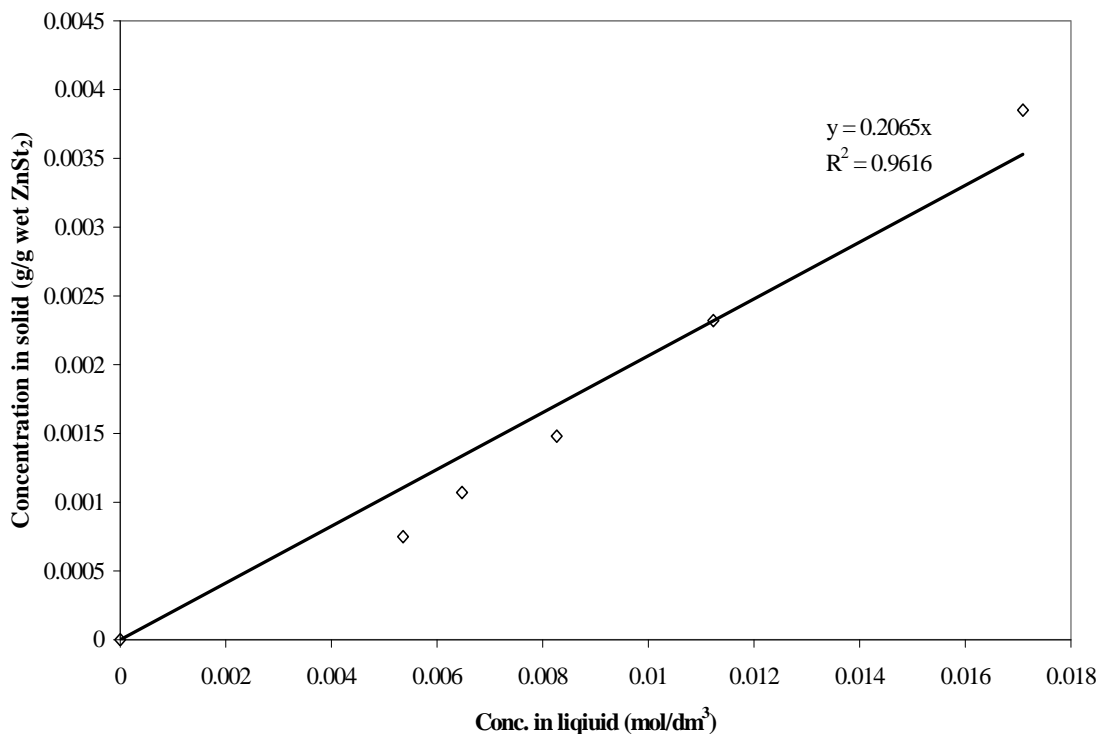
Figure 6.14. Adsorption isotherm of Na_2SO_4 on $ZnSt_2$.

6.5. Selection of Process Variables for Fusion Process

Fusion process is used for manufacturing of metallic soaps with melting points below 140°C, which produce relatively nonviscous melts. The decomposable metallic soaps can not be produced by this method. Transition metal soaps, for example, lead, zinc, or cadmium stearates are suited to produce by using this technique (Elvers, 1990).

Stearic acid and zinc oxide were used for manufacturing of $ZnSt_2$ in fusion process. Since stearic acid has a melting point at 60°C, the reaction temperature was selected higher than this value namely 120°C and 140°C. All the reactions were studied

in theoretical amounts of raw materials. Since, the reaction between zinc oxide and stearic acid is solid-liquid reaction, mixing of the reactants becomes important parameter. In order to determine the effect of mixing rate, reaction was studied under three different mixing rates 400, 600, 750 rpm.

On the other hand, the examining of fusion process in the presence of water was studied in theoretical amounts. The amount of water used in the reaction was 200 ml. The reaction was studied at 80°C and 500 rpm. for 1 hr. In order to increase the dispersion of stearic acid in water 1.5% (w) sodium stearate was added into the reaction mixture as a surfactant (Odashima and Kondo, 1982).

6.6. Characterization of Raw Materials in Fusion Process

Stearic acid and zinc oxide were used in the fusion process to manufacture zinc stearate. These materials were examined by using different techniques to determine their purities. The IR spectra of zinc oxide and stearic acid are shown in Figure 6.15.
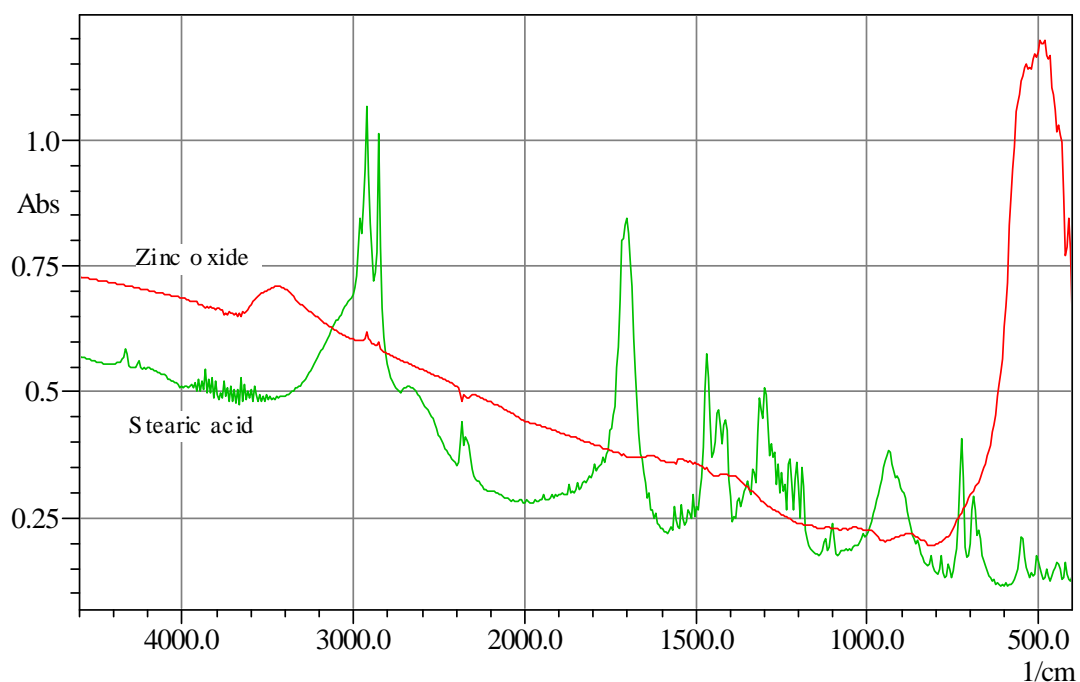

Figure 6.15. IR spectra of zinc oxide and stearic acid.

The characteristic band of stearic acid at 1700 cm^{-1} due to C=O asymmetric stretching vibration was observed in the IR spectrum. This result shows that there is no impurity in the stearic acid and it is consistent with the value, which is given in the

literature (Colthup et al., 1990). The presented IR spectrum of zinc oxide has a characteristic band at 400cm^{-1}. Porous zinc oxide samples show two characteristic bands with maxima at 420 and 565cm^{-1} and the splitting of these characteristic maximas depends on the particle morphology (Sigoli et al., 1997).

Particle size distribution of zinc oxide as shown in Figure 6.16. was found using particle size analyzer (Sedigraph-5100). The reaction between ZnO and stearic acid at a temperature, which is higher than the melting point of stearic acid is liquid-solid reaction. At this point, the surface area of ZnO becomes important to provide an adequate surface area for the reaction. As shown in Figure 6.16., 99% (w) of the particles have sizes lower than 7.5 μm, while 30 % (w) of the particles have diameters lower than 1 μm. The mean diameter calculated from the size distribution is 1.53 μm.
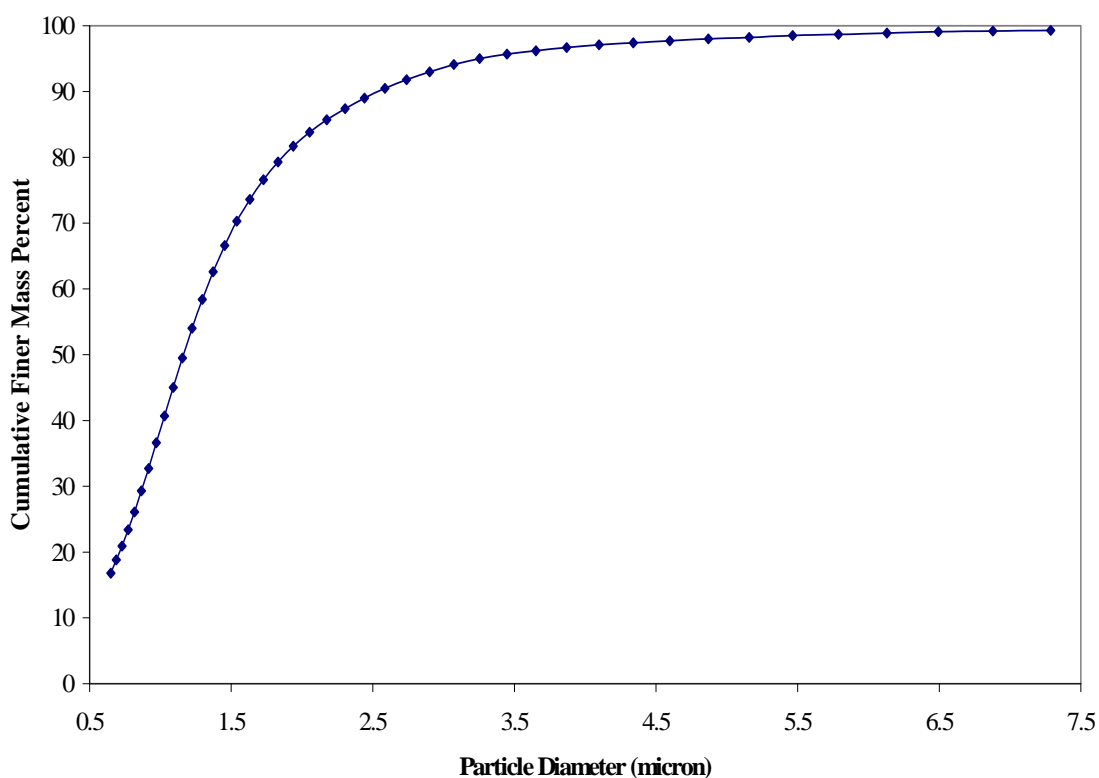

Figure 6.16. Particle size distribution of zinc oxide.

XRD pattern of zinc oxide and stearic acid as shown in Figure 6.17. were obtained for determination of their purities and obtaining the unreacted raw materials in product. The (100), (002), and (101) characteristic diffraction peaks of zinc oxide were observed at 2θ values 31.82, 34.47, 36.27, and 47.57 respectively. They are consistent

with literature (Lee et al., 2002). The characteristic 2θ values for stearic acid were observed at 6.72, 21.62, and 23.97 which are consistent with the data library of the Philips Xpert-Pro., (PCPDFWIN v. 2.1.).
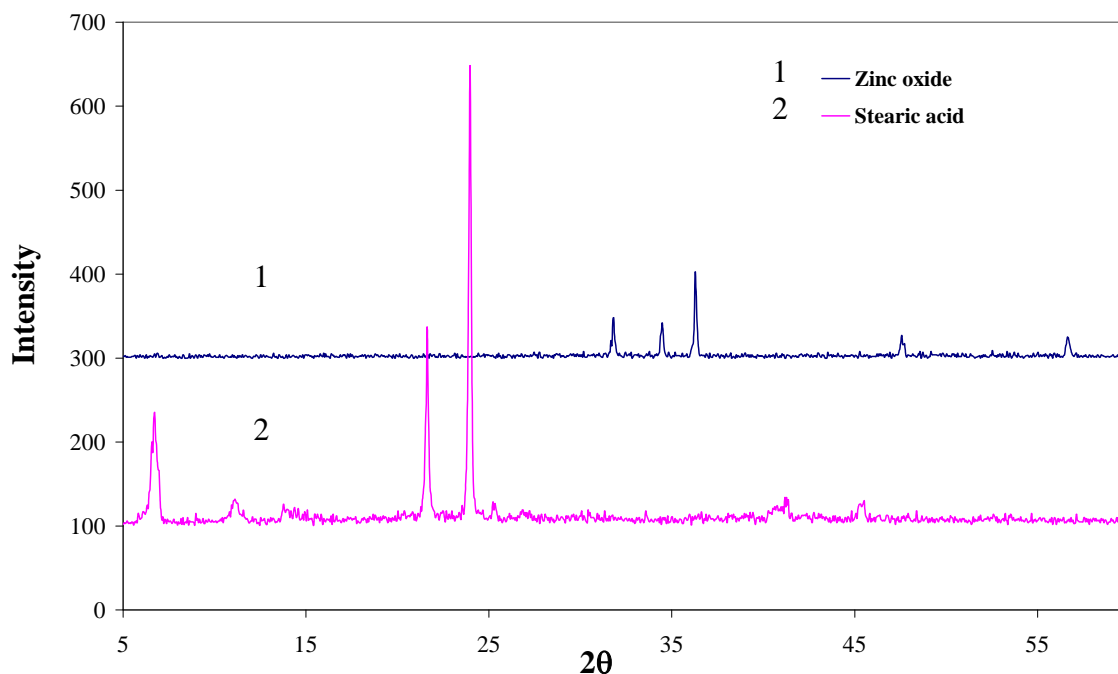
Figure 6.17. XRD pattern of zinc oxide and stearic acid.

6.7. Investigations on ZnSt$_2$ Produced by Fusion Process

6.7.1. Effect of Temperature

In order to determine the effect of temperature on reaction between stearic acid and zinc oxide it was carried out at 500 rpm; 120°C and 140°C for 60 minute reaction time. The change of reactant, stearic acid, to product zinc stearate was observed IR analysis. The IR spectra of the samples for different reaction temperature given in Figure 6.18. indicated lower conversion to zinc stearate at 120°C. It was found that 120°C reaction temperature is not as effective as the 140°C since the melting point of zinc stearate is higher than this value. In the 120°C reaction temperature case, with formation of ZnSt$_2$ it was observed that mixing of the reactants became difficult due to the increasing viscosity at this temperature.

Figure 6.18. IR spectra of ZnSt$_2$ sample at different reaction temperatures.

6.7.2. Effect Mixing Rate

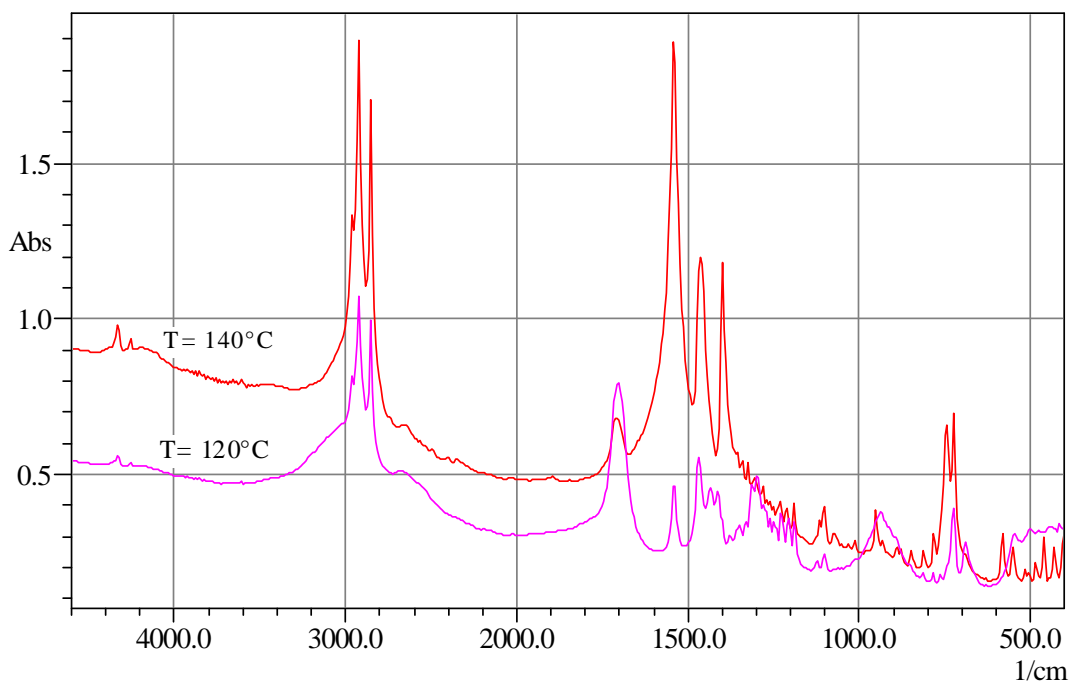In order to determine the effect of mixing on reaction, three different stirring rates 400, 600 and 750 rpm at 140°C were studied in the fusion process. The proceeding of the reaction was monitored by IR analysis. The characteristic peaks of stearic acid at 1700cm^{-1} and zinc stearate at 1540cm^{-1} due to the C=O and COO$^-$ stretching vibrations respectively were used in the determination of conversion.

The IR spectra used in conversion calculation are shown in Figure 6.19. through Figure 6.21. for stirring rates 400, 600, and 750 rpm respectively. The two spectra given in the figures belong to IR spectrum of samples collected at the beginning of the reaction and at the end of reaction. As it can be seen in Figure 6.19. through Figure 6.21., with elapsing time, the characteristic peak of stearic acid at 1700 cm^{-1} due to C=O stretching vibration decreased and the characteristic band of zinc stearate at 1540 cm^{-1} due to COO$^-$ stretching vibration increased. However, after a certain time, no change was observed in the height of stearic acid band which shows unreacted stearic acid remained in the product. Increasing of the mixing rate decreased the delay time in the reaction. This delay may be resulted from the existing product, which forms a barrier film on the surface of the zinc oxide particles.
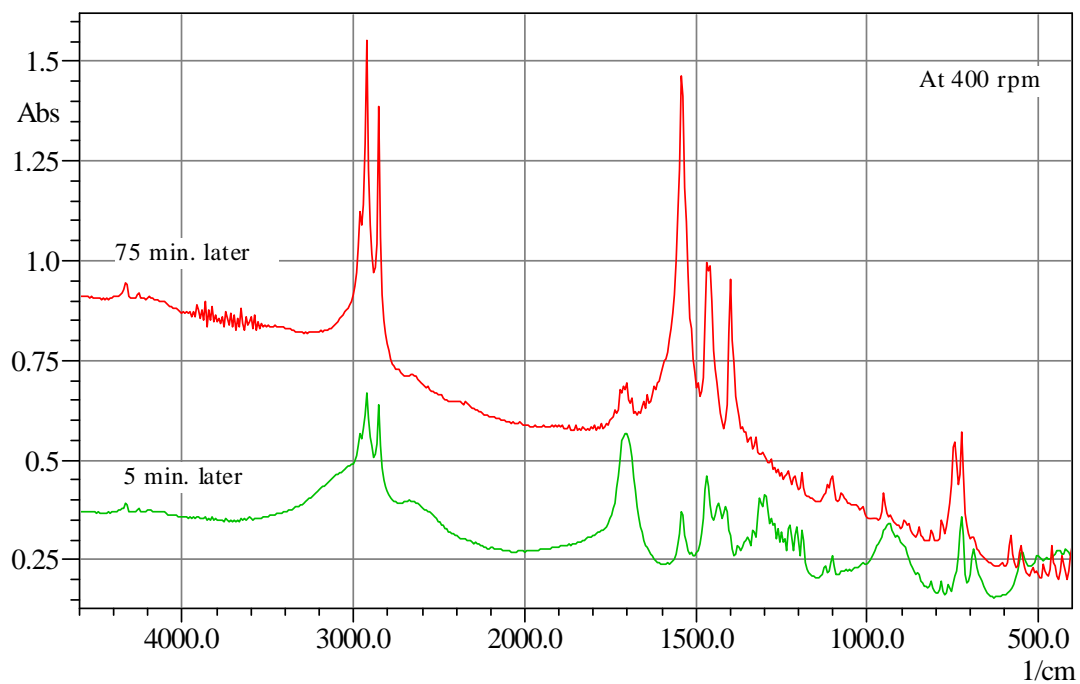
Figure 6.19. IR spectra of ZnSt$_2$ at different times for 400 rpm.
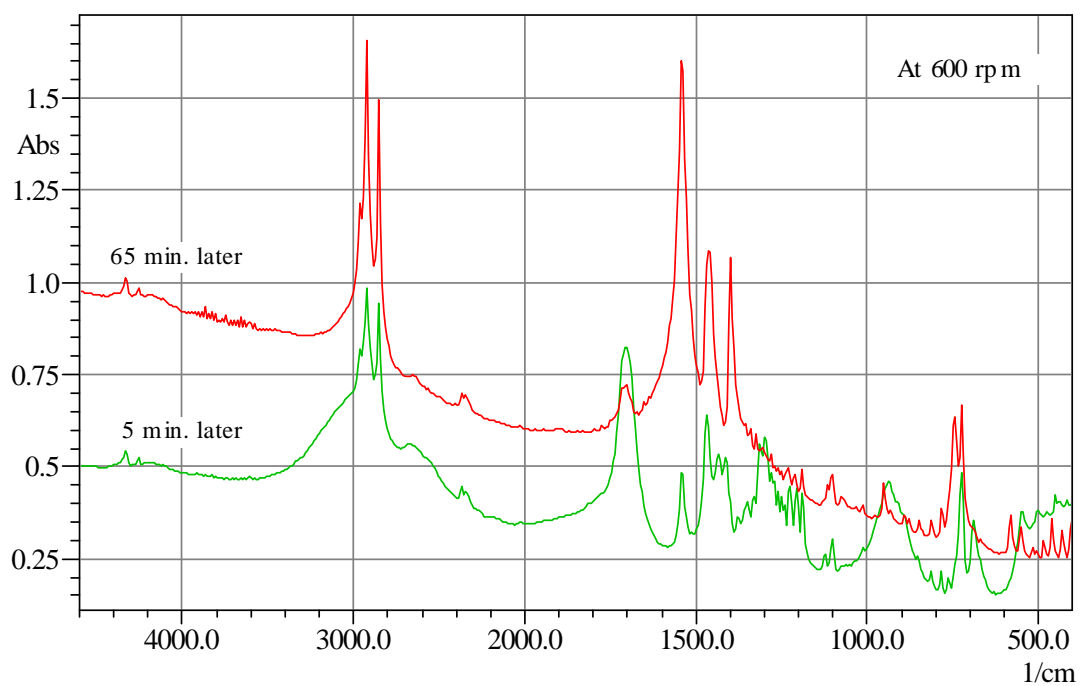
Figure 6.20. IR spectra of ZnSt$_2$ at different times for 600 rpm.
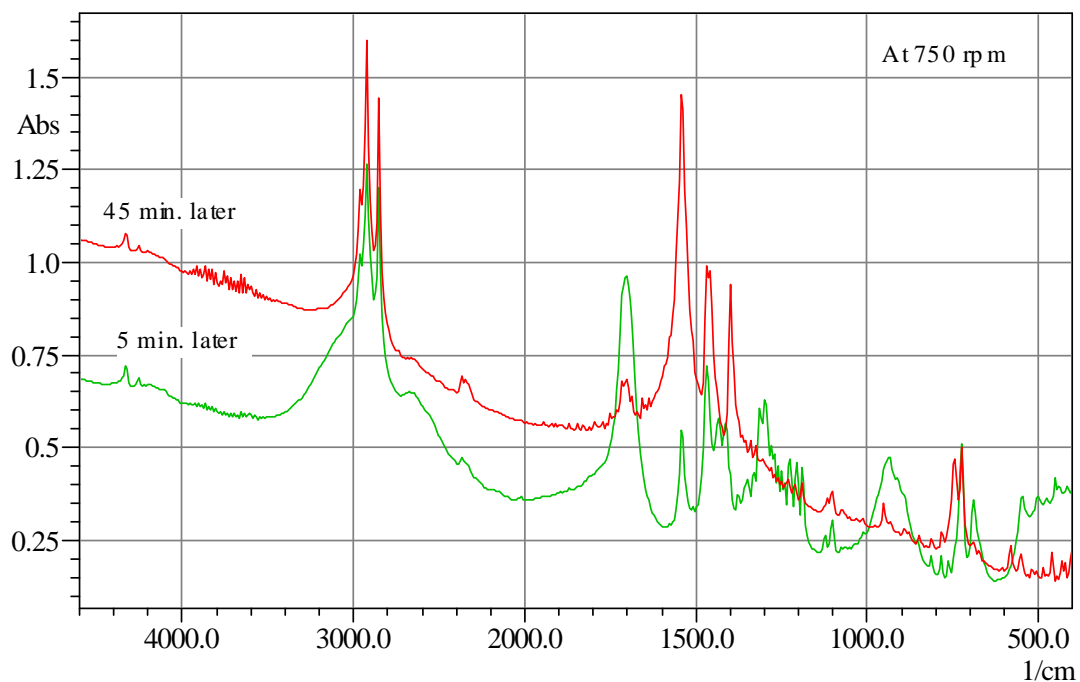
Figure 6.21. IR spectra of ZnSt$_2$ at different times for 750 rpm.

The XRD patterns of ZnSt$_2$ samples as shown in Figure 6.22. manufactured at different stirring rates 400, 600, 750 rpm were obtained for the determination of their structures and constitutes. Since the XRD analysis is unable to determine the concentrations lower than 3% (w), the characteristic peaks of ZnO and stearic acid were not observed. The characteristic peaks of stearic acid if any, were overlapped with that of ZnSt$_2$.

All samples obtained by fusion process taken at the first 5 minute of the reaction contained free ZnO as understood from the ZnO peak at 500cm^{-1}. At the completion of the reaction this peak disappears completely. In other words, all ZnO reacted with stearic acid and some free acid remained in the system. This may be due to the lower molecular weight of the commercial stearic acid than the pure stearic acid. Commercial stearic acid contained C16-C18 alkyl chains. Its molecular weight was 284.48. Thus an excess amount than the equivalent amount was used in the reaction.
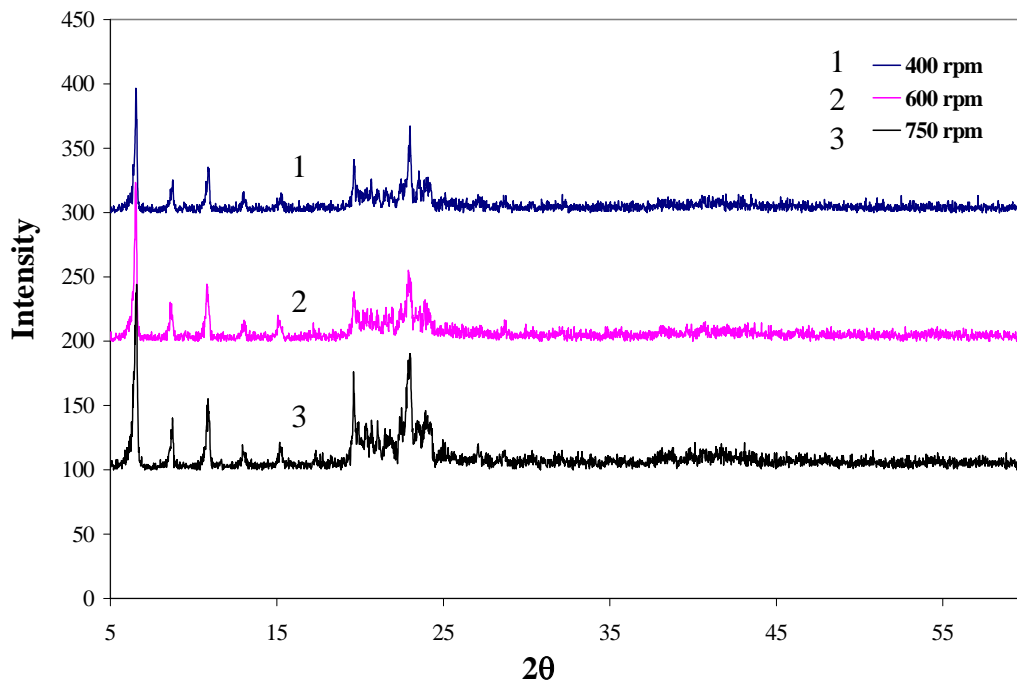
Figure 6.22. XRD patterns of ZnSt$_2$ samples produced at different mixing rates.

Figure 6.22. shows that ZnSt$_2$ samples have it's own characteristic peaks at 2θ values of 6.55, 8.77, 10.93, 19.67, 22.99. except the 2θ at 37.93. These results are consistent with diffraction data library of the Philips Xpert-Pro. (PCPDFWIN v. 2.1.), which is given in Table 6.6. and literature values (Jona et al., 2002).

Table 6.6. XRD data of ZnSt$_2$ (diffraction data library of the Philips Xpert-Pro)

2θ	Intensity
6.40	100
8.4	13
10.59	27
19.58	100
22.66	67
37.93	33

SEM micrographs of the $ZnSt_2$ samples obtained by fusion technique at different stirring rates are given in Figure 6.23 through Figure 6.25.
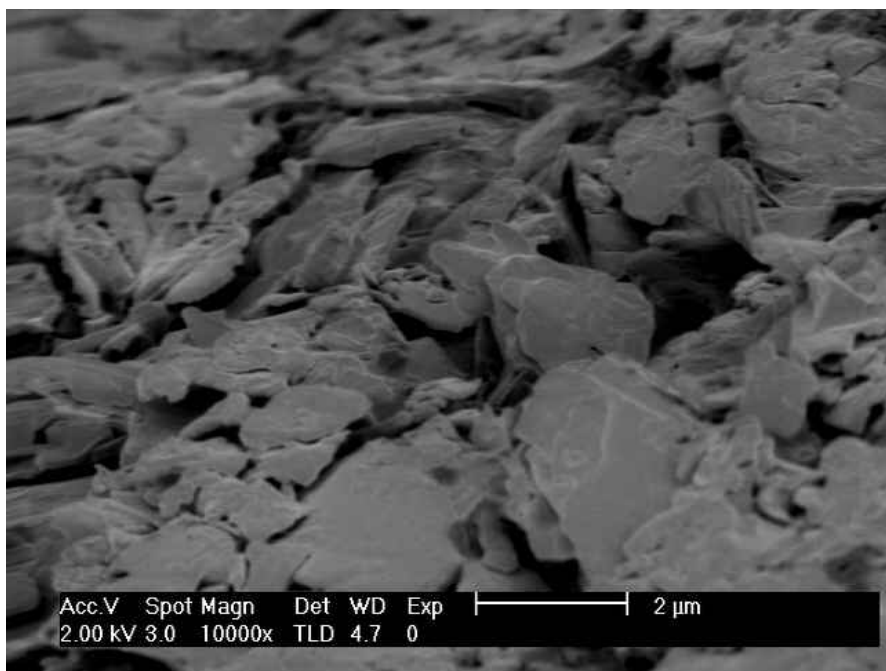
Figure 6.23. SEM micrograph of the $ZnSt_2$ sample obtained at 400 rpm.
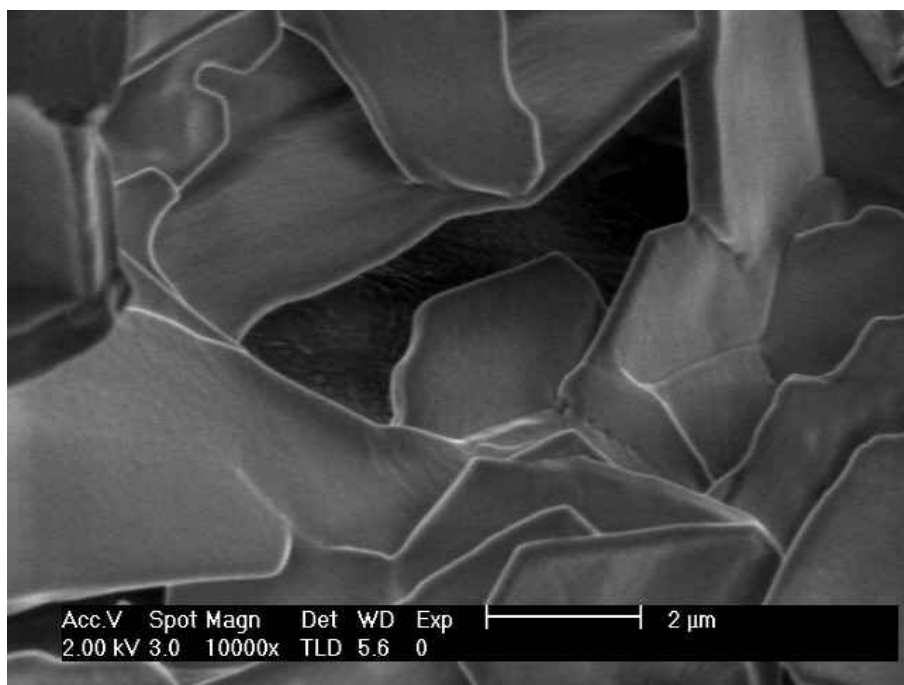
Figure 6.24. SEM micrograph of the $ZnSt_2$ sample obtained at 600rpm.
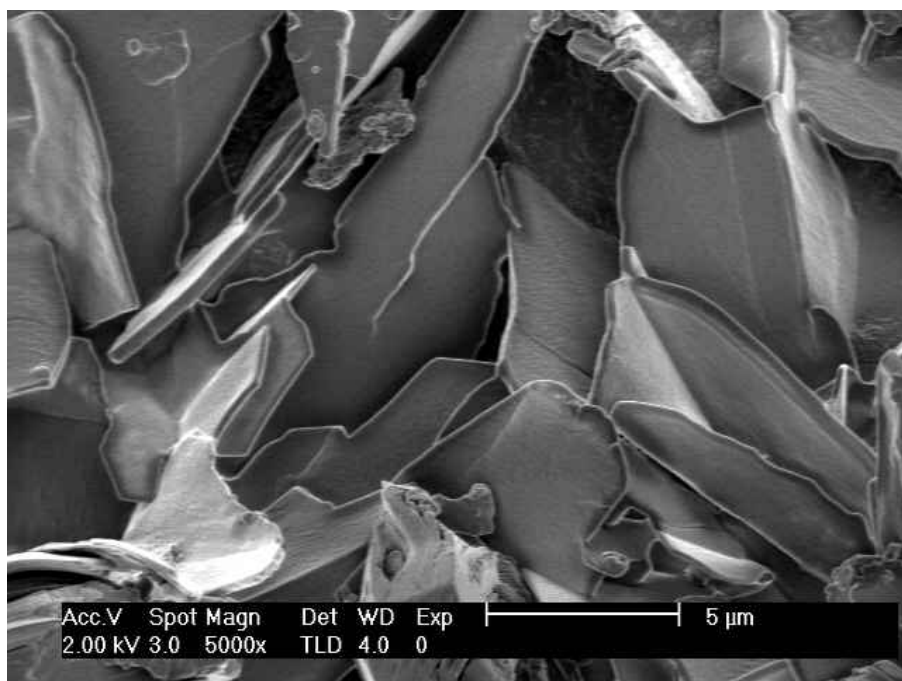
Figure 6.25. SEM micrograph of the ZnSt$_2$ sample obtained at 750 rpm.

It is seen from Figure 6.23. through Figure 6.25. that the particle size of ZnSt$_2$ samples change between 4-6 μm. The crystal shapes of the particles are different than the ZnSt$_2$ particles obtained by precipitation process. The particles produced by the fusion process have sharp edge and were packed more orderly than the ones from precipitation process.

The melting point of zinc stearate samples from fusion process for different stirring rates was determined by transmission optic microscopy with hot stage controlled by temperature controller. The samples taken at the beginning of the reaction melted at about of 65°C as shown in Figure 6.26. (a), Figure 6.26. (b), Figure 6.27.(a), Figure 6.27.(b), Figure 6.28.(a) and Figure 6.28.(b). This low melting temperature shows the presence of stearic acid in the samples at the beginning of reaction. And black points in these microphotographs belong to zinc oxide particles. The melting point of the ZnSt$_2$ samples were found to be slightly lower than 122 °C as shown in Figure 6.26. (c), Figure 6.26. (d), Figure 6.27.(c), Figure 6.27.(d), Figure 6.28.(c) and Figure 6.28.(d). Although the microphotographs were taken at 122°C melting started before that temperature and this quick phase change could not be captured. The reported temperatures under microphotographs are the hot stage temperatures of the microscope.

(a). at 30 °C	(b). at 65 °C

(c). at 120 °C	(d). at 122 °C
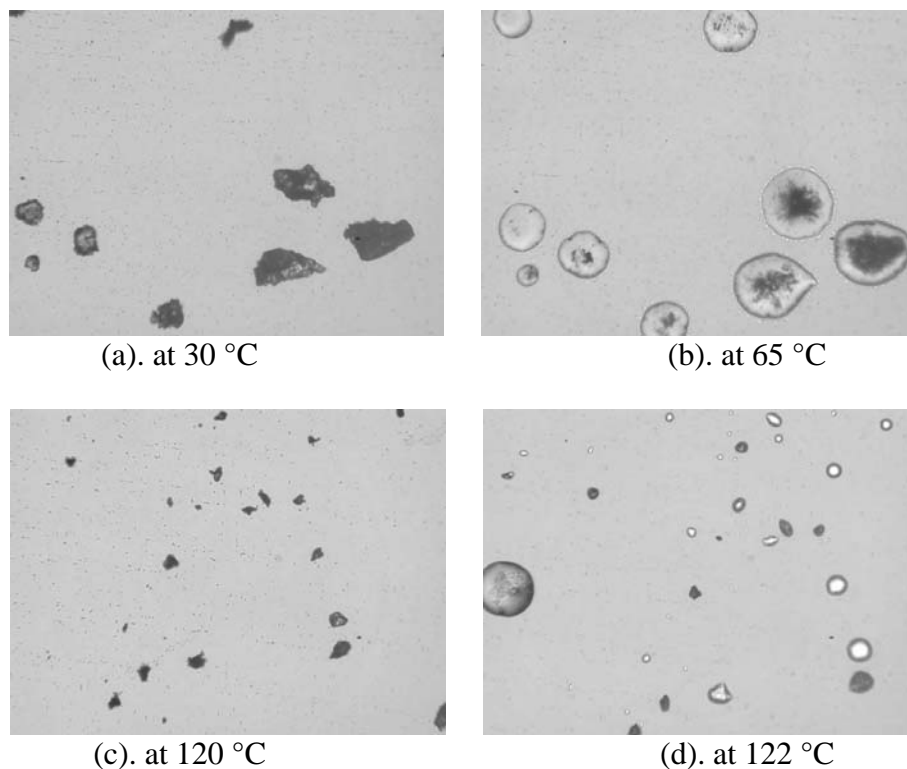
Figure 6.26. The transmission optic microscope microphotographs of ZnSt$_2$ samples at 400 rpm; (a),(b) samples taken at the beginning of reaction ,(c),(d) samples taken at the end of the reaction.

(a). at 30 °C	(b). at 65°C

(c). at 120 °C	(d). at 122 °C
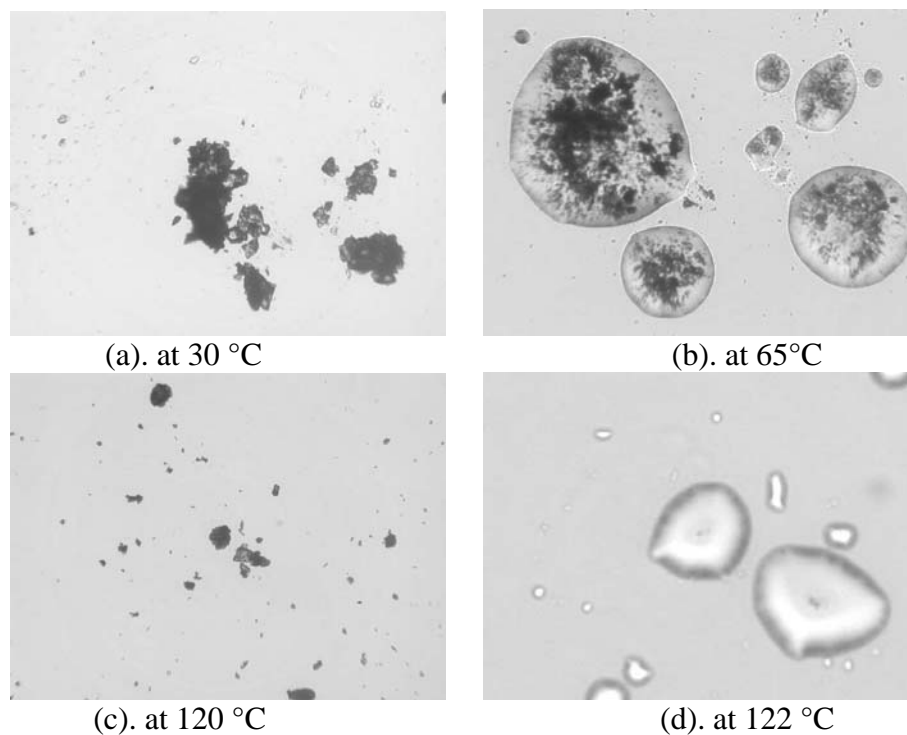
Figure 6.27. The transmission optic microscope microphotographs of ZnSt$_2$ samples at 600 rpm; (a),(b) samples taken at the beginning of reaction ,(c),(d) samples taken at the end of the reaction.

(a). at 30 °C   (b). at 65 °C

(c). at 120 °C   (d). at 122°C
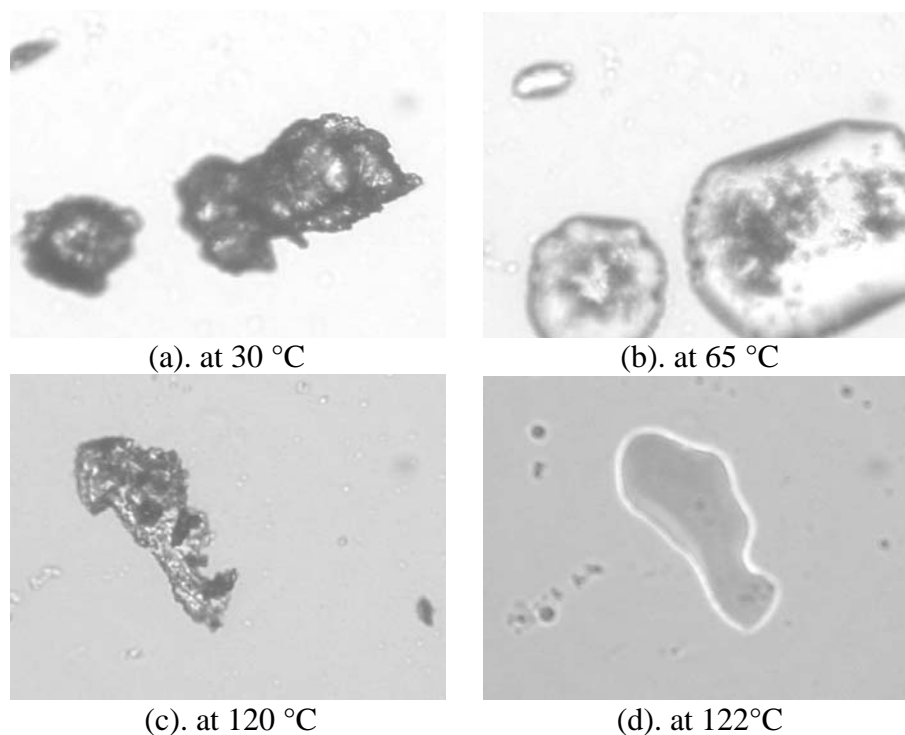
Figure 6.28. The transmission optic microscope microphotographs of $ZnSt_2$ samples at 750 rpm; (a),(b) samples taken at the beginning of reaction ,(c),(d) samples taken at the end of the reaction.

6.8. Investigations on $ZnSt_2$ Produced by Modified Fusion Process

The reaction of stearic acid and zinc oxide was studied in the presence of water in this set. Reaction was carried out at 80°C with a stirring rate of 500 rpm and for 60 min. The increase in reaction temperature is not possible due to vaporizing of water under atmospheric reaction condition. The effect of sodium stearate was examined for this modified process. Since stearic acid is insoluble in water it was thought that the addition of surfactant would increase the dispersion of stearic acid in the form of micelles.
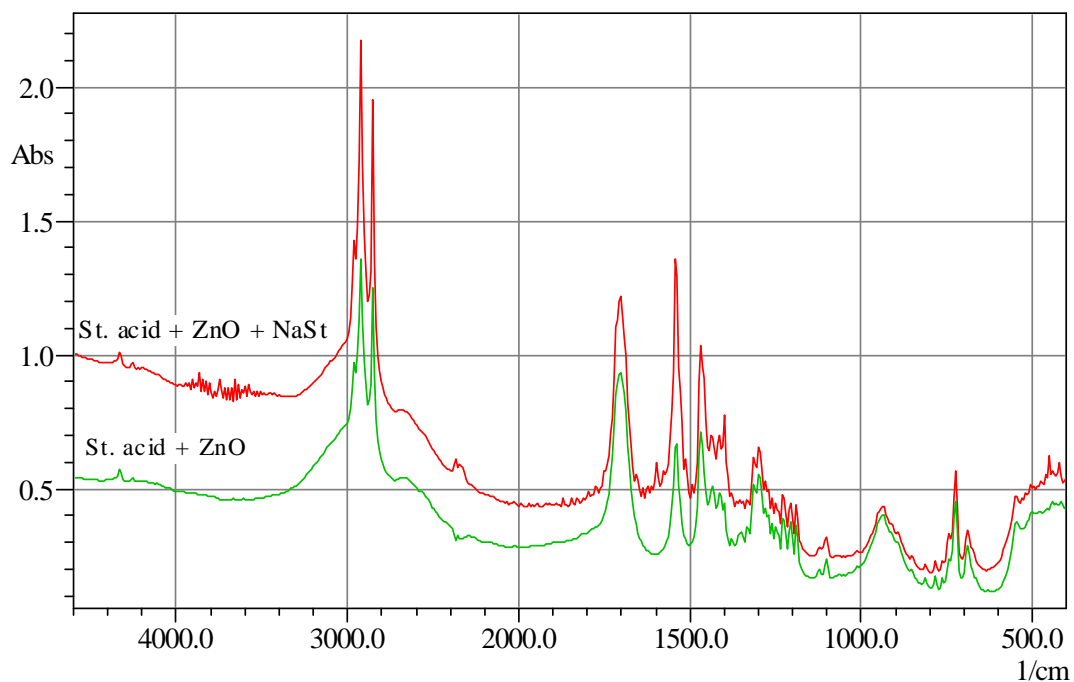
Figure 6.29. IR spectra of zinc stearate from modified fusion process.

As it seen in Figure 6.29., the addition of 0.5 g of NaSt did not produce a significant result based on raw material consumption. In theory, insoluble stearic acid does not dissolve in water and it floats due to its low density, and zinc oxide sinks in water due to its high density. In order to increase the dispersion of stearic acid in water, surfactant was used to overcome the above situation.

The presence of stearic acid in zinc stearate is understood from the characteristic stearic acid peak at 1700cm^{-1} band due to C=O stretching vibration. The synthesized product was observed from IR spectrum at 1540cm^{-1} due to COO^{-} stretching vibration.

As shown in Figure 6.30., zinc stearate samples have impurities. The 2θ values at 31.72, 34.43 and 36.19 shows the presence of unreacted ZnO in the product. At this point mixture contains also a theoretical amount of stearic acid with respect to zinc oxide.
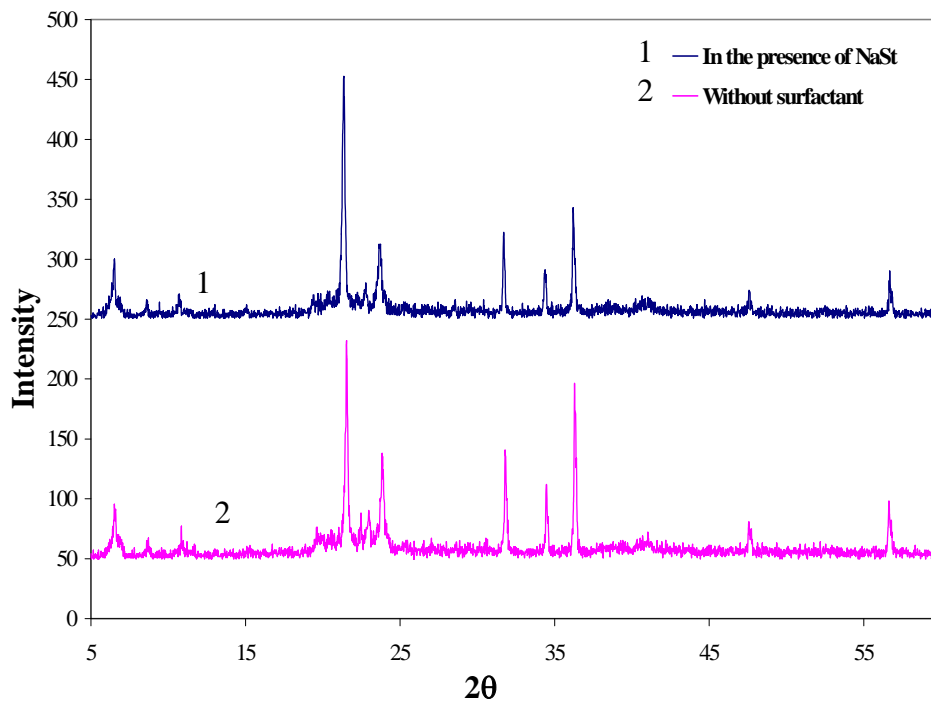
Figure 6.30. XRD Patterns of zinc stearate from modified fusion process.

SEM micrographs of zinc stearate samples are shown in Figure 6.31. and Figure 6.32.
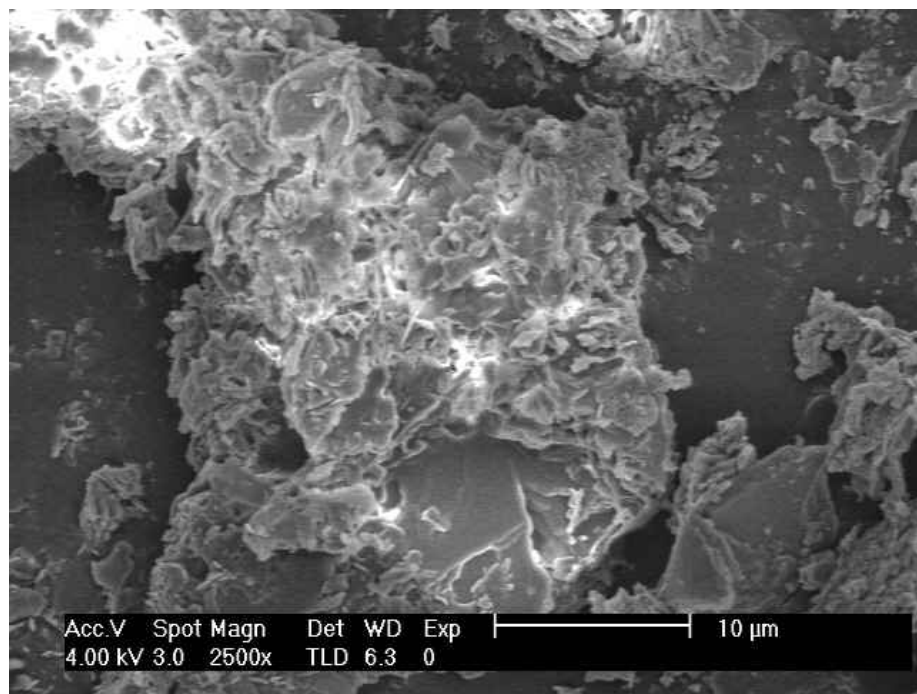
Figure 6.31. SEM micrograph of zinc stearate sample from modified fusion process
in the absence of surfactant, NaSt.
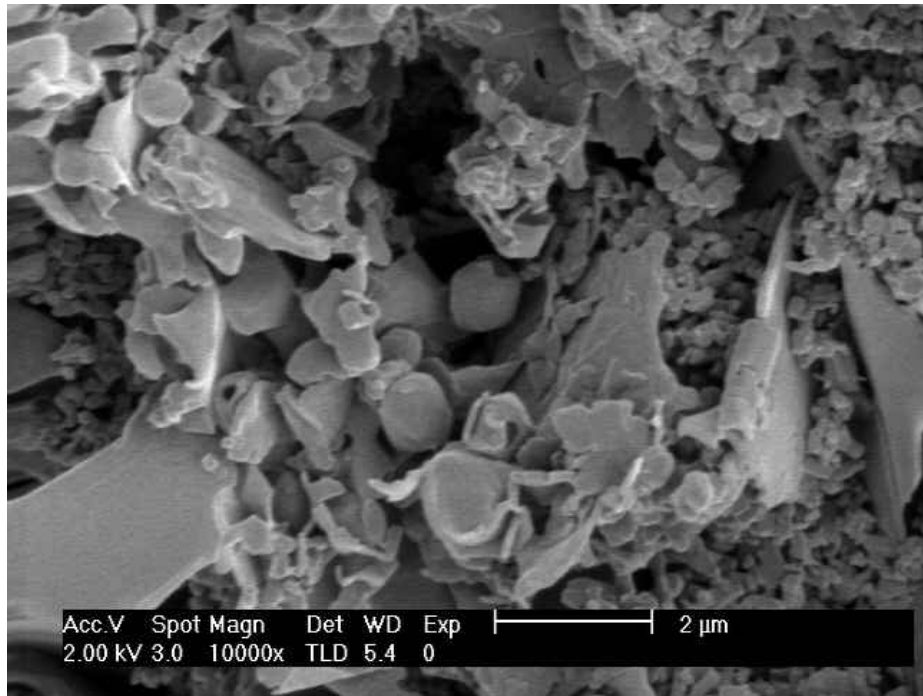
Figure 6.32. SEM micrograph of zinc stearate sample from modified fusion process in the presence of surfactant, NaSt.

As it seen in Figure 6.31. and Figure 6.32. both zinc stearate samples contain unreacted ZnO and stearic acid. The shape of particles and comparison of Figure 6.32. and Figure 6.33. showed that they are zinc oxide.
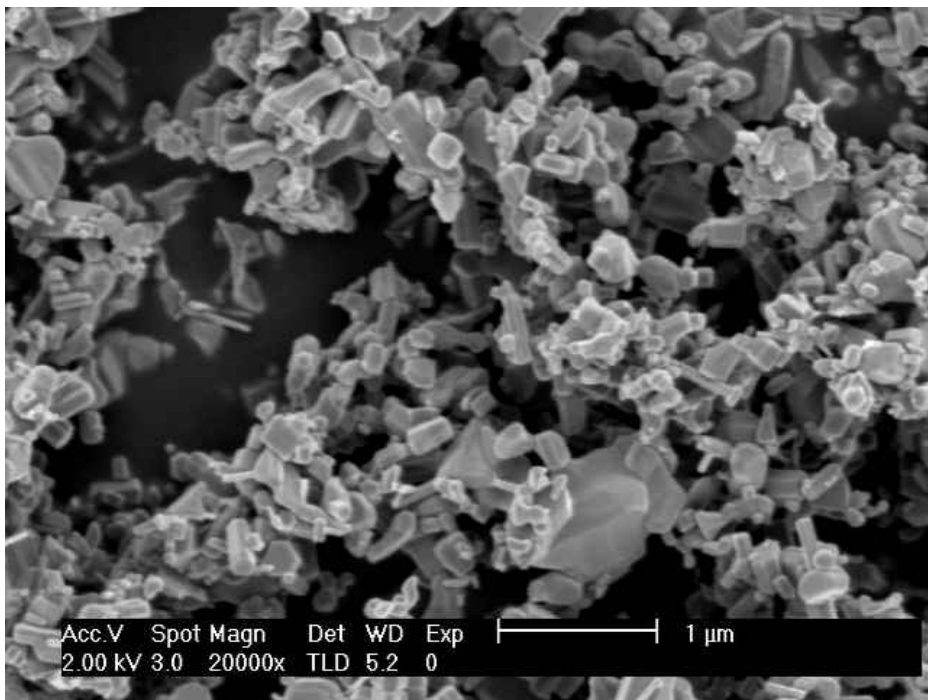
Figure 6.33. SEM micrograph of zinc oxide.

6.9. Kinetic Studies of Both ZnSt₂ Production Processes

For the determination of conversion in the fusion and precipitation processes, a new method was developed by using IR spectra of the samples throughout the reaction. In this method, calibration curve of sodium stearate, stearic acid and zinc stearate were obtained using known compositions of these compounds. In fusion process, powder ZnO was added into molten stearic acid and reaction started. Samples have been taken from reaction mixture in constant time intervals. In precipitation process, zinc sulfate solution was added into dissolved sodium stearate and sampling was begun. Finally, conversion was calculated by comparing the measured characteristic band of raw material and product and calibration curve.

6.9.1. Developing of Model for Conversion Calculations

The absorption law is commonly called Beer's law and is usually written as a function of absorbance (A) as shown in Equation 6.1.;

$$A = \varepsilon.b.C \qquad\qquad \text{-6.1.-}$$

The concentration of product (C), and the thickness (b), is a measure of the relative number of the absorbing molecules in the infrared beam. The absorptivity (ε) is a constant specific for the substance at a particular wavelength and also varies with the units used for b and C.

Ratio Methods:

In solid state spectra of the films, KBr discs, the thickness or concentration in the KBr is not known and is different preparations. In these cases, band ratios can be used since the absorbance ratio of two bands in the same spectrum should be independent of sample thickness. The mixture comprises two components stearic acid and zinc stearate, each of which has an analytical band, which has no interference from the other component . In this case, the absorbance ratios for the two analytical bands are from Beer's law.

$$\frac{A_1}{A_2} = \frac{\varepsilon_1.b_1.C_1}{\varepsilon_2.b_2.C_2} \qquad\qquad \text{-6.2.-}$$

Since $b_1=b_2$ and ($\varepsilon_1/\varepsilon_2$) is a constant, the above equation states that the absorbance ratio is proportional to the concentration ratio.

A relationship can be rearranged for the conversion calculations of the fusion process as shown in Equation 6.3.

$$\frac{C_1}{C_2} = \frac{\varepsilon_2.A_1}{\varepsilon_1.A_2}$$

-6.3.-

Postulated reaction model is given in Table 6.7.

Table 6.7. Conversion calculation

	2 A	+ B $\longrightarrow$	C	+ D
Initial	$[A_0]$	$[B_0]$ $\longrightarrow$	-	-
Consumption $-[A_0].X$		$-[A_0].X/2 \longrightarrow$	$[A_0].X/2$	$[A_0].X/2$
Remaining $[A_0]-[A_0X/2]$		$[B_0]-[A_0X/2] \longrightarrow$	$[A_0]X/2$	$[A_0].X/2$

Conversion (X) can be obtained by taking the ratio of remaining raw material concentration to formed product concentration.

$$\frac{A}{CorD} = \frac{[A_0](1-X)}{[A_0](X/2)} \qquad (A: C_1, D: C_2)$$

$$\frac{C_1}{2C_2} = \frac{(1-X)}{X} \qquad \Rightarrow \qquad \frac{C_1}{C_2} = \frac{2(1-X)}{X}$$

-6.4.-

When the Equation 6.3. is inserted in the Equation 6.4., the conversion equation can be calculated as shown in Equation 6.5.

$$X = \frac{2\varepsilon_1 A_2}{\varepsilon_2 A_1 + 2\varepsilon_1 A_2}$$

-6.5.-

(C_1: concentration of reactant A, C_2: concentration of product D, ε_1: absorptivity of reactant A, ε_1: absorptivity of product D, A_1 and A_2 absorbance values of reactant A and product D respectively.)

6.9.2. Kinetic Study of The Precipitation Process

The reaction between NaSt and $ZnSO_4$ in aqueous phase as shown in Equation 5.1. was studied at 70°C and 500 rpm for 30 minutes for the kinetic analysis. The samples taken at different time periods were subjected to IR analysis. From IR analysis of the samples, characteristic NaSt and $ZnSt_2$ peaks were measured by taking their absorbance values of their characteristic peaks. These measured absorbance values ratio (A_1/A_2) was used in the Equation 6.5. to determine the conversion..

$$2C_{17}H_{35}COONa_{(aq)} + ZnSO_4.7H_2O_{(aq)} \longrightarrow (C_{17}H_{35}COO)_2Zn_{(s)} + Na_2SO_{4(aq)} \quad -5.1-$$
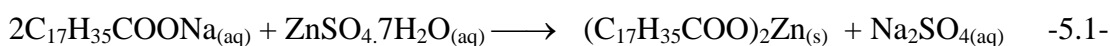
(Sodium stearate:1, Zinc stearate:2)

Calibration curve of compounds as shown in Figure 6.34. was obtained by performing conventional IR analysis with known compound compositions. 1, 2, 3, and 4 mg of material completed to 200 mg with KBr. Calibration curves were drawn by measuring the absorbance values of NaSt ($1560cm^{-1}$), $ZnSt_2$ ($1540cm^{-1}$), and stearic acid ($1700cm^{-1}$), for every composition. In this figure, the absorptivities of NaSt, $ZnSt_2$ and stearic acid were obtained by linearization of the absorbance data. The characteristic bands and structures of the every compound and specific absorptivity values are shown in Table 6.8.
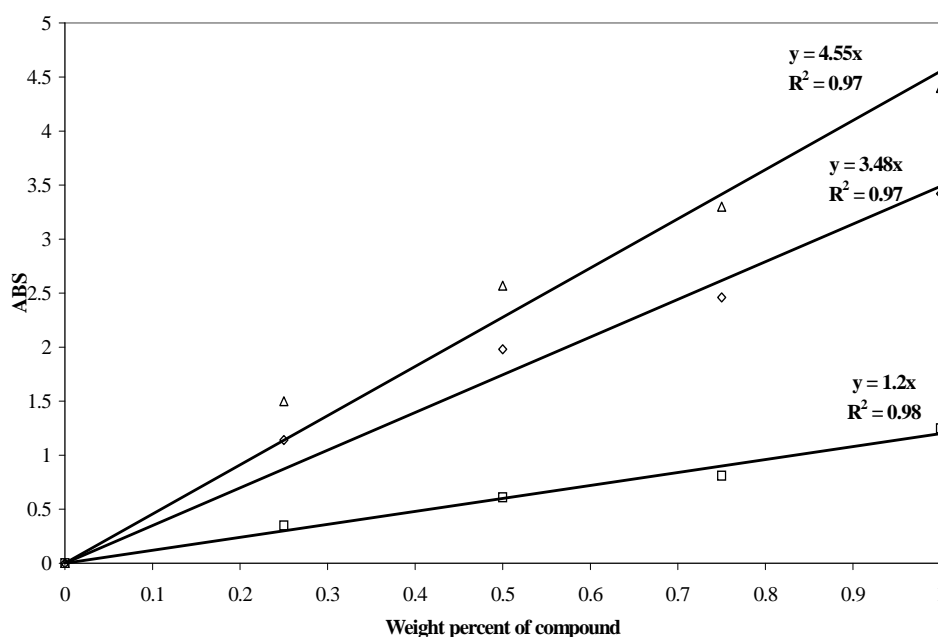
Figure 6.34. Calibration curves of NaSt (Δ), $ZnSt_2$ (◊), Stearic acid (□).

Table 6.8. The characteristic structure, band and absorptivity of compounds.

Compound	Vibration type	Band (cm^{-1})	Absorptivity (ε)
NaSt	COO^- stretching	1560	4.55
$ZnSt_2$	COO^- stretching	1540	3.48
Stearic acid	$C=O$ stretching	1700	1.2
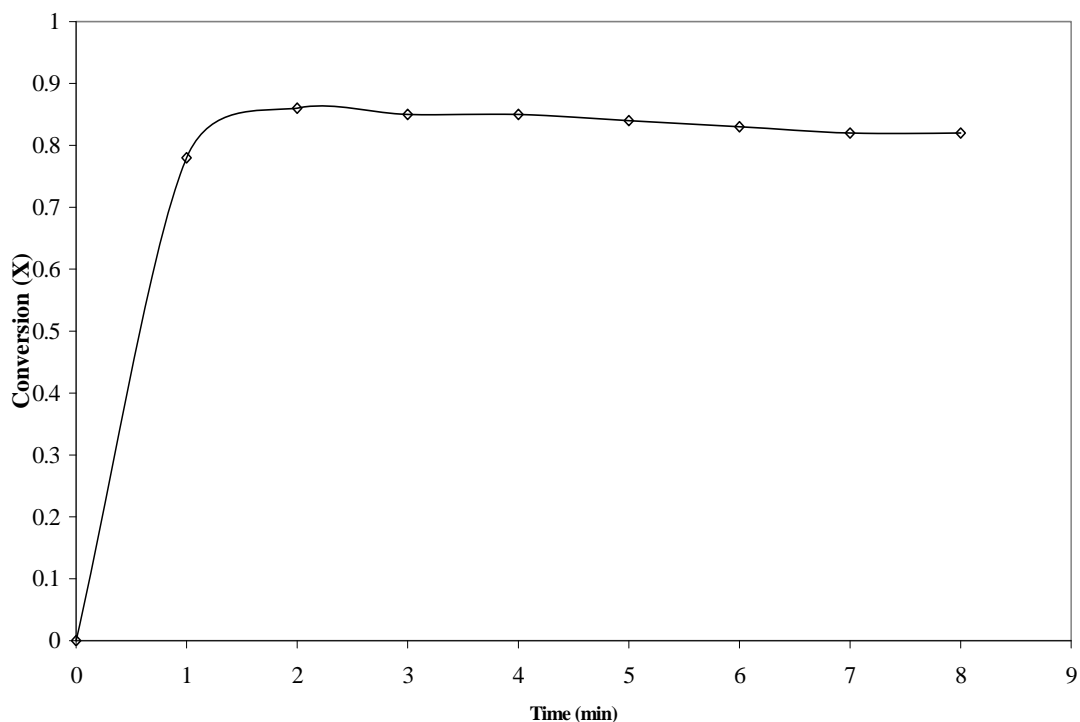
Figure 6.35. The change of conversion with elapsing time.

The change of conversion with elapsing time is shown in Figure 6.35. The ratio of NaSt characteristic absorbance to $ZnSt_2$ absorbance was obtained from IR spectra of every sample taken during the reaction. By using this ratio, conversion was calculated according to Equation 6.5. The fast ionic reaction between NaSt and $ZnSO_4$ occurred within few minutes and the conversion was reached a value of about 80%. The fluctuations seen in Figure 6.35. are attributed to unmixed sample taken for IR analysis. The change of NaSt into $ZnSt_2$ could be better observed by taking samples with shorter time intervals at the initial period of the reaction.

6.9.3. Kinetic Study of The Fusion Process

The liquid-solid reaction between stearic acid and ZnO as shown in Equation 5.2. was studied at 140°C and 400 rpm. for the kinetic analysis. The samples which were taken throughout the reaction were subjected to IR analysis. From IR analysis of the samples, characteristic stearic acid and $ZnSt_2$ peaks were measured by taking their absorbance values. These measured absorbance values ratio (A_1/A_2) was used in the Equation 6.5. to determine the conversion of the reaction.

$$ZnO_{(s)} + 2C_{17}H_{35}COOH_{(l)} \longrightarrow (C_{17}H_{35}COO)_2Zn_{(l)} + H_2O_{(g)} \qquad \text{-5.2-}$$

(Stearic acid:1, Zinc stearate:2)

The calibration curves of stearic acid and zinc stearate are shown in Figure 6.34. Curves were determined by using the measured absorbance values of stearic acid and $ZnSt_2$ for every composition. The ratios of stearic acid characteristic absorbance to $ZnSt_2$ characteristic absorbance was obtained from IR spectra for every sample taken during the reaction.

It is obvious that an increase of mixing rate decreased the delay time of the reaction between zinc oxide and stearic acid. The existing delay time might be caused by the zinc stearate formed shell on the surface of the zinc oxide particles. That shell constitutes a resistance against the diffusion of stearic acid onto solid particles. The reaction between solid ZnO particles and liquid stearic acid is conventional solid liquid reaction. The conversion obtained for three cases was about the value of 82%. The increase in mixing rate affected the required reaction time but not the overall conversion of the reactants as shown in Figure 6.36.

Figure 6.36. The change of conversion with elapsing time for different mixing rates
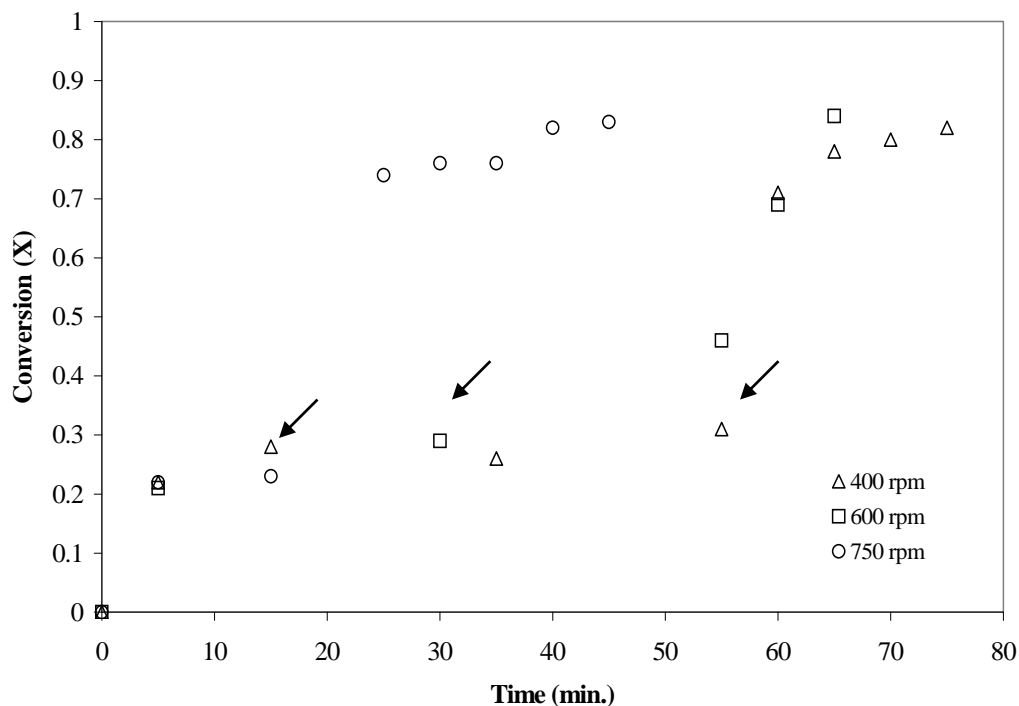(arrows indicate start of the second step in the reaction).

The change of conversion with elapsing time is shown in Figure 6.36. The reaction occurs in two steps. In the first step reaction takes places between the solid zinc oxide particles and molten stearic acid. The synthesized zinc stearate forms a shell at the surface of zinc oxide and decreases the diffusion of the stearic acid onto the zinc oxide surface. With elapsing time, the shell of zinc stearate is removed from zinc oxide surface and second step begins. In the second step, the highest conversion reached is 82% and no progress of the reaction was observed beyond this value.

6.9.4. Comparison of Experimental Data with Kinetic Models

The reaction taking place in precipitation process is a fast ionic reaction and it's proceeding could not be observed with elapsing time. In order to examine the this reaction steps, the compositional change of the reactants must be observed at the very first minute of reaction by using appropriate devices.

In the fusion process, reaction, as given in Equation 5.2., between solid ZnO particles and liquid stearic acid is a solid-liquid reaction and formed by product water is in the gas phase at the reaction temperature. The extensively used model for explanation of solid-liquid reactions is "unreacted core model" for shrinking spherical particles. In

this model, the reaction starts at the outer skin of the particle than moves into the solid and may leave behind completely converted materiel and inert solid, which is referred as ash. Thus, at any time there exists an unreacted core of material, which shrinks in size during reaction as shown in Figure 6.37 (Levenspiel, 1972). Experimental conversion values were compared with this model result as shown in Figure 6.38.
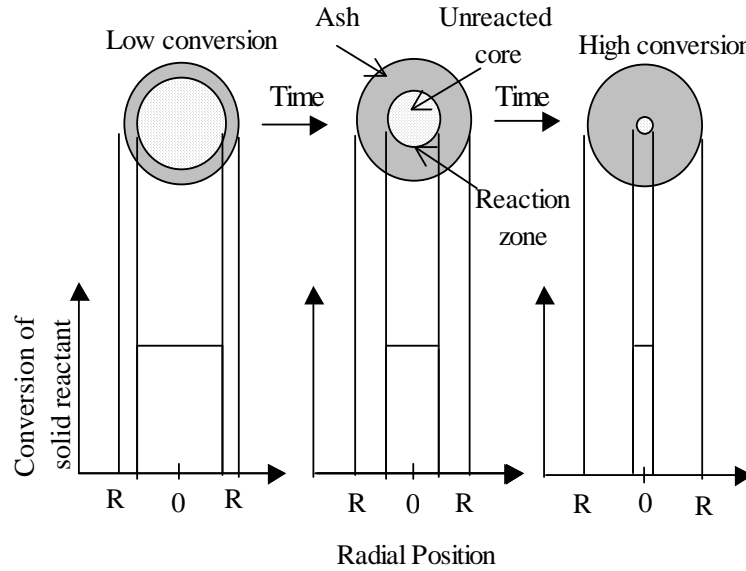

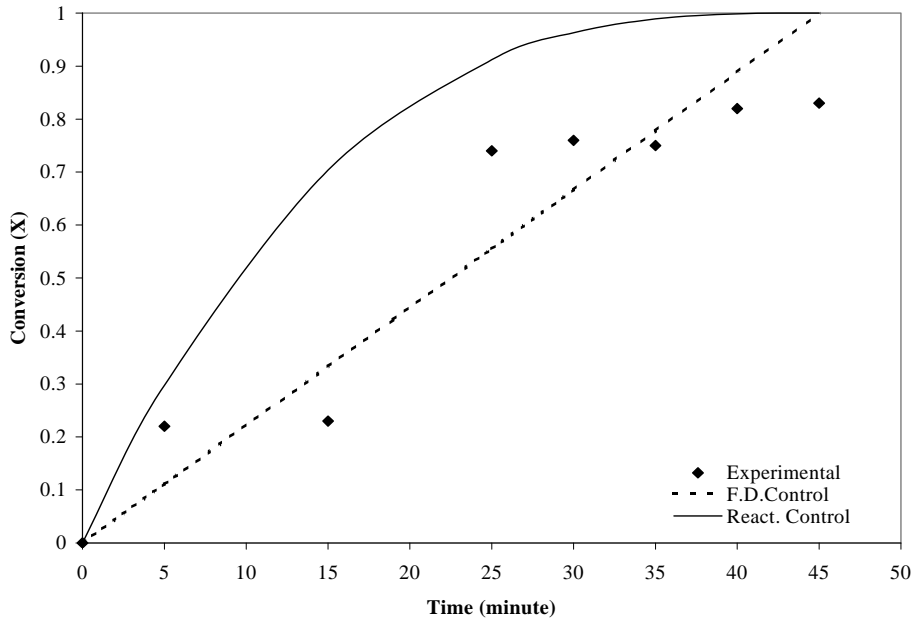Figure 6.37. Schematic representation of unreacted core model.

Figure 6.38. Calculated conversion vs. time from unreacted core model.

In unreacted core model, the conversion was calculated using film diffusion control equation and reaction control equation. The conversion data obtained from the reaction of zinc oxide and stearic acid at 140°C and 750 rpm. was used in these calculations. The equations used are given in Equation 6.6. and Equation 6.7. (Levenspiel, 1972).

$$\frac{t}{\tau} = 1 - (1 - X_B)^{2/3} \quad \text{for film diffusion control} \quad \text{-6.6-}$$

$$\frac{t}{\tau} = 1 - (1 - X_B)^{1/3} \quad \text{for reaction control} \quad \text{-6.7-}$$

(t: time, τ: total time, X_B: conversion of reactant B)

As it seen in Figure 6.38., the model equation conversion values do not overlap with the experimental results. Because, the synthesized $ZnSt_2$ forms a resistance against the diffusion of fresh stearic acid and a delay occurs in the reaction. That delay causes long reaction times. Unreacted core model must be reconsidered taking into account that phenomenon.

6.10. Thermal Decomposition of Zinc Stearate and Stearic Acid

Thermal behavior of $ZnSt_2$ samples produced by precipitation method and fusion technique was examined in thermal gravimetric analysis (TGA). TGA curves of samples are given in Figure 6.39.

The remaining mass of $ZnSt_2$ samples at 1000°C obtained from precipitation and fusion processes are 27.34% and 17.98% respectively. $ZnSt_2$ from precipitation process began to lose weight at 100°C. On the other hand, $ZnSt_2$ from fusion process started to lose weight at 270°C at which degradation starts. Total loss for fusion process product occurred as 82.01% (w) and above 550°C, no loss was observed. The precipitation product lost 72.64 percent of its initial weight and above 550°C, no weight loss was observed. The remained compound at the end of thermal treatment could be oxide and carbonate of zinc metal as pointed out in literature (Akanni et al., 1992). Although decomposition products analysis was not performed, it is thought that major decomposition products of $ZnSt_2$ might be carbondioxide, alkanes, ketones as gas product as given in the literature (Artok and Schobert, 2000).
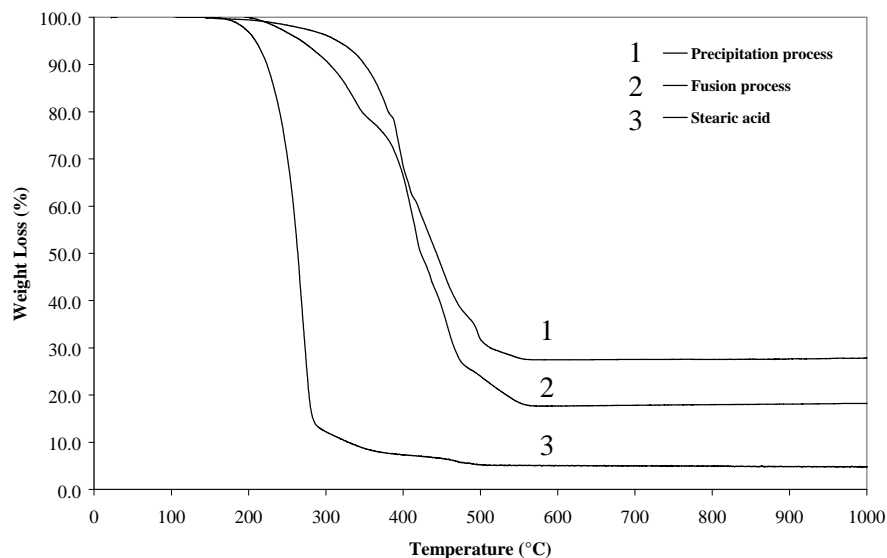
Figure 6.39. TGA curves of ZnSt$_2$ samples from precipitation and fusion process.

The unreacted stearic acid in ZnSt$_2$ produced by fusion process also decomposes to volatile or nonvolatile products. 5% remaining mass at 500°C was observed by (Jaw et al., 2000). The difference between ash contents of ZnSt$_2$ produced by fusion and precipitation methods as seen in Figure 6.39. could be attributed to the presence of easily degradable stearic acid in ZnSt$_2$ produced by fusion process.

6.11. The Effect of Zinc Stearate on n-Paraffin Decomposition
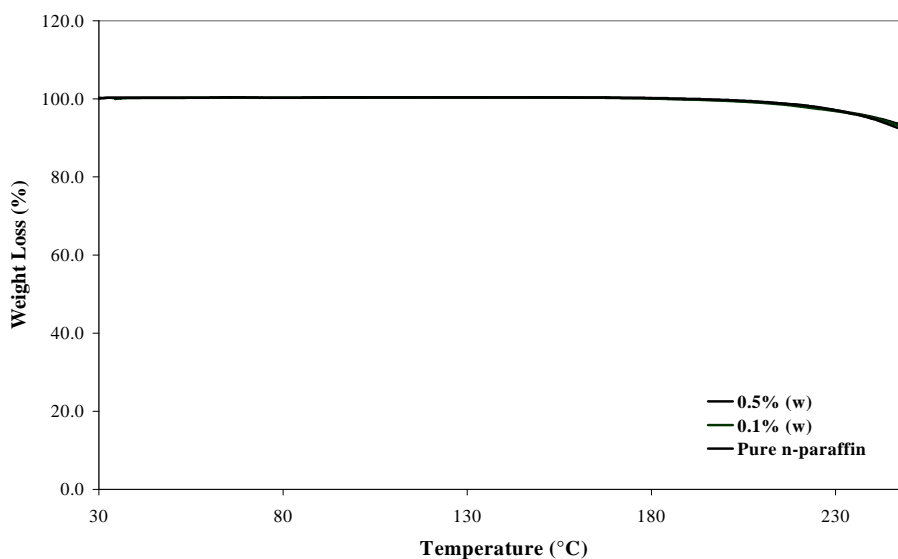
Figure 6.40. TGA curves of n-paraffin in the presence of ZnSt$_2$ 30-250°C range.
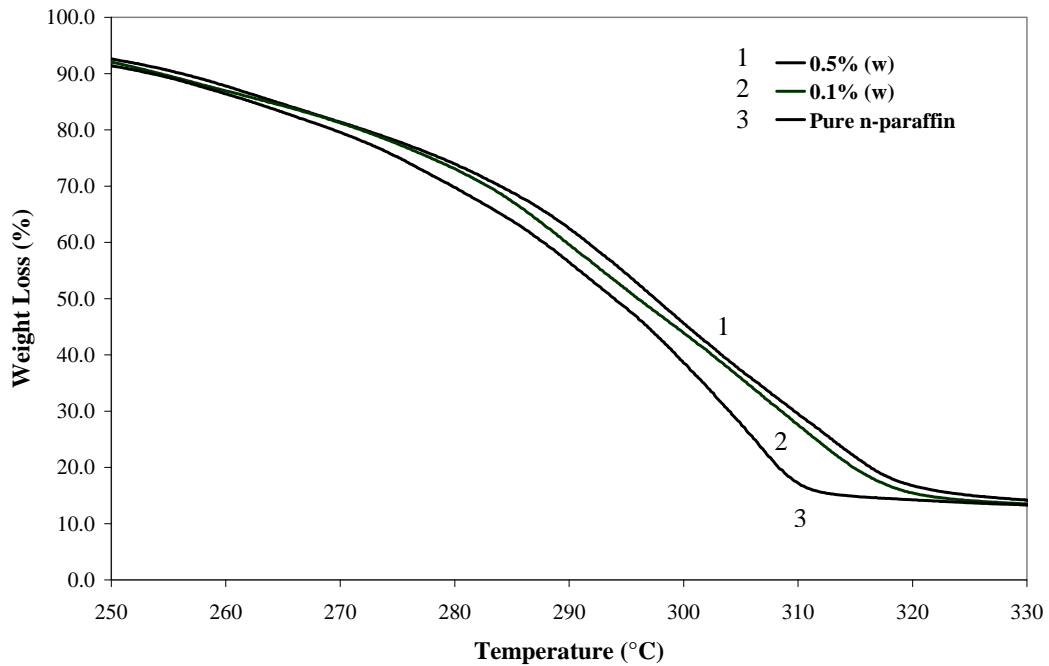
Figure 6.41. TGA curves of n-paraffin in the presence of ZnSt$_2$, 250-330°C range.

In this part of study, 0.1% (w) and 0.5% (w) of zinc stearate were added in n-paraffin and TGA analysis was performed. The result of the analysis is given in Figure 6.40. and Figure 6.41. As it can be seen in the Figure 6.40. n-paraffin does not decompose at 200°C. The addition of zinc stearate shifted the decomposition temperature of n-paraffin as seen in the Figure 6.41. The addition of zinc stearate into n-paraffin increased desired properties of n-paraffin in fuel industry. The thermal decomposition behavior of paraffin wax was found to be consistent with literature (Jaw et al., 2000).

Table 6.3. Elements % (w), for ZnSt$_2$ samples

Experiment name		Equivalent			10% Excess Zn			10% Deficient Zn		
Elements	Theoretical	ICP	EDX	E.A.*	ICP	EDX	E.A.*	ICP	EDX	E.A.*
C	68.43	-	70.23	64.84	-	68.15	63.96	-	68.54	65.72
O	10.12	-	7.14	-	-	8.75	-	-	9.06	-
Zn	10.34	13.53	12.17	-	14.84	13.18	-	12.33	10.52	-
Na	-	0.1	-	-	0.02	-	-	0.521	1.04	-
H	11.09**	-	11.09**	9.41	-	11.09**	9.07	-	11.09**	9.92

* for elemental analysis (E.A.) results, ** for theoretical values of hydrogen

Table 6.4. ICP analyses of reaction aqueous phase and washing water in ppm

Experiment name	Equivalent		10% Excess Zn		10% Deficient Zn	
Ions	Na	Zn	Na	Zn	Na	Zn
Reaction water	1169	0.11	1131	9.06	1141	3.49
Washing water-I	165	0	80.30	9.0	203.91	2.54
Washing water-II	-	-	5.78	1.0	35.57	1.87

CHAPTER VII

CONCLUSIONS

In this study, the production of zinc stearate by precipitation technique, fusion method and modified fusion process was studied to obtain highly pure product. The process parameters of three processes were examined based on product purity.

In precipitation process, the following conclusions were drawn: The solubility of the sodium stearate determines the important parameters e.g., amount of water required, reaction temperature in this process. 2.5% (w) of NaSt is an optimum solubility value at 70°C for the reaction. However, this low solubility of NaSt caused an increase in the amount of water used in the reaction. Therefore, further washing and filtration processes were required. The other anticipated result is the treatment of wastewater effluent from process. It was concluded from XRD patterns that zinc stearate crystallinity is low and not orderly packed. SEM micrographs showed that zinc stearate crystal morphology is in lamellar form. The particle size was found to be between 2-4 μm. From their IR spectra, it was seen that highly pure zinc stearate was obtained from precipitation process with equivalent raw materials ratio when it is compared to fusion process.

The amount of washing water to zinc stearate ratio was found to be 40 dm^3/kg for effective removal of by products and unreacted raw materials at room temperature. Any further increase in amount of water did not bring any significant change in the results. The interesting situation occurring in the washing was the floatation of the zinc stearate particles although its density is greater than the water. This result was attributed to its porous structure. The adsorption of sodium sulfate on zinc stearate was not observed in washing experiments.

In fusion process the following conclusions were drawn: The lowest reaction time was obtained at 750 rpm stirring rate and 140°C for same conversion value of 80%. Vigorous agitation increased the collision of the reactants and under this turbulence regime formed zinc stearate on the surface of zinc oxide was removed into the bulk phase. Although the reaction temperature is two times greater than the precipitation process, synthesized zinc stearate samples contained unreacted raw material, stearic acid. The presence of unreacted stearic acid in the product was

observed in IR spectrum. Fusion reaction should be studied for longer reaction periods and under vigorous agitation for high conversion.

XRD patterns showed that zinc stearate crystallinity is greater than the precipitation process product crystallinity. Since the product was obtained from melt, it was more orderly packed. From SEM micrographs, zinc stearate crystal structure was observed as layered lamellar form. The particle size of zinc stearate was found to be between 4-6 μm from SEM micrographs.

The phase change of the zinc stearate samples was observed as from solid to liquid directly for both processes. In the precipitation process melting point of samples were found to be 122°C. The melting points of samples from fusion process were found to be slightly lower than 122°C due to the presence of stearic acid.

In modified fusion process the following conclusions were drawn: Since the reaction was carried out at 80°C in the presence of water, the reaction did not go to completion in the period of 60 min. and formed product comprises unreacted raw material. From IR spectra, XRD patterns and SEM micrographs of the samples collected at the end of reaction, the presence of unreacted raw materials was confirmed. The addition of sodium stearate into reaction mixture as a surfactant did not bring a significant effect for reaction proceeding.

Thermal decomposition of zinc stearate was examined in TGA analysis. It was concluded that fusion process product includes stearic acid because its remaining mass is less than the precipitation process product's remaining mass. The use of zinc stearate in n-paraffin wax shifted the thermal decomposition temperature of wax 10°C. Increasing the amount of zinc stearate in n-paraffin shifts the decomposition temperature of wax.

Finally, the precipitation process is favored for the production of highly pure zinc stearate at the expense of high water consumption in reaction and separation. The fusion reaction should be examined further to decrease the reaction time and increase the conversion. The zinc stearate manufactured with high purity will be used in industrial applications such as PVC thermal stabilization, Langmuir-Blodgett film formation and fuel additive in further studies.

REFERENCES

- Akanni M. S., Okoh E. K., Burrows H. D., and Ellis H. A. "The thermal behavior of divalent and higher valent metal soaps-arewiev", Thermochimica Acta, 208, 1-41, 1992

- Antony P. and De S. K., "The effect of zinc stearate on melt-processable ionomeric blends based on zinc salts of maleated high-density polyethylene and maleated EPDM rubber", Polymer, 40, 1487-1493, 1999.

- Artok L. and Schobert H. H., "Reaction of carboxylic acids under coal liquefaction conditions 1. Under nitrogen atmosphere", Journal of Analytical and Applied Pyrolysis, 54, 215-233, 2000

- Baltacıoğlu H. and Balköse D., "Effect of zinc stearate and/or epoxidized soybean oil on gelation and thermal stability of PVC-DOP plastigels", Journal of Applied Polymer Science, 74, 2488-2498, 1999.

- Baltacıoğlu H., "Thermal stabilization of PVC plastisols", Ph.D. Thesis, Ege University, Graduate School of Natural Applied Science, 1994 (in Turkish).

- Blachford J., U.S. Patent, 4,316,852, 1982

- Chen H. Z., Li-ming S., "Design of orthogonal test and determination of optimum technological conditions for direct synthesis of zinc stearate", Plastics Manufacture and Processing, CA:37 15-17, 2000

- Colthup N. B., Daly H. L. and Wiberley s. E., "Introduction to infrared and raman spectroscopy", Academic Press, pp. 291-320, Calfornia, 1990

- Cutler W. G. And Davis R.C., "Detergency Theory and Test Methods", Marcel Dekker Inc., p. 8, 1972, Newyork

- Elvers B, Hawkins S., and schulz G., "Ullmann's Encyclopedia of Industrial Chemistry", Volume A16, 5th Edition, pp. 361-371, 1990

- Gökçel H. I., Balköse D., and Köktürk U., "Effects of mixed metal stearates on thermal stability of rgid PVC", European Polymer Journal, 35, 1501-1508, 1999.

- Hayasaka I., Makino N. And Okada T., U.K. Patent, 2,103,616, 1983

- Howe-Grant M., "Kırk-Othmer Encyclopedia of Chemical Technology", Volume 8, 4th Edition, pp. 433-445, 1990

- Hudson J. R. And Nelson E. N., U.S. Patent, 5,164,523, 1992

- Hui Y. H., "Bailey's Industrial Oil and Fat Products", Volume 5, 5th Edition, John Wiley & Sons Inc., New York, 1996

- Ishioka T., Maeda K., Watanabe I., Kawauchi S. and Harada M., "Infrared and XAFS study on structure and transition behavior of zinc stearate", Spectrochimica Acta Part A: Molecular Spectroscopy, 56, 1731-1737, 2000

- Ishioka T., Shibata Y., Takahashi M. and Kanesaka I., "Vibrational spectra and structures of zinc carboxylate II. Anhydrous zinc acetate and zinc stearate", Spectrochimica Acta Part A: Molecular Spectroscopy, 54, 1811-1818, 1998

- Jaw K. S., Hsu C. K., and Lee J. S., "The thermal decomposition behaviour of stearic acid, paraffin wax and polyvinyl butyral", Thermochimica Acta, 367-368, 165-168, 2001

- Jona E., Pajtasova M., Ondrusova D., and Simon P., "Influence of temperature on curative interactions with participation of metal carboxylate as adhesive promotors: the interactions Cu(II) hexadecanoate with stearic acid, N,N'-dicyclohexylbenzothiazole-2-sulfenamide, sulfur and zinc oxide", Journal of Analytical and Applied Pyrolysis", 63, 17-27, 2002

- Kato Y., U.S. Patent, 6,162,836, 2000

- Lally R. E. and Cunder J., U.S. Patent, 3,476,786, 1969

- Lee J. H., Ko K. H., Park B. O., "Electrical and optical properties of ZnO transparent conducting films by the sol-gel method", Journal of Crystal Growth, 247, 119-125, 2003

- Lee S. J., Han S. W., Choi H. J. And Kim K., "Phase behavior of organic-inorganic crystal", The European Physical Journal D, 16, 293-296, 2001

- Liao Z., Wang X. and Lu A., CN Patent, 101,941, 1997

- Levenspiel O., "Chemical Reaction Engineering", 2nd Edition, John Wiley & Sons pp 357-376, Toronto, 1972

- Martinus C. D., Bolt-Westerhoff J. A. and Wijngaarden G. L., U.K. Patent, 2,097,417, 1981

- Mul M. N. G., Davis H. T., Evans D. F., Bhave A. V., and Wagner J. R., "Solution phase behavior and solid phase structure of long chain sodium soap mixtures", Langmuir, 16, 8276-8284, 2000.

- Odashima O. and Kondo O., U.S. Patent 4,473,504, 1984

- Odashima O. and Kondo O., U.K. Patent, 2,080,804, 1982

- (PCPDFWIN v. 2.1.), Data library of the Philips Xpert-Pro.

- Perry J.H., "Chemical Engineering Handbook", Kogakuska Company Ltd., 3-94, Tokyo, 1963

- Ross R. A. and Takacs A. M., "Surface reactions of ethyl stearate and stearic acid with zinc, manganese and their oxides", Surface Technology, 84, 361-377, 1984

- Sakai H. and Umemura J., "Evaluation of molecular structure in Langmuir monolayers of zinc stearate and zinc 12-hydroxystearate by IR external reflection spectroscopy", Colloid Polymer Science, 280, 316-321, 2002

- Sakai A. and Kojima Y., "On the infrared absorption spectra of zinc stearate complex", Spectrochimica Acta Part A: Molecular Spectroscopy, 71, 581-592, 1971

- Scott L. F., Strachan H. D. and McCloskey C. M., U.S. Patent 3,803,188, 1974

- Sigoli F. A., Davolos M. R., and Jafelicci Jr., "Morphological evolution of zinc oxide originating from zinc hydroxide carbonate", Journal of Alloy and Compounds, 262:263, 292-295, 1997

- Simons M. J., U.S. Patent, 3,839,049, 1974

- Tandon P., Raudenkolb S., Neubert R. H. H., Rettig W., and Wartewig S., "X-ray diffraction and spectroscopic studies of oleic acid-sodioum oleate", Chemistry and Physics of Lipids, 109, 37-45, 2001.

- Valor A., Reguear E., Torres-Garcia E., Mendoza S. and Sanchez-Sinencio F., "The thermal decomposition of the calcium salts of several carboxylic acids", Thermochimica Acta, 389, 133-139, 2002

- Wade L. G., "Lipids", Organic Chemistry, pp. 1264-1271, Prentice Hall Inc., New Jersey, 1987

- Walas S.M., "Chemical Process Equipment", pp. 287-304, Butterworth-Heinemann, Boston, 1990

- Wu X. and Xiao C., "Synthesis of calcium and zinc stearate by saponification", Surface Active Agents and Detergents, CA:46, 19-21, 1998

- Yoshizawa F., Kikuchi F., Kojima S. and Yuasa K., U.S. Patent 5,175,322, 1992

- Zhou C., Wenjuan Z., Wangeng S. and Shixian Y., Plastics Manufacture and Processing CA:37, 2000